SANDIA REPORT
SAND2011-2896
Unlimited Release
Printed May 2011

Allowable Pillar to Diameter Ratio for Strategic Petroleum Reserve Caverns

Byoung Yoon Park and Brian L. Ehgartner

Prepared by
Sandia National Laboratories
Albuquerque, New Mexico 87185 and Livermore, California 94550

Sandia National Laboratories is a multi-program laboratory managed and operated by Sandia Corporation, a wholly owned subsidiary of Lockheed Martin Corporation, for the U.S. Department of Energy's National Nuclear Security Administration under contract DE-AC04-94AL85000.

Issued by Sandia National Laboratories, operated for the United States Department of Energy by Sandia Corporation.

Available to DOE and DOE contractors from
U.S. Department of Energy
Office of Scientific and Technical Information
P.O. Box 62
Oak Ridge, TN 37831

Telephone: (865) 576-8401
Facsimile: (865) 576-5728
E-Mail: reports@adonis.osti.gov
Online ordering: http://www.osti.gov/bridge

Available to the public from
U.S. Department of Commerce
National Technical Information Service
5285 Port Royal Rd.
Springfield, VA 22161

Telephone: (800) 553-6847
Facsimile: (703) 605-6900
E-Mail: orders@ntis.fedworld.gov
Online order: http://www.ntis.gov/help/ordermethods.asp?loc=7-4-0#online

SAND2011-2896
Unlimited Release
Printed May 2011

Allowable Pillar to Diameter Ratio for Strategic Petroleum Reserve Caverns

Byoung Yoon Park[1] and Brian L. Ehgartner[2]

[1]-Geomechanics Department
Sandia National Laboratories
P.O. Box 5800
Albuquerque, NM 87185-MS0751

[2]-Geotechnology and Engineering Department
Sandia National Laboratories
P.O. Box 5800
Albuquerque, NM 87185-MS0706

Abstract

This report compiles 3-D finite element analyses performed to evaluate the stability of Strategic Petroleum Reserve (SPR) caverns over multiple leach cycles. When oil is withdrawn from a cavern in salt using freshwater, the cavern enlarges. As a result, the pillar separating caverns in the SPR fields is reduced over time due to usage of the reserve. The enlarged cavern diameters and smaller pillars reduce underground stability. Advances in geomechanics modeling enable the allowable pillar to diameter ratio (P/D) to be defined. Prior to such modeling capabilities, the allowable P/D was established as 1.78 based on some very limited experience in other cavern fields. While appropriate for 1980, the ratio conservatively limits the allowable number of oil drawdowns and hence limits the overall utility and life of the SPR cavern field. Analyses from all four cavern fields are evaluated along with operating experience gained over the past 30 years to define a new P/D for the reserve. A new ratio of 1.0 is recommended. This ratio is applicable only to existing SPR caverns.

ACKNOWLEDGMENTS

This research is funded by SPR programs administered by the Office of Fossil Energy (FE) of the U.S. Department of Energy.

Dr. Courtney G. Herrick (SNL, Dept. 6211) and Dr. Stephen J. Bauer (SNL, Dept. 6914) provided a technical review and Dr. David J. Borns (SNL, Dept. 6912) provided a management review. We also acknowledge and thank Dr. John D. Osnes of RE/SPEC (Rapid City, SD) for his review and concurrence on the recommendation to reduce the existing pillar to diameter ratio to 1.0. His endorsement is based in part on experience with numerous cavern fields and his expertise in modeling. This report has been improved by these individuals.

CONTENTS

ACKNOWLEDGMENTS 4
CONTENTS 5
FIGURES 7
TABLES 11
NOMENCLATURE 12
1. INTRODUCTION 13
1.1. Background 13
1.2. Objectives 13
1.3. Approach 13
1.4. Applications 14
1.5. Report Organization 14
2. DEFINITIONS 15
2.1. Pillar to Diameter Ratio 15
2.2. Salt Dilation Criteria 17
2.2.1. Van Sambeek Criterion 17
2.2.2. RESPEC Dilation Criterion 18
3. MODEL DESCRIPTION 21
3.1. Wedge Symmetry Plane Model for West Hackberry 23
3.2. Wedge Symmetry Plane Model for Cavern Shape Study 25
3.3. Wedge Symmetry Plane Model for Big Hill 26
3.4. Salt Dome Model for Bayou Choctaw 27
3.5. Salt Dome Model for Bryan Mound 28
3.6. Half of Salt Dome Model for West Hackberry 30
4. RESULTS 32
4.1. Wedge Symmetry Plane Model for West Hackberry 32
4.2. Wedge Symmetry Plane Model for Cavern Shapes 37
4.2.1. Cylindrical Cavern 37
4.2.2. Enlarged Bottom Cavern 39
4.2.3. Enlarged Middle Cavern 41
4.2.4. Enlarged Top Cavern 43
4.3. Wedge Symmetry Plane Model for Big Hill 45
4.4. Salt Dome Model for Bayou Choctaw 49
4.5. Salt Dome Model for Bryan Mound 53
4.5.1. Caverns 103 and 111 53
4.5.2. Caverns 112 and 114 60
4.5.3. Caverns 105 and 108 65
4.6. Half of Salt Dome Model for West Hackberry 69

5. SUMMARY AND CONCLUDING REMARKS 77
6. REFERENCES 80
APPENDIX I: MEMORANDUM ABOUT PILLAR TO DIAMETER RATIOS OF SPR CAVERNS AND ALLOWABLE NUMBERS OF DRAWDOWNS 82
APPENDIX II: SPR SITE SPECIFIC DILATION AND STRENGTH DATA 96
APPENDIX III: ALGEBRA SCRIPTS FOR POST-PROCESS 103
III-A. Units.txt 103
III-B. An example for wedge symmetry plane model 103
III-C. An example for the zoomed volume of the web salt 104
III-D. An example for the zoomed volume containing two caverns 106
DISTRIBUTION 108

FIGURES

Figure 1: Relationship between 3D-P/D and standard single valued P/D. 16
Figure 2: Dilation criterion in I_1 and $\sqrt{J_2}$ stress space [DeVries et al., 2003]. 18
Figure 3: RESPEC dilation criteria in I_1 and $\sqrt{J_2}$ stress space with laboratory test data from Cayuta salt [DeVries et al., 2003]. 20
Figure 4: Wedge symmetry plane mesh for 19-cavern and 18-drawdown model showing the stratigraphy at West Hackberry and boundary conditions [Ehgartner and Sobolik, 2002]. . 24
Figure 5: The layout of 19 cavern model in West Hackberry salt dome. Cavern numbering in red. 24
Figure 6: Wedge symmetry plane mesh for the enlarged middle cavern model showing the stratigraphy and boundary conditions [Sobolik and Ehgartner, 2006]. 25
Figure 7: Wedge symmetry plane mesh for 19-cavern and 15-drawdown model showing the stratigraphy at Big Hill and boundary conditions. 26
Figure 8: Overview of the finite element mesh showing the stratigraphy and cavern field at Bayou Choctaw and the cavern geometry within the salt [Park et al., 2006]. 28
Figure 9: Computational mesh showing the stratigraphy and cavern field at Bryan Mound and the cavern geometry within the salt dome (derived from the model constructed by Sobolik and Ehgartner [2009 b]). 29
Figure 10: Computational mesh showing the stratigraphy and cavern field at West Hackberry and the cavern geometry within the salt dome (derived from the model constructed by Sobolik and Ehgartner [2009 a]). 31
Figure 11: Salt dome mesh of the 19-cavern, 18-drawdown leaches model for the West Hackberry site. Since the cavern diameter (D) increases with each drawdown leach while the pillar size (P) decreases, a smaller P/D indicates more leaches have taken place. 34
Figure 12: Minimum safety factor for dilatancy as a function of standard P/D. The numbers on the graph indicates the number of drawdown leaches 35
Figure 13: Predicted safety factor history for dilatancy using the Van Sambeek criterion with C=0.18. The numbers on the history line indicates the number of drawdown leaches. 35
Figure 14: Predicted safety factor contours for dilatancy during workover when the minimum values occur after 13^{th} (A), 14^{th} (B), 15^{th} (C), and 16^{th} (D) drawdown leaches, respectively. Van Sambeek criterion with C=0.18 is used. The vertical cross-section through the centers of caverns and the horizon cross-section at the elevation where the minimum safety factor occurs. The lines A-A* show where the section was cut. Units of time are in years. 36
Figure 15: Salt dome mesh with the cylindrical caverns, and safety factor as a function of standard P/D. 38
Figure 16: Predicted safety factor contours for dilatancy during workover of Cavern 2 when the minimum values occurs (cavern diameters are 600 ft). Van Sambeek criterion with C=0.18 is used. The vertical cross-section through the centers of caverns and the horizon cross-section at the section A-A* and B-B*. Dash-dot lines show where the section was cut. Time is in years. 38
Figure 17: Computational mesh for the enlarged bottom caverns, and safety factor as a function of minimum and standard P/Ds. 40
Figure 18: Predicted safety factor contours for dilatancy during workover of Cavern 4 when the minimum safety factor occurs (cavern diameters at bottom are 600 ft). The Van Sambeek

criterion with C=0.18 is used. The vertical cross-section through the centers of caverns and the horizon cross-section at the elevation where the minimum safety factor occurs. Dash-dot lines show where the section was cut. Time is in years. 40
Figure 19: Computational mesh for the enlarged middle caverns (left), and safety factors as a function of minimum and standard P/Ds. 42
Figure 20: Predicted safety factor contours for dilatancy during workover of Cavern 4 when the minimum safety factor occurs (cavern diameters at middle are 600 ft). Van Sambeek criterion with C=0.18 is used. The vertical cross-section through the centers of caverns and the horizon cross-sections at the elevations where the minimum safety factor occurs (A-A*). Dash-dot lines show where the section was cut. Time is in years. 42
Figure 21: Computational mesh for the enlarged top caverns (left), and safety factor as a function of minimum (right, top) and standard P/D (right, bottom). 44
Figure 22: Predicted safety factor contours for dilatancy when the minimum value occurs during workover of Cavern 4 (Cavern radius at top is 200 ft). Van Sambeek criterion with C=0.18 is used. The vertical cross-section through the centers of caverns and the horizon cross-section at the elevation where the minimum safety factor occurs (A-A*). Dash-dot lines show where the section was cut. Time is in years. 44
Figure 23: Salt dome mesh of the 19-cavern, 15-drawdown leach model for the Big Hill site. Since the cavern diameter (D) increases with each drawdown leach while the pillar size (P) decreases. 47
Figure 24: Minimum safety factor for dilatancy as a function of standard P/D. The numbers on the graph indicates the graph indicates the number of drawdown leaches. 47
Figure 25: Computational mesh for the 31-cavern model in Big Hill (left), and safety factor as a function of P/D (right). 48
Figure 26: Computational mesh for Cavern 5 and dome perimeter in Big Hill (left and center), and safety factor as a function of P/D (right). 49
Figure 27: Computational mesh for Caverns 15 and 17 in Bayou Choctaw (left), and safety factor as a function of P/D (right). 50
Figure 28: Predicted safety factor contours for dilatancy during workover when the minimum values of safety factor occur after 1st, 2nd, 3rd, 4th, and 5th drawdown leach, respectively. The RD criterion for the Cayuta salt is used. The vertical cross-section through the centers of caverns and the horizon cross-section at the elevation where the minimum safety factor occurs. Dash-dot lines show where the section was cut. Time is given in years. 51
Figure 29: Computational mesh for Cavern 20 and dome perimeter in Bayou Choctaw model (left), and safety factor as a function of P/D (right). 52
Figure 30: The mesh of web salt between Caverns 103 and 111 in Bryan Mound. 55
Figure 31: Minimum safety factor for dilatancy using the RD criterion for the Cayuta salt in the web between Caverns 103 and 111 as a function of time. 55
Figure 32: Minimum safety factor of dilatancy as a function of minimum and standard P/D for Cavern 103. 56
Figure 33: Predicted safety factor contours for dilatancy around Caverns 103 and 111 during workover of Cavern 103 at 5/19/2025 (15115 days) (center) with an enlarged view of the location where the dilatancy damage is predicted in Cavern 103 (left). Horizontal cross-section at the elevation where the damage occurs (right-top). Horizontal cross-section at the elevation where the minimum P/D (right-bottom). Time is given in days. 56

Figure 34: Predicted safety factor contours for dilatancy around Caverns 103 and 111 during workover of Cavern 111 at 1/20/2027 (15725 days) (center) with an enlarged view of the location where the dilatancy damage is predicted in Cavern 111 (left). Horizontal cross-section at the elevation where the damage occurs (right-top). Horizontal cross-section at the elevation where the minimum P/D (right-bottom). Time is given in days. 57
Figure 35. The mesh of web salt between Caverns 103 and 111 excluding the roof and floor in Bryan Mound. 57
Figure 36: Minimum safety factor for dilatancy as a function of minimum and standard P/D for Caverns 103 and 111. 59
Figure 37: Predicted safety factor contours for dilatancy in the web salt between Caverns 103 and 111 during workover of Cavern 111 at 12/30/2031 (17530 days). The vertical cross-section through the centers of caverns (left) and the horizontal cross-section at the elevation (-3320 ft) where the minimum safety factor value occurs (right). The minimum P/D is calculated at the same elevation. Time is given in days. 59
Figure 38: The mesh of web salt between Caverns 112 and 114 in Bryan Mound. 61
Figure 39: Minimum safety factor of dilatancy as a function of minimum and standard P/D for cavern 112. 61
Figure 40: Predicted safety factor contours for dilatancy around Caverns 112 and 114 during workover of Cavern 112 at 9/1/2031 (17410 days) (center) with an enlarged view of the location where the dilatancy damage occurs in Cavern 112 (left). Horizontal cross-section at the elevation where the damage occurs (right-top). Horizontal cross-section at the elevation where the minimum P/D (right-bottom). 62
Figure 41: Predicted safety factor contours for dilatancy around Caverns 112 and 114 during workover of Cavern 114 at 12/24/2032 (17890 days) (center) with an enlarged view of the location where the dilatancy damage occurs in Cavern 114 (left). Horizontal cross-section at the elevation where the damage occurs (right-top). Horizontal cross-section at the elevation where the minimum P/D (right-bottom). 62
Figure 42: The mesh of web salt between Caverns 112 and 114 excluding the roof and floor in Bryan Mound. 63
Figure 43: Minimum safety factor for dilatancy as a function of minimum and standard P/D for Caverns 112 and 114. 64
Figure 44: The mesh of web salt between Caverns 105 and 108 excluding the roof and floor in Bryan Mound. 66
Figure 45: Minimum safety factor for dilatancy as a function of minimum and standard P/D for Cavern 105 in the pillar as shown Figure 44. 66
Figure 46: Predicted safety factor contours for dilatancy around Caverns 105 and 108 during workover of Cavern 105 at 15230 days (Center) with an enlarged view at the location where the dilatancy damage occurs in Cavern 105 (left). Horizontal cross-section at the elevation where the damage occurs (right-top). Horizontal cross-section at the elevation where the minimum P/D (right-bottom). 67
Figure 47: The mesh of web volume and Caverns 105 and 108 above the waist of Cavern 105. 67
Figure 48: Minimum safety factor for dilatancy as a function of minimum and standard P/D for Caverns 105 and 108. 69
Figure 49: The mesh of web salt modeled between Caverns 101 and 105 within West Hackberry salt dome. 71

Figure 50: Minimum safety factor for dilatancy as a function of minimum and standard P/D for Cavern 105 in the pillar as shown Figure 49. 72
Figure 51: Predicted safety factor contours for dilatancy around Caverns 101 and 105 during workover of Cavern 105 after the 4th drawdown leach (Center) with an enlarged view of the location where the dilatancy damage occurs in Cavern 105 (left). Horizontal cross-section at the elevation where the minimum P/D (right-top). Horizontal cross-section at the elevation where the damage occurs (right-bottom). 72
Figure 52: The mesh of web volume between Caverns 101 and 105 (left) and the volume between the roof and 500 ft below the roof (center), and minimum safety factor of dilatancy as a function of minimum (right-top) and standard P/D (right-bottom) in this volume. 73
Figure 53: Minimum safety factor for dilatancy as a function of minimum and standard P/D for Caverns 101 and 105..... 73
Figure 54: The mesh of web volume between Caverns 109 and 110 (left) and the volume between the roof and 500 ft below the roof. 74
Figure 55: Minimum safety factor for dilatancy as a function of minimum and standard P/D for Caverns 109 and 110 within the web volume as shown in Figure 54..... 75
Figure 56: The mesh of web salt between Caverns 8 and 9 in West Hackberry salt dome (left), predicted safety contours for dilatancy during workover of Cavern 8 after the 5th drawdown leach (center, the vertical cross-section through the center of caverns and the horizon cross-section at the elevation where the dilatancy damage occurs). 76
Figure 57: Minimum safety factor for dilatancy as a function of minimum and standard P/D for Caverns 8 and 9..... 76

TABLES

Table 1: RESPEC Dilation criterion parameter values for Cayuta salt and Big Hill salt [DeVries et al., 2003; Sobolik and Ehgartner, 2009a]..... 20
Table 2: Stratigraphy and cavern dimensions used in the analysis for each site. 21
Table 3: Material parameters used in the analyses for each site. 22
Table 4: West Hackberry caverns drawdown leach properties, P/Ds, and predicted minimum safety factors for dilatancy in the salt dome. 33
Table 5: P/D and minimum safety factor for dilatancy in the salt dome for the cylindrical caverns. 37
Table 6: P/D and minimum safety factor for dilatancy in the salt dome for the enlarged bottom caverns. 39
Table 7: P/D and minimum safety factor for dilatancy in the salt dome for the enlarged middle caverns. 41
Table 8: P/D and minimum safety factor for dilatancy in the salt dome for the enlarged top caverns. 43
Table 9: P/D and minimum safety factor for dilatancy in the salt dome for the cylindrical caverns. 46
Table 10: P/D and minimum safety factor for dilatancy in the pillar between Cavern 5 and dome perimeter. 48
Table 11: P/D and minimum safety factor for dilatancy in the web salt between Caverns 15 and 17 in Bayou Choctaw salt dome. 50
Table 12: P/D and minimum safety factor for dilatancy in the web salt between Caverns 20 and the surrounding rock in Bayou Choctaw salt dome. 52
Table 13: Minimum P/Ds in the web salt between Caverns 103 and 111. 58
Table 14: Standard P/Ds and minimum safety factor for dilatancy in the web salt between Caverns 103 and 111..... 58
Table 15: Minimum P/Ds for Caverns 112 and 114 in the web salt between Caverns 112 and 114. 63
Table 16: Standard P/Ds and minimum safety factor for dilatancy in the web salt between Caverns 112 and 114..... 64
Table 17: Minimum P/Ds in the web salt between Caverns 105 and 108. 68
Table 18: Standard P/Ds in the web salt between Caverns 105 and 108 as shown Figure 44; and minimum safety factor for dilatancy in the web salt between Caverns 105 and 108 above the waist of Cavern 105. 68
Table 19: Minimum and standard P/Ds for Caverns 101 and 105..... 70
Table 20: Minimum and standard P/Ds for Caverns 109 and 110..... 71
Table 21: Minimum safety factor for dilatancy within the web salts between Caverns 101 and 105; Caverns 109 and 110..... 74
Table 22: P/Ds at the onset of dilatant damage for various webs of salt between caverns. 77
Table 23: Current minimum P/D and the predicted minimum safety factors for dilatancy using three dilatation criteria for Caverns 1, 2, 3, and 4 in Bryan Mound salt dome..... 78

NOMENCLATURE

BC	Bayou Choctaw
BH	Big Hill
BM	Bryan Mound
DP	Damage Potential
FEM	Finite Element Method
MSF	Minimum Safety Factor
MMB	Million Barrels
RD	RESPEC Dilation
SF	Safety Factor
SPR	Strategic Petroleum Reserve
P/D	Pillar to Diameter ratio
VS	Van Sambeek
WH	West Hackberry

1. INTRODUCTION

1.1. Background

Many of the Strategic Petroleum Reserve (SPR) caverns will likely be out of compliance with the SPR Level III Design Criterion, which specifies that each cavern possesses a pillar to diameter ratio (P/D) of 1.78 or greater after five complete fill and drawdown cycles [DOE, 2001]. While some of the caverns were acquired by the SPR, most caverns were leached by the SPR. Many of these are also in violation of this criterion well before five oil drawdowns. This subtask addresses this issue by examining what the current ratios are, and what the criteria should be, based on modeling and advances in geomechanics. To evaluate what safe ratio is, the existing geomechanical analyses results were post-processed using conventional and new salt damage criteria. The results are presented in terms of P/D versus minimum safety factor for dilatancy.

1.2. Objectives

The goal is to establish a limit for the remaining pillar thickness between salt caverns used by SPR without threatening the structural integrity of the caverns. Scripts for the code ALGEBRA using the conventional Van Sambeek and a newer RESPEC dilatant damage criteria were constructed for post processing of existing geomechanics models. The impacts on cavern stability with drawdowns will be established. The results from the new criteria will be compared to the conventional results and presented in terms of P/D.

1.3. Approach

To identify the relationship between P/D and the safety factor for dilatancy, the existing geomechanical analyses results were post-processed using the Van Sambeek (VS) and RESPEC dilation (RD) criteria for Cayuta and Big Hill (BH) salt. Evaluating the sensitivity of the results to these various damage criteria for salt is important because the properties at SPR sites are believed to vary and are not well characterized considering the recent advances in dilation based damage criteria. The webs of salt between the caverns, which are relatively close to each other, are selected to examine the P/D effect assuming these caverns will exhibit the lowest safety factors. Those are Caverns 15 and 17 in the Bayou Choctaw (BC) salt dome; Cavern 103 and 111, 112 and 114, 105 and 108 in the Bryan Mound (BM) salt dome; Cavern 101 and 105, 109 and 110, 8 and 9 in the West Hackberry (WH) salt dome. All caverns in the wedge symmetric plane model are chosen for this study. The out most caverns, Cavern 5 in the BH and Cavern 20 in the BC models, are chosen for examining the P/D effect between the cavern and the dome perimeter. The post-processing code ALGEBRA is used with JAS3D output (EXODUS) to determine the dilatant damage potential in a salt dome. The analyses results used in this study are as follows:

1. The EXODUS output files from computational analyses performed to determine the structural integrity of different cavern shapes in salt domes [Sobolik and Ehgartner, 2006].
2. Constructed the 19-cavern, 15-drawdown leach model to investigate the P/D effect. This model was modified from the 19-cavern, 5-drawdown model to evaluate the structural integrity of caverns located at the SPR BH site [Park et al., 2005].

3. The EXODUS output files from the 3-D finite element analyses performed to evaluate the structural integrity of caverns located at the SPR BC site [Park et al., 2006].
4. The EXODUS output files from the computational analyses that simulate the structural response of caverns at the SPR WH site [Ehgartner and Sobolik, 2002; Sobolik and Ehgartner, 2009a].
5. The EXODUS output files from the computational analyses that simulate the structural response of caverns at the SPR BM site [Sobolik and Ehgartner, 2009b].

1.4. Applications

The P to D ratio limits from this study will help the SPR project manage their existing caverns more effectively.

1.5. Report Organization

The remainder of this report describes the analyses details. Section 2 describes the definitions of P/D, and the Van Sambeek and RESPEC salt dilation criteria. Section 3 presents an overview of the geomechanical models including salt dome geometry, cavern geometries and layout, and material properties. This section provides the discretized finite element meshes for examining the effect of P/D on the dilatant damage. Section 4 describes the post-processed results such as the plots between the P/D and minimum safety factor for dilatancy, and minimum safety factor contours to see where dilatant damage is predicted to occur. Section 5 provides a summary of these calculations and concluding remarks. References are listed in Section 6. Memorandum about P/Ds of SPR caverns and impacts on the numbers of drawdowns are described in Appendix I. SPR site specific dilation and strength data are provided in Appendix II. ALGEBRA scripts for computing the safety factor for dilatancy are also provided in Appendix III.

2. DEFINITIONS

2.1. Pillar to Diameter Ratio

The P/D is a measure used to establish a limit for the spacing between salt caverns used by the SPR. This quantity is defined in the Level III Design Criteria [DOE, 2001]. "Pillar" refers to the thickness of the web of salt remaining between any two adjacent caverns, or between the cavern and salt dome perimeter. "Diameter" refers to the cavern diameter. However, there are inconsistencies in the definition of "Pillar" as (i) the overall average web thickness, or (ii) the minimum web thickness:

(i) Page 2-9, last paragraph under 2.4.2 "Physical Characteristics",

*The ratio of the web or pillar **average** thickness (P), between two adjacent caverns, to **average** final cavern diameter (D) shall not be less than 1.78.*

(ii) Page 2-10, under 2.4.2.2 "Spacing and Proximity Criteria",

*"Pillar" refers to **minimum** thickness of the web of salt remaining between any two adjacent caverns after the last leaching process, or between cavern and salt dome perimeter. . . D **is cavern diameter** after five complete fill and drawdown cycles; P **is pillar width** after five complete fill and drawdown cycles.*

To ensure cavern structural integrity, the Level III Design Criteria mandate that the P/D for each cavern must remain greater than 1.78 after five complete oil drawdown cycles. This criterion applies to caverns constructed by the SPR. A number of acquired caverns are already in violation of the criteria. These caverns have unique shapes and sizes, therefore must be evaluated on a case-by-case basis.

Lord et al. [2009] defined two following P/Ds to consider both definitions above, and calculated the allowable number of full drawdowns until P/Ds of 1.78 and 1.0 for both the average web thickness and the minimum web thicknesses:

$$\text{Minimum 3D-P/D} = \frac{P_{3D}}{2R_{3D}} \quad (1)$$

$$\text{Standard single value P/D} = \frac{P_{L3}}{2R_{L3}} \quad (2)$$

The relationship between these definitions is shown in Figure 1 using Big Hill caverns 101 and 102 average radius profiles after 5 leaches. P_{3D} is the distance between the closest nodes on both cavern meshes, and R_{3D} is the radius of the cavern at each elevation of the closest nodes. P_{L3} and R_{L3} are determined from the volume conserving cylinders as shown as blue boxes. Note that the Minimum 3D-P/D uses the actual 3D mesh data, but not the average radius representation to determine the minimum pillar thickness and location. The single-value P/D will always be larger because $P_{L3} > P_{3D}$ and $R_{L3} < R_{3D}$ and can be thought of as an "average" P/D. Note that the P/Ds by Equations (1) and (2) (based on BH101) are not the same as the P/Ds based on BH102 when R_{3D} and R_{L3} of BH102 are not the same as those of BH101. Hereafter, "Minimum 3D-P/D" and "Standard single value P/D" will be called "Minimum P/D" and "Standard P/D", respectively. The details are provided in Appendix I.

In this study, both pillar definitions will be applied to calculate the P/Ds. In practice though, the minimum P/D is suggested as it relates the proximity of the nearest cavern. This is crucial in preventing caverns from expectantly merging or preventing communication of cavern fluids through cracks or geologic anomalies. The caverns in the numerical analyses models for WH, BH, and BC sites were simplified to the cylinder shapes using the volume conserving cylinders. Therefore, "Standard P/D" only will be calculated to identify the relationship between P/D and the safety factor for dilatancy using the analyses results for those sites. The caverns in the modified model for WH and the model for BM were simplified using the average radius profiles at each elevation of the caverns. Therefore, both "Minimum P/D" and "Standard P/D" will be calculated to identify the relationship between P/D and the safety factor for dilatancy using the analyses results from those models. Note that the creep deformation was not accounted for in calculating the P/D, i.e. the cavern diameters and the pillar thicknesses with drawdown leaches obtained from the initial mesh rather than the deformed mesh due to salt creep were used.

In applying these results to the caverns in the SPR, we recognize that the models represent approximations to actual cavern geometries. As such, the P/Ds found in the models do not necessarily equal those of the caverns in the field. The analysis results are presented in terms of the P/Ds in the model. Once the acceptable minimum P/D is defined, the result can be applied to Appendix I to define the allowable number of oil drawdowns until the criterion is violated.

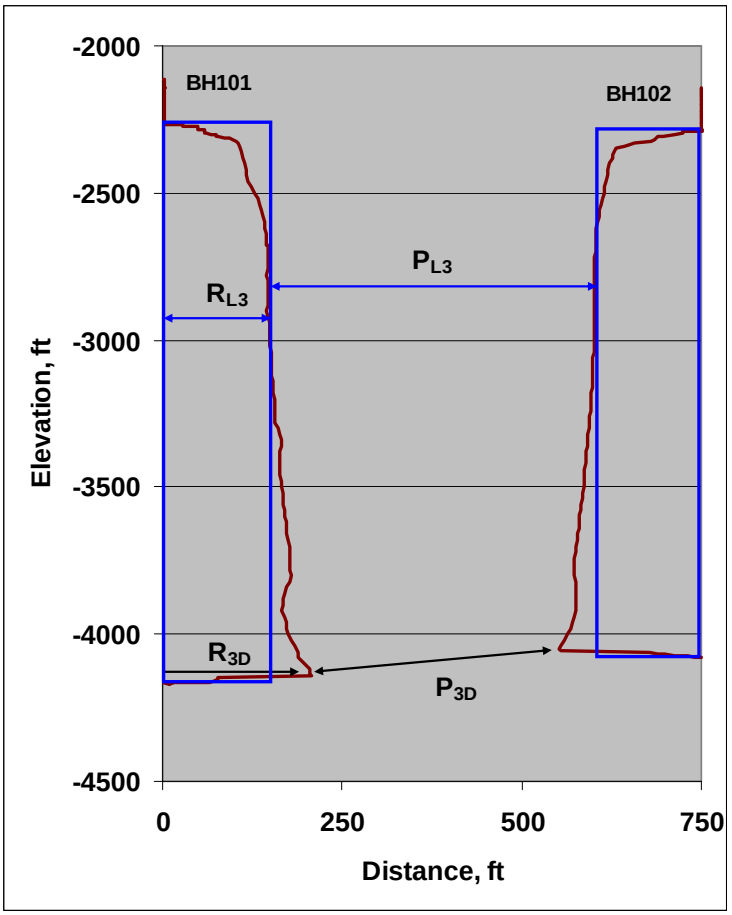

Figure 1: Relationship between 3D-P/D and standard single valued P/D.

2.2. Salt Dilation Criteria

2.2.1. Van Sambeek Criterion

Extensive laboratory salt creep data has demonstrated that damage can be assessed in terms of volumetric strain and principal stresses. The damage potential (DP) criterion has been used since the mid-1990's to evaluate the integrity of salt storage caverns. Mathematically, the DP criterion is:

$$\sqrt{J_2} = C \cdot I_1 \tag{3}$$

where I_1 is the first invariant of the stress tensor ($=\sigma_1+\sigma_2+\sigma_3=3\sigma_m$); J_2 is the second invariant of the deviatoric stress tensor ($=[(\sigma_1-\sigma_2)^2+(\sigma_2-\sigma_3)^2+(\sigma_3-\sigma_1)^2]/6$); σ_1 is maximum principal stress; σ_2 is intermediate principal stress; σ_3 is minimum principal stress and σ_m is the mean stress; C is a material constant with a value typically near -0.27 (tension is considered to be positive) [Van Sambeek et al, 1993].

The test data can be plotted in I_1 and $\sqrt{J_2}$ stress space where the data trend generally indicates that $\sqrt{J_2}$ increases as I_1 increases. The trend is often modeled as a linear relationship, although nonlinear functions have also been fit to such data. A linear line fitted to the data will divide the stress space into two distinct regions as shown in Figure 2. The safety factor for dilatancy can be defined in terms of the ratio of stress invariants:

$$SF_{VS} = \frac{C \cdot I_1}{\sqrt{J_2}} \tag{4}$$

When $SF_{VS} < 1$ (Dilating Region in Figure 2), the shear stresses in the salt (J_2) are large relative to the mean stress (I_1), and dilatant behavior is predicted.

Site specific dilation and strength data for the SPR is compiled in Appendix II along with a discussion on what an acceptable safety margin is. The available data show considerable variation, but general agreement with Equation (4). As discussed in Appendix II, the safety margin of 1.5 needs to be applied to Equation (4) to cover the variation. A safety margin of 1.5 is equivalent to a value of 0.18 (=0.27/1.5) of *C*. This is close to the *C* value in the dilatancy criterion determined from ultrasonic velocity data measured at Location 1 within the WIPP S-90 drift [Park et al., 2008].

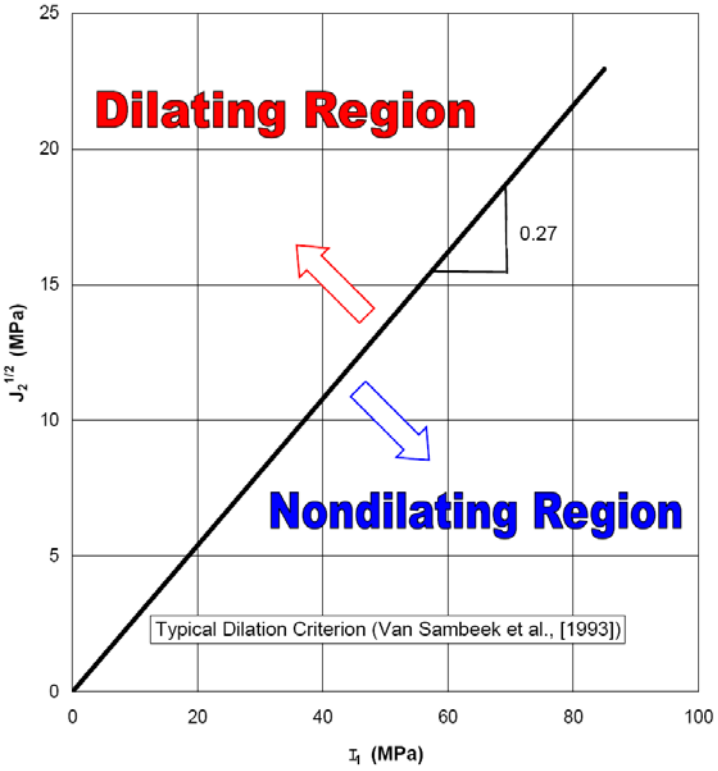

Figure 2: Dilation criterion in I_1 and $\sqrt{J_2}$ stress space [DeVries et al., 2003].

2.2.2. RESPEC Dilation Criterion

Equation (4) predicts the same dilation potential for triaxial extension states of stress as it does for triaxial compress. Similar to many other types of rock, salt is weaker (dilates more readily) in triaxial extension than in triaxial compression. This known behavior has not been taken into account during the development of many dilatancy criteria because nearly all strength testing on salt has been done under triaxial compression. The triaxial extension results indicate a nearly identical trend for the dilation limit dependency on mean stress; however, the dilation limit is approximately 30% lower than the results obtained during triaxial compression. As a result, the dilatancy boundary predicted by models that do not account for the difference in Lode angle may not be conservative if stress states other than triaxial compression are encountered. To consider this problem, RESPEC proposed a new dilation criterion which provides a dilation limit for states of stress ranging from triaxial compression to triaxial extension (i.e., Lode angles ranging from 30º to -30º). The proposed criterion is based on a Mohr-Coulomb-type of failure criterion to represent salt failure as a function of shear stress, mean stress, and Lode angle. Because the experimental evidence suggests that the dilation limit is better represented by a nonlinear function, the follow relationship was developed for the dilatant failure criterion of salt [DeVries et al., 2003];

$$\sqrt{J_2} = \frac{-D_1\left(\frac{I_1}{\sigma_0}\right)^n + T_0}{\sqrt{3}\cos\psi - D_2\sin\psi} \tag{5}$$

where σ_0 is a dimensional constant equal to -1 with the same units as I_1; T_0 is the unconfined tensile strength; ψ is the Lode angle; and n, D_1, and D_2 are parameter estimates that must be determined for each salt formation. The Lode angle can be expressed in terms of the principal stresses as follows:

$$\psi = \tan^{-1}\frac{1}{\sqrt{3}}\left[\frac{2\sigma_2 - \sigma_1 - \sigma_3}{\sigma_1 - \sigma_3}\right] \tag{6}$$

where σ_1 is maximum principal stress; σ_2 is intermediate principal stress; σ_3 is minimum principal stress.

The safety factor for dilatancy is defined as:

$$SF_{RD} = \frac{\left[\frac{-D_1\left(\frac{I_1}{\sigma_0}\right)^n + T_0}{\sqrt{3}\cos\psi - D_2\sin\psi}\right]}{\sqrt{J_2}} \tag{7}$$

The RD criterion was developed to address the following shortcomings identified in the Van Sambeek criterion: (1) a nonzero intercept, (2) a nonlinear relation for the dilatancy boundary in I_1 and $\sqrt{J_2}$ stress space, and (3) the effect of Lode angle. Figure 3 plots the dilation criterion given by Equation (7) with the constant mean stress test data using the fitted parameter values determined for Cayuta salt. The Lode angle (ψ) is 30 degrees for triaxial compression stress states and −30 degrees for triaxial extension stress states. The original linear stress-based criterion given by Ratigan et al. [1991] is also provided in Figure 3. The original criterion represents the best linear fit to both the triaxial compression and triaxial extension test data. However, provision for the different stress states (triaxial compression and triaxial extension) is inherent in the new criterion represented by Equation (7) [DeVries et al., 2003].

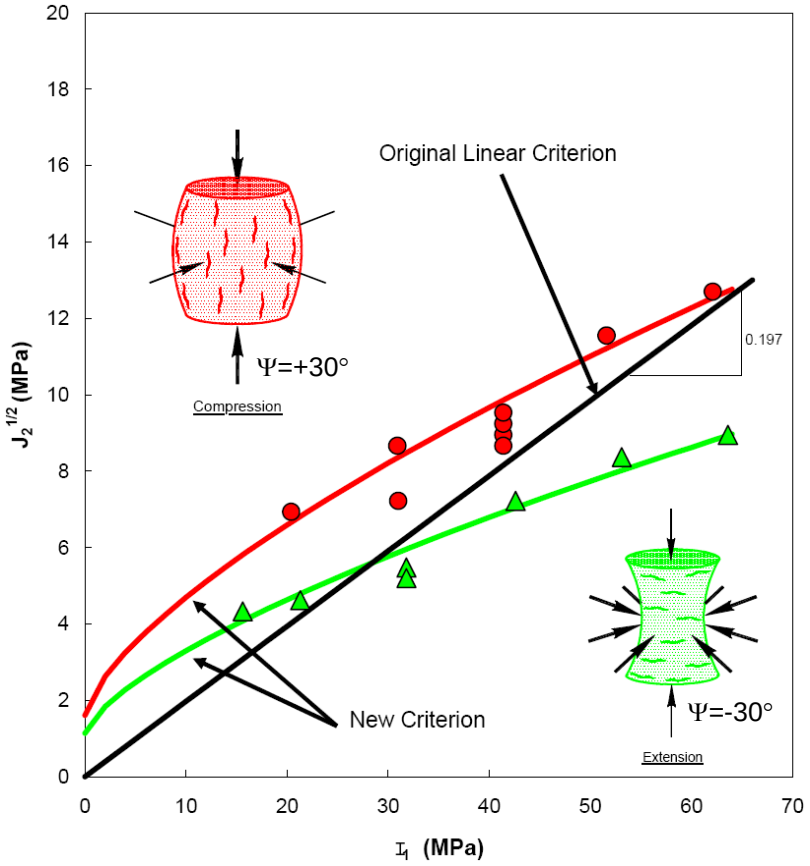

Figure 3: RESPEC dilation criteria in I_1 and $\sqrt{J_2}$ stress space with laboratory test data from Cayuta salt [DeVries et al., 2003].

Parameter values for the RD criterion determined for Cayuta salt and Big Hill salt are provided in Table 1. The values were obtained through experimental work for each site. However, the required RD criterion parameter values are not available for WH, BC and BM salt dome. When the RD criterion for Cayuta or BH salt is applied to the dilatancy calculation in the following sections, the calculation results assume the salt used in each analysis behaves like Cayuta or BH salt. This suggests the RD criterion is applied as a general criterion like the Van Sambeek criterion, but not a site specific criterion.

ALGEBRA scripts for post-processing the results from the FEM analyses with the Van Sambeek criterion and RD criteria for Cayuta salt and Big Hill salt are provided in Appendix III.

Table 1: RESPEC Dilation criterion parameter values for Cayuta salt and Big Hill salt [DeVries et al., 2003; Sobolik and Ehgartner, 2009a]

Parameters	Cayuta Salt	Big Hill Salt
σ_0	-1 MPa (-20885 psf)	-1 MPa (-20885 psf)
n	0.693	0.3668
D_1	0.773 MPa (16144 psf)	2.164 MPa (45200 psf)
D_2	0.524	0.5632
T_0	1.95 MPa (40726 psf)	4.0 MPa (83540 psf)

3. MODEL DESCRIPTION

To identify the relationship between P/D and the safety factor for dilatancy, the existing FEM analyses results from the WH wedge symmetry plane model, the cavern shape study model, the modified WH model, the BH wedge symmetry plane model, the BC model and the BM model were post-processed. The model configurations such as the dimensions, internal cavern pressure history, and material properties will be briefly described in this chapter. The stratigraphy and cavern dimensions used in the FEM analyses for each site are listed in Table 2. The material parameter values used in the analysis for each site are summarized in Table 3. Figure 4 through Figure 9 show the overview of the finite element mesh showing the stratigraphy, cavern geometry, and the boundary conditions at each site. For comparison purpose to show how large the caverns are, a silhouette of the Sears Tower (currently known as Willis Tower) in Chicago, IL is shown.

Table 2: Stratigraphy and cavern dimensions used in the analysis for each site.

	West Hackberry	Cavern Shape	Big Hill	Bayou Choctaw	Bryan Mound	Modified West Hackberry
Overburden thickness (ft)	1000	300	300	500	760	1600
Caprock thickness (ft)	400	900	900	150	280	400
Caprock 2 thickness (ft)	N/A	400	400	N/A	N/A	N/A
Salt dome height (ft)	4900	4400	4400	7350	4960	4000
Surrounding rock thickness (ft)	N/A	5700	5700	7500	5240	4400
Cavern height (ft)	2000	2000	1890	Various	Various	Various
Well depth (ft)	2500	2300	2286	Various	Various	Various
Related figure	Figure 4	Figure 6	Figure 7	Figure 8	Figure 9	Figure 10

Table 3: Material parameters used in the analyses for each site.

Material	Parameter	Unit	Value					
			West Hackberry	Cavern Shape	Big Hill	Bayou Choctaw	Bryan Mound	Modified West Hackberry
Salt Dome	Elastic modulus (E)	GPa	31	31	31	31	31	31
	Density (ρ)	kg/m^3	2300	2300	2300	2300	2300	2300
	Poisson's ratio (ν)	-	0.25	0.25	0.25	0.25	0.25	0.25
	Elastic modulus reduction factor (RF)	-	12.5	12.5	12.5	12.5	12.5	12.5
	Bulk modulus (K)	GPa	1.65	1.65	1.65	1.65	1.65	1.65
	Shear modulus (μ)	GPa	0.992	0.992	0.992	0.992	0.992	0.992
	Stress exponent (n)	-	4.9	4.9	4.9	4.9	5.0	5.0
	Secondary creep constant (A_{SC})	s^{-1}	1.245E15	2.571E14	2.571E14	1.994E13	2.994E12† / 2.167E13‡	4.532E13
	Power law creep constant (A)	Pa^{-n}/s	4.34E-35	8.96E-36	8.96E-36	6.95E-37	1.02E-38† / 7.39E-38‡	1.55E-37
	Structure multiplication factor (SMF)	-	7.5	1.5	1.5	0.12	1.8† / 13.0‡	4.0
	Activation energy (Q)	cal/mol	12000	12000	12000	12000	10000	10000
	Universal gas constant (R)	cal/(mol·K)	1.987	1.987	1.987	1.987	1.987	1.987
	Input thermal constant (Q/R)	K	6034	6034	6034	6034	5033	5033
Overburden	Elastic modulus (E)	GPa	0.1	0.1	0.1	0.1	0.1	0.1
	Density (ρ)	kg/m^3	1874	1874	1874	1874	1874	1874
	Poisson's ratio (ν)	-	0.33	0.33	0.33	0.33	0.33	0.33
Caprock	Elastic modulus (E)	GPa	7.0	7.0	21	15.7	7.0	7.0
	Density (ρ)	kg/m^3	2500	2500	2500	2319	2500	2500
	Poisson's ratio (ν)	-	0.29	0.29	0.29	0.288	0.29	0.29
Caprock (Anhydrite)	Elastic modulus (E)	GPa	N/A	75.1	75.1	N/A	N/A	N/A
	Density (ρ)	kg/m^3	N/A	2300	2300	N/A	N/A	N/A
	Poisson's ratio (ν)	-	N/A	0.35	0.35	N/A	N/A	N/A
	Bulk modulus (K)	GPa	N/A	83.4	83.4	N/A	N/A	N/A
	Shear modulus (μ)	GPa	N/A	27.8	27.8	N/A	N/A	N/A
	A_0*	-	N/A	2338	2338	N/A	N/A	N/A
	A_1*	-	N/A	2.338	2.338	N/A	N/A	N/A
	A_2*	-	N/A	0	0	N/A	N/A	N/A
Surrounding rock	Elastic modulus (E)	GPa	N/A	N/A	70	35	7.33	7.33
	Density (ρ)	kg/m^3	N/A	N/A	2500	2500	2140	2140
	Poisson's ratio (ν)	-	N/A	N/A	0.33	0.33	0.33	0.33
Related figure			Figure 4	Figure 6	Figure 7	Figure 8	Figure 9	Figure 10
References			Ehgartner and Sobolik, 2002	Sobolik and Ehgartner, 2006	Park and Ehgartner, 2005	Park and Ehgartner, 2006	Sobolik and Ehgartner, 2009b	Sobolik and Ehgartner, 2009a

†: 'Hard' salt
‡: 'Soft' salt in Bryan Mound
*: material constant for Soil and Foams model in JAS3D which is a Sandia National Laboratories 3-D FEM internal software package.

3.1. Wedge Symmetry Plane Model for West Hackberry

The caverns are approximately 2500 ft deep to the roof, stand approximately 2000 ft high, and are nominally 200 ft in diameter. The caverns are spaced at approximately 750 ft apart. The WH field contains 22 SPR caverns and a number of smaller industrial caverns. The finite element model used for this study includes stratigraphy with a 4900 ft height salt dome, a 400 ft thick caprock, and 1000 ft thick of overburden as listed in Table 2. Since the caverns are located in the central portion of the dome, symmetry planes can be used in the model. The model simulates 19 caverns in a systematic pattern with equal spacing and uniform cavern size and geometry.

The 19-cavern, 18-drawdown leach model was constructed as shown Figure 4. The material properties for the model are listed in Table 3. The pressure condition applied to the cavern was based on a wellhead pressure of 975 psi, which is considered typical for WH caverns operating at normal pressure, and assumed caverns that are full of oil (a pressure gradient of 0.37 psi/ft of depth). In these analyses, a constant pressure is applied over time and pressure drops are periodically included to simulate times when caverns are operated at lower than normal pressures and during workover conditions (0 psi wellhead). Workover pressures were applied every 5 years for a duration of 3 months in each cavern.

The analysis simulated caverns that were leached to full size over a one year period, filled with petroleum, and then permitted to creep for 20 years to approximate the current age of the caverns. At 20 years and subsequently every five years, the caverns were instantaneously leached by deleting elements along the wall of the caverns to produce an increased volume of 15% for each leach. The drawdown leach was assumed to occur uniformly along the entire height of the cavern and not permitted in the floor or roof. Actual cavern dimensions will vary from the idealized geometries presented in Table 4. Workover conditions can only be approximated in the calculations.

The schedule for oil withdrawals (drawdowns) is based on dividing the cavern array into "cavern rings" of constant radius, where the numbered caverns shown in the 30º wedge section of Figure 5 each represent the several caverns of the ring. The solution results for the representative cavern are identical for all of the caverns in the given ring. Thus, Cavern Ring 1 (which is a degenerate ring) represents one cavern; Cavern Ring 2 represents six caverns, as does Cavern Ring 3 and Cavern Ring 4. One year after the initial point, i.e., at 21 years, Cavern Ring 1 undergoes a drawdown, with subsequent drawdowns every five years thereafter until 18 drawdowns have occurred. Caverns in Ring 2 start the schedule sequence two years after the initial point with subsequent drawdowns every five years. Cavern Rings 3 and 4 start the schedule sequence at three and four years after the initial point, respectively. The details of the analysis are provided by Ehgartner and Sobolik [2002].

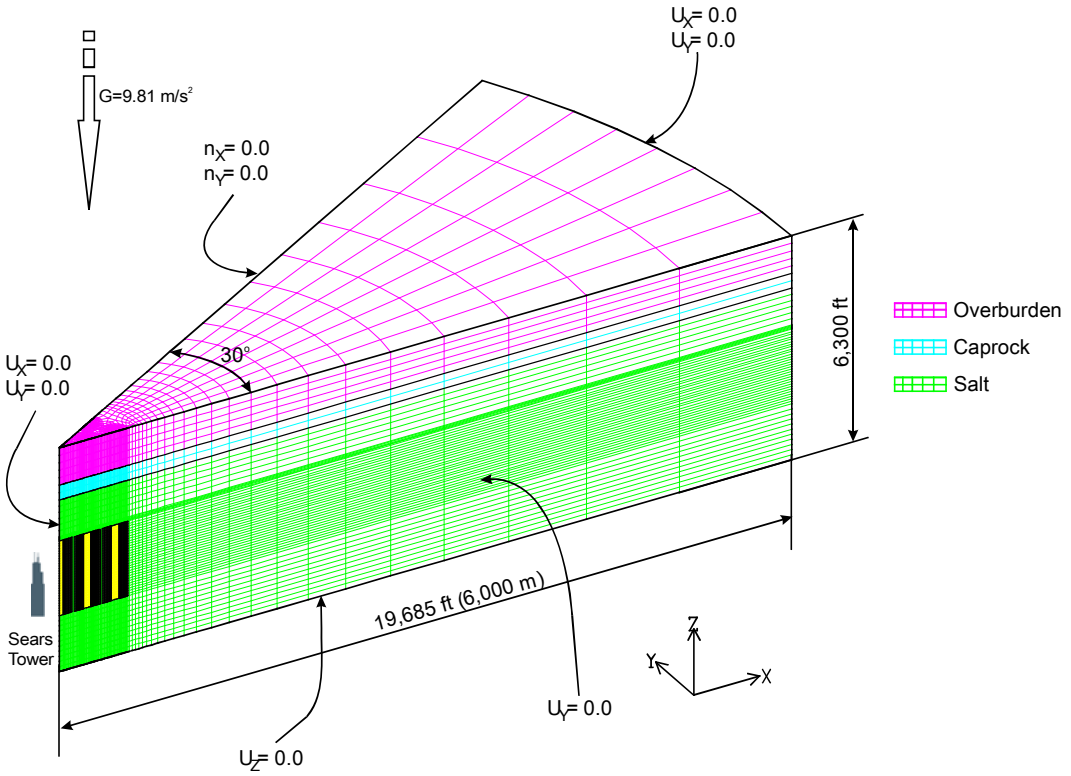

Figure 4: Wedge symmetry plane mesh for 19-cavern and 18-drawdown model showing the stratigraphy at West Hackberry and boundary conditions [Ehgartner and Sobolik, 2002].

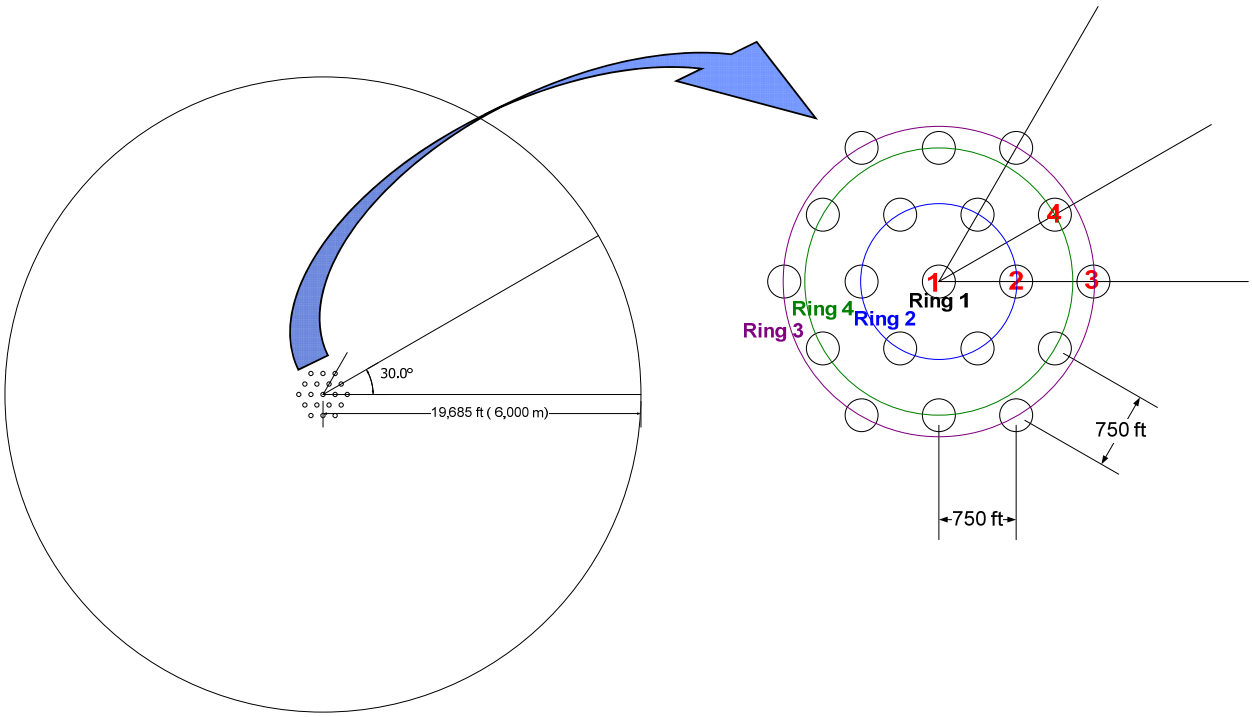

Figure 5: The layout of 19 cavern model in West Hackberry salt dome. Cavern numbering in red.

3.2. Wedge Symmetry Plane Model for Cavern Shape Study

The caverns are 2300 ft deep to the roof and stand approximately 2000 ft high. The caverns are spaced at 750 ft apart. The finite element model used for this study includes stratigraphy with a 4400 ft height salt dome, a 900 ft thick caprock, 400 ft thick caprock 2 and 300 ft thick of overburden as listed in Table 2. The material properties for the lithologies are listed in Table 3. The model simulates 19 caverns in a systematic pattern with equal spacing and uniform cavern size and geometry as shown in Figure 6.

The analytical model to investigate the cavern shape effect is similar to that used in Section 3.1. The analysis simulates caverns that were leached to full size over a one year period, filled with oil, and then permitted to creep for an additional 45 years. No additional leaching, and hence cavern growth, occurs after 1 year. This will allow the impact of initially small P/Ds to be compared to similar ratios that were obtained through time due to oil withdrawals found in the other wedge models where cylindrical caverns were simulated. The standard pressure condition applied to the cavern was based on an average wellhead pressure of 945 psi. This constant pressure is applied except for planned workover periods, during which the wellhead pressure is dropped to 0 psi. These workover periods are designed to last for three months, and to occur once every 5 years. These durations of the simulated workover may be slightly longer than are typically encountered in the field, but are chosen to provide an adverse condition and closely simulate actual subsidence measurements. Details of the model description are provided by Sobolik and Ehgartner [2006].

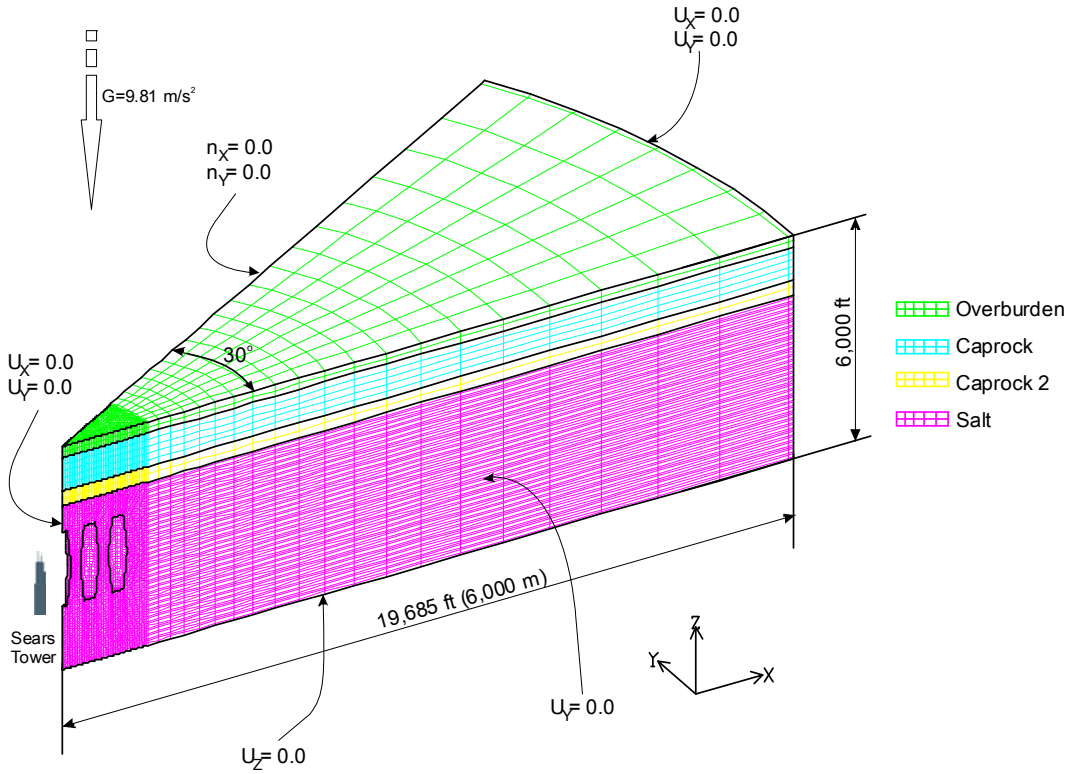

Figure 6: Wedge symmetry plane mesh for the enlarged middle cavern model showing the stratigraphy and boundary conditions [Sobolik and Ehgartner, 2006].

3.3. Wedge Symmetry Plane Model for Big Hill

The wedge symmetry model for BH is similar to the WH model as mentioned in Section 3.1. To investigate the P/D effect, the 19-cavern, 15-drawdown leach model was constructed as shown Figure 7. Two layers of caprock exist over the BH salt dome rather than one layer of caprock over the WH salt dome. The upper caprock, consisting of gypsum and limestone, is 900 ft thick. The lower caprock, consisting of anhydrite, is 400 ft thick. The top layer of overburden, which consists of sand and soil, has a thickness of 300 ft. The salt dome height is 1890 ft and the depth of the roof of cavern is 2286 ft as listed in Table 2. The material properties for each layer are listed in Table 3. The salt thickness over the caverns is 686 ft. The salt dome and caprock layers are surrounded by rock (sandstone) as shown Figure 7. Modeling of the leaching process of the caverns was accomplished by deleting elements along the walls of the caverns so that the volume increased by 16 percent for each leach rather than 15 percent used in WH modeling. The exact volume increase depends on the insoluble content of salt. The pressure condition applied to the cavern was based on an average wellhead pressure of 905 psi, and workovers were simulated as per other wedge models. The drawdown leach procedure is similar to that for WH model as described in Section 3.1 except 15 drawdowns rather than 18 drawdowns ware simulated. Details of the model description are provided in Park, et al. [2005].

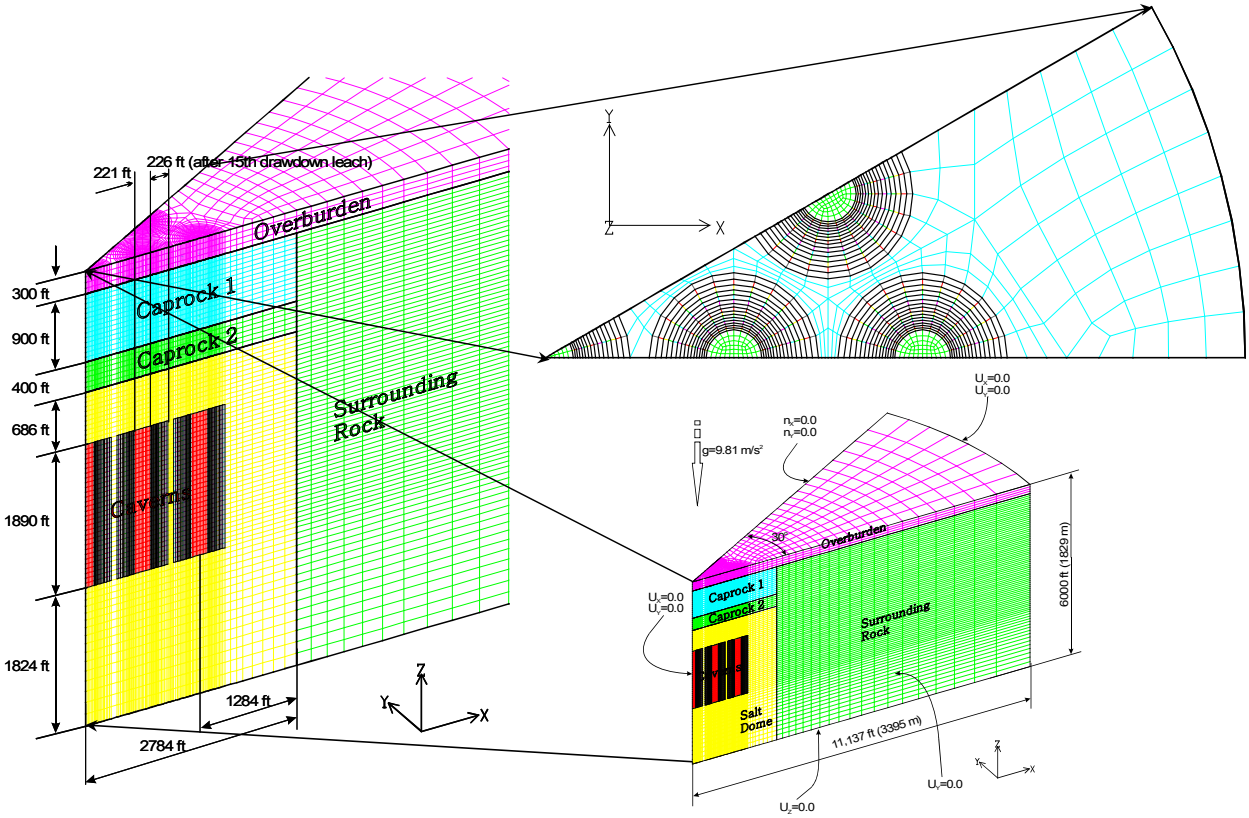

Figure 7: Wedge symmetry plane mesh for 19-cavern and 15-drawdown model showing the stratigraphy at Big Hill and boundary conditions.

3.4. Salt Dome Model for Bayou Choctaw

The 3D mesh allowing control of each cavern individually was constructed as shown Figure 8 because the location and depth of caverns at the BC site are irregular. Fifteen active and nine abandoned caverns exist at BC, producing a total cavern volume of some 164 million barrels (MMB). This includes 81 MMB in six SPR caverns, 31 MMB in nine Union Texas Petroleum (UTP) caverns, and about 52 MMB in abandoned caverns. The top layer of overburden, which consists of sand, silts and clays, has a thickness of 500 ft. The caprock, consisting of gypsum, anhydrite, and sand, is 150 ft thick as listed in Table 2. The material properties for each layer are listed in Table 3. The bottom of the deepest cavern (Cavern 25) is at a depth of 5790 ft. The depth of the salt dome bottom is 8,000 ft below the surface in the model. All SPR caverns are located below 2,000 ft. Cavern 20 is closest to the dome edge. The structural integrity of the web between Cavern 20 and the edge was checked in this simulation. The elevation of Cavern 20 is approximately 4,000 ft below the surface.

The analysis simulates caverns that were leached to full size over a one year period by means of gradually switching from salt to fresh water in the caverns. It was assumed that the SPR caverns were filled with petroleum and non-SPR caverns were filled with brine at year one, and then permitted to creep for twenty years. Subsequently, every 5 years after twenty-one years, the SPR caverns were instantaneously leached. Modeling of the leaching process of the caverns was accomplished by deleting elements along the walls of the caverns so that the volume increased by 15% with each leach. However, leaching is not permitted in the floor or roof of the caverns. The 5-year period between each drawdown allows the stress state in the salt to return to a steady-state condition. The simulation executed up to the 5th leach to investigate the structural behavior of the dome for 46 years.

The pressure conditions applied to the caverns were based on an average wellhead pressures. Cavern 15 operates over a range of pressures from 815 to 990 psi under normal conditions. The pressure starts at 815 psi, then, due to creep and thermal expansion of fluids, the pressure gradually rises to 990 psi. At that time the brine is removed from the cavern to reduce the pressure to 815 psi. Thus, on average, a pressure of 903 psi is used for the Cavern 15 wellhead pressure operating under normal conditions. In the same manner, the pressures of 903, 715, 925, 850, and 913 psi are used for the normal operating wellhead pressures of Cavern 17, 18, 19, 20, and 101, respectively.

Caverns 15 and 17 are operated as a gallery maintaining equal pressures at all times including the workover periods, because the two caverns are close to each other as shown Figure 27 (left). For workover conditions, zero wellhead pressure is used for all SPR caverns. The workovers on Caverns 15 and 17 are performed one year after switching from brine to petroleum. Cavern 19 is worked over 1 month after the workover of Caverns 15 and 17 have been completed. The workover of Cavern 18 starts as soon as the workover of Cavern 19 has been completed. Then, Cavern 20 is worked over 2.5 years later. Finally, Cavern 101 is worked over as soon as the workover of Cavern 20 has been completed. As in the other analyses, this workover cycle is repeated every 5 years, and the workover durations are 3 months for all caverns. For both normal and workover conditions, the caverns are assumed to be full of oil with a pressure gradient of 0.37 psi/ft of depth. The details of the simulation are provided by Park et al. [2006].

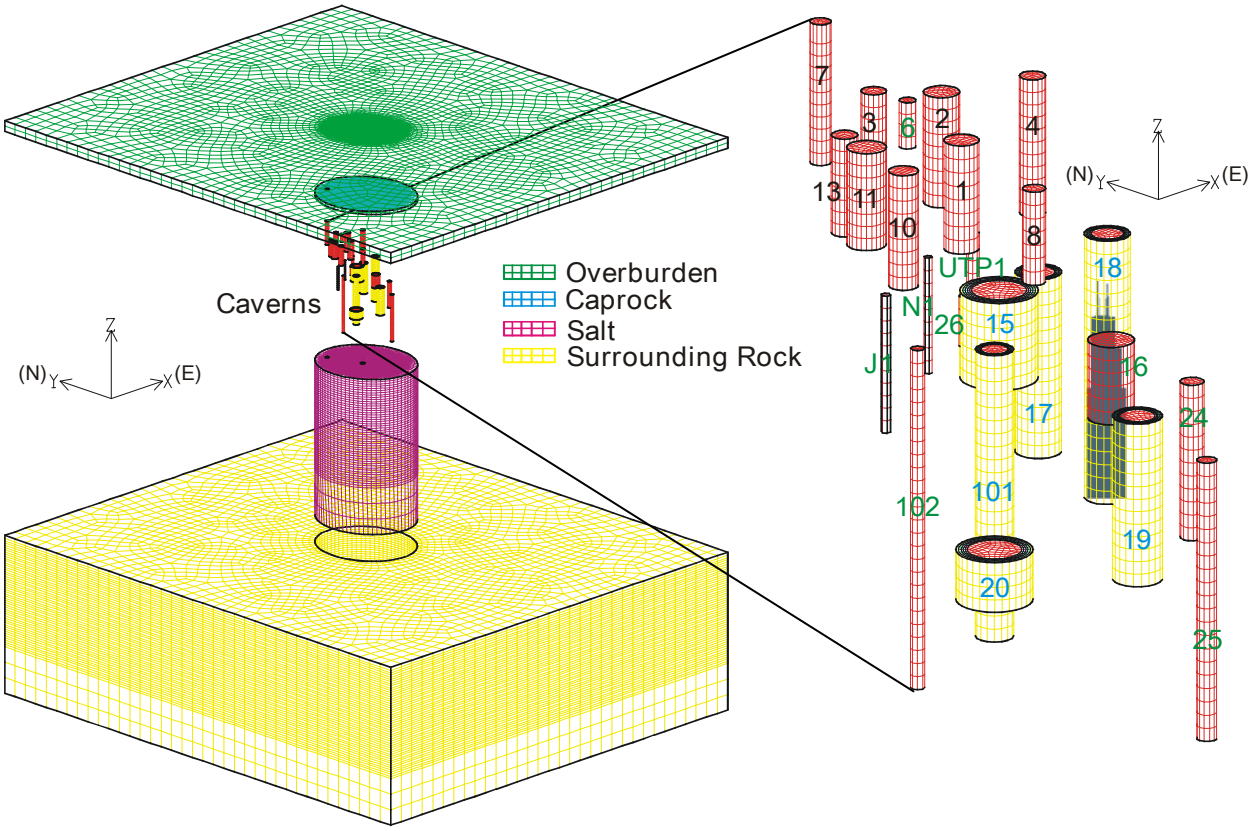

Figure 8: Overview of the finite element mesh showing the stratigraphy and cavern field at Bayou Choctaw and the cavern geometry within the salt [Park et al., 2006].

3.5. Salt Dome Model for Bryan Mound

Five material blocks are used in the model as shown Figure 9 to describe the stratigraphy layers: the overburden, caprock, soft salt dome, hard salt dome and the rock layers surrounding the salt dome. The overburden is made of sand, and the caprock layer is made of gypsum or limestone. The rock layers surrounding the salt dome comprise several layers of sandstone and shale; they have been modeled as one large layer of sandstone due to the minimal deviation in densities and rock mass moduli throughout those layers. The overburden and caprock thicknesses are reasonably constant over the entire salt dome, so for meshing purposes they have been given constant values; the overburden layer is 760 feet thick, and the caprock is 280 feet thick as listed in Table 2. The material properties for the blocks are listed in Table 3.

The analysis simulates the caverns that were leached to full size over time and filled with brine until 1981 and then filled with oil. The analysis also simulates the leaching of the post-1981 caverns and subsequent filling with oil. In general, these caverns have been maintained at constant operating pressures except during workovers. The standard pressure condition applied to the cavern is based on an average wellhead pressure ranging between 900 and 975 psi. Beginning in the simulation year 1984, a series of five-year cycles of cavern workovers was initiated. During the five year cycle, every cavern is scheduled for a workover. During the workover, the affected cavern is held at 0 psi wellhead pressure for three months. The pressures

for all caverns are at normal operating pressure for the fourth month (so that the workover rig can be moved to a new well) and then the workover of the next scheduled well begins.

After 2008, the simulation incorporates an additional feature. Each of the caverns is expected to experience five leaching operations to grow the cavern, with a volume growth of approximately 15% for each leach. (There are some exceptions to this: cavern 5 is not further developed due to its unwieldy shape; caverns 1 and 2 are leached only four times due to potential interference with other caverns; and cavern 113 is increased by 10% for each leach, also due to potential interference issues.) The leaching operations are simulated to begin in September 2008, which is the final four-month window in that particular five-year workover cycle. This is repeated in 2013, 2018, 2023, and 2028, and the calculation then performs one more workover for each cavern through 2033. Caverns 101-116 and 4 were meshed as axisymmetric caverns, using the average radius as a function of elevation based on sonar measurement data. Because of their highly non-cylindrical and asymmetric geometries, the 16 meshes for caverns 1, 2, and 5 were created from extrusions based on a representative shape derived from the sonar data. Details of the simulation are provided in Sobolik and Ehgartner [2009 b].

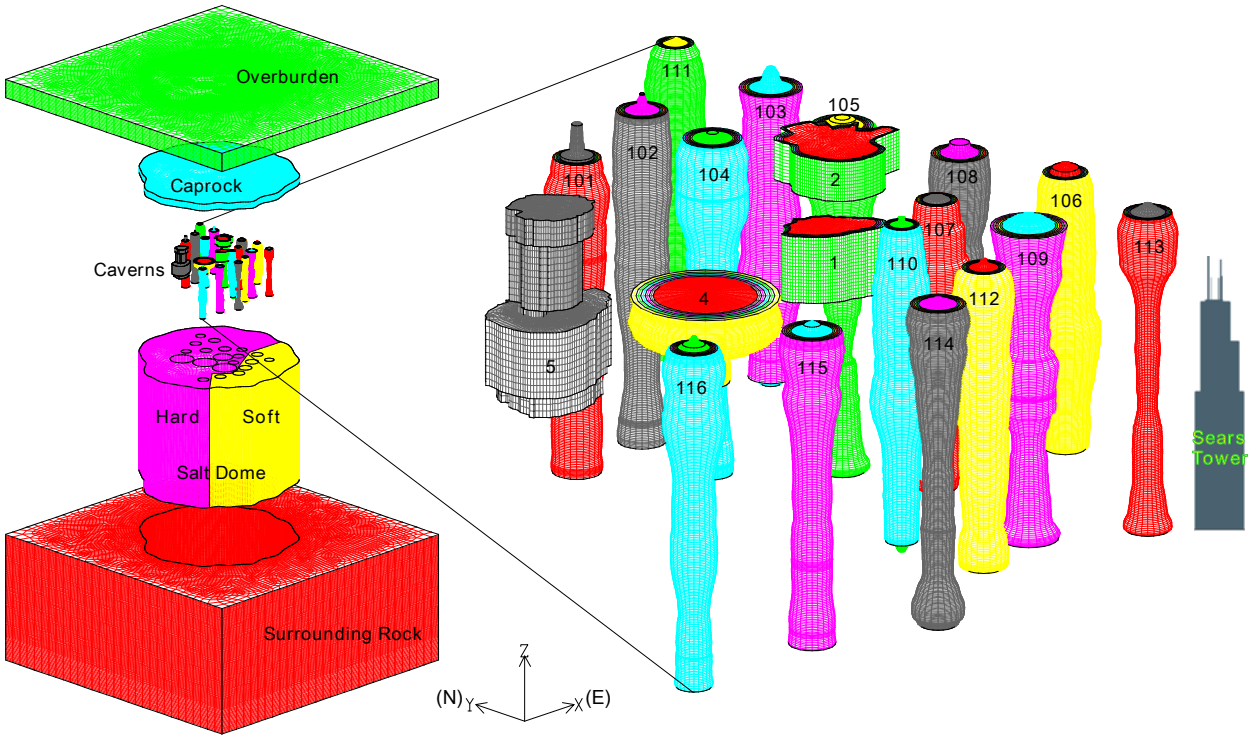

Figure 9: Computational mesh showing the stratigraphy and cavern field at Bryan Mound and the cavern geometry within the salt dome (derived from the model constructed by Sobolik and Ehgartner [2009 b]).

3.6. Half of Salt Dome Model for West Hackberry

Four material blocks are used in the model as shown Figure 10 to describe the stratigraphy layers: the overburden, caprock, salt dome and sandstone surrounding the salt dome. The overburden is made of sand, and the caprock layer is made of gypsum or limestone. The caprock closely matches that used for Big Hill [Park et al., 2005], and it is thought to be reasonably accurate for the other SPR sites. The overburden layer is 1600 feet thick, the caprock 400 feet thick, the salt dome 4000 ft height, and the surrounding rock 4400 ft thick as listed in Table 2. The material properties for the blocks used in the analysis are listed in Table 3.

At the West Hackberry site, the five caverns known as Phase 1 – Caverns 6, 7, 8, 9, and 11 – were created as early as 1946 and were used for brining and storage before the SPR took ownership of them in 1981. After that time, seventeen other storage caverns were created over an eight-year period. Six of these post-1981 caverns (110, 109, 103, 101, 105, and 117) are arranged in a nearly linear fashion, allowing for the use of a vertical symmetry plane through them. The post-1981 caverns were typically constructed on 750-feet center-to-center spacing. A seventh cavern, 108, is also included in the computational field, for a total of all five Phase 1 and seven post-1981 caverns.

The analysis simulates the Phase 1 caverns that were leached to full size over some period of time and filled with brine until 1981 and then filled with oil. The analysis also simulates the leaching of the post-1981 caverns and subsequent filling with oil. In general, these caverns have been maintained at constant operating pressures except during workovers. The standard pressure condition applied to the cavern is based on an average wellhead pressure ranging between 900 and 975 psi.

Beginning in 1984, a series of five-year cycles of cavern workovers was initiated. During the five year cycle, every cavern is scheduled for a workover. During the workover, the affected cavern is held at 0 psi wellhead pressure for three months. The pressures for all caverns are then at normal operating pressure for the fourth month (so that the workover rig can be moved to a new well), and then the workover of the next scheduled well begins. Previous analyses have shown that the abrupt pressure drop during the workover will induce the greatest potential for damage. The duration of the simulated workover may be slightly longer than is typically encountered in the field, but is chosen to provide an adverse condition and closely simulate actual subsidence measurements, which reflect periods of low to intermediate operating pressures associated with fluid transfers.

After 2008, the simulation incorporates an additional feature. Each of the caverns (except 103) is expected to experience ten leaching operations to grow the cavern, with a volume growth of approximately 15% for each leach. The leaching operations are simulated to begin in September 2008, which is the final four-month window in that particular five-year workover cycle. This is repeated in 2013, 2018, 2023, 2028, 2033, 2038, 2043, 2048, and 2053. Caverns 6, 8, and 9 have significant potential interference issues which must be addressed in operational planning; this analysis has made assumptions about how those caverns will be enlarged. Details of the simulation are provided in Sobolik and Ehgartner [2009 a].

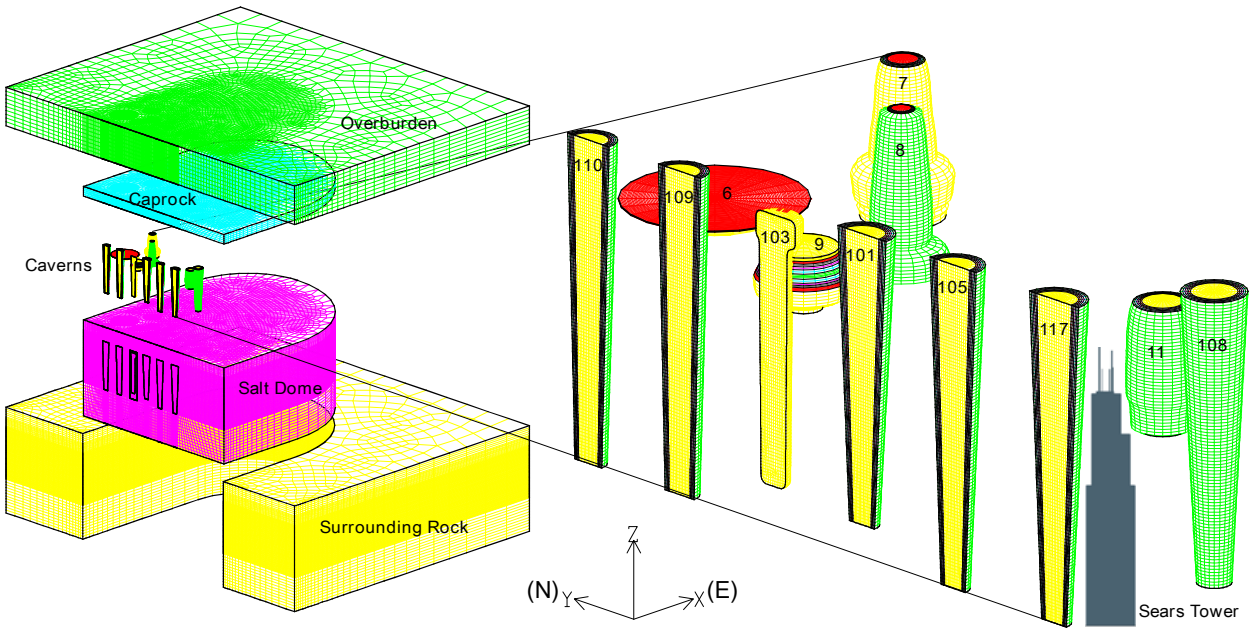

Figure 10: Computational mesh showing the stratigraphy and cavern field at West Hackberry and the cavern geometry within the salt dome (derived from the model constructed by Sobolik and Ehgartner [2009 a]).

4. RESULTS

4.1. Wedge Symmetry Plane Model for West Hackberry

To investigate the P/D effect, the EXODUS output, which was obtained from the 3-D finite element analysis using the wedge symmetry plane model for WH [Ehgartner and Sobolik, 2002], was post-processed using the algebra scripts in Appendix III.

Figure 11 shows the zoomed computational mesh around the caverns (the entire mesh is shown Figure 4). The diameter of caverns increases from 200 ft to 704 ft in 7.24% increments with each of 18 drawdown leaches. The pillar thickness between the caverns decreases from 550 ft to 46 ft with drawdown leaches.

Figure 12 shows the minimum safety factor for dilatancy as a function of standard P/D calculated with three dilation criteria. Note that the caverns in the numerical analyses model for WH were simplified to the cylinder shapes using the volume conserving cylinders. Therefore, "Standard P/D" only was calculated to identify the relationship between P/D and the safety factor for dilatancy. The standard and minimum P/Ds are equivalent for cylindrical geometries. When the Van Sambeek criterion with C=0.18 and RD criteria for the Cayuta and Big Hill salt are applied to the dilatancy calculation, the onsets of dilatant damage are predicted at the P/D values of 0.55, 0.20, and 0.37, respectively. The value of safety factor decreases remarkably after the 11th, 12th, and 15th drawdown leach when the Van Sambeek criterion with C=0.18, the RD criterion for the Cayuta salt and the Big Hill salt are applied, respectively. The Van Sambeek criterion with C=0.18 yields the largest critical P/D value for the onsets of damage. Therefore, this criterion should be applied to calculate the limit of the P/D in this WH model. The "P/D limit" is defined as the P/D when the safety factor equals 1.0.

Figure 13 shows the predicted minimum safety factor history for dilatancy using the Van Sambeek criterion with C=0.18. The analysis has shown that each abrupt pressure drop (downward peaks) due to the workover will induce large damage potentials. Dilatant damage is predicted to occur during workover of Cavern 2 (second peak) after the 13th drawdown leach ($SF_{VS} < 1$). At that time the diameter of the caverns is 496 ft and the pillar thickness is 254 ft, i.e. P/D is calculated to be 0.51 (see Table 4). The onsets of dilatant damage may occur when the P/D value is between 0.62 and 0.51, i.e. when the P/D value is 0.55 as shown in Figure 12.

Figure 14 shows the minimum safety factor contours for dilatancy during workovers of Cavern 2 after the 13th (A), 14th (B), 15th (C), and 16th (D) drawdown leaches, respectively. The Van Sambeek criterion with C=0.18 is applied to the dilatancy calculation. The damage is predicted to occur at the roof of Cavern 4 after the 13th drawdown leach. The damage zone grows with the drawdown leaches.

Table 4: West Hackberry caverns drawdown leach properties, P/Ds, and predicted minimum safety factors for dilatancy in the salt dome.

Number of Drawdowns	Age of Cavern (year)	Cavern Volume (MMB)	Cavern Diameter (ft)	Pillar Thickness (ft)	P/D	Minimum Safety Factor		
						Van Sambeek C=0.18	RD for Cayuta salt	RD for Big Hill salt
initial	0	11.2	200	550	**2.75**	**1.467**	**1.528**	**1.661**
1	20	12.9	214	536	**2.50**	**1.529**	**1.571**	**1.618**
2	25	14.8	230	520	**2.26**	**1.536**	**1.560**	**1.629**
3	30	17.0	247	503	**2.04**	**1.533**	**1.503**	**1.579**
4	35	19.6	265	486	**1.84**	**1.530**	**1.490**	**1.570**
5	40	22.5	284	466	**1.64**	**1.528**	**1.475**	**1.558**
6	45	25.9	304	446	**1.47**	**1.523**	**1.457**	**1.544**
7	50	29.8	326	424	**1.30**	**1.504**	**1.431**	**1.522**
8	55	34.2	350	400	**1.14**	**1.476**	**1.411**	**1.505**
9	60	39.4	375	375	**1.00**	**1.459**	**1.410**	**1.513**
10	65	45.3	402	348	**0.86**	**1.431**	**1.387**	**1.495**
11	70	52.1	431	319	**0.74**	**1.262**	**1.383**	**1.499**
12	75	59.9	463	287	**0.62**	**1.089**	**1.304**	**1.509**
13	80	68.9	496	254	**0.51**	**0.950**	**1.203**	**1.490**
14	85	79.2	532	218	**0.41**	**0.787**	**1.066**	**1.432**
15	90	91.1	571	179	**0.31**	**0.602**	**0.909**	**1.292**
16	95	104.7	612	138	**0.23**	**0.407**	**0.722**	**1.113**
17	100	120.4	656	94	**0.14**	**0.064**	**0.364**	**0.785**
18	105	138.5	704	46	**0.07**	**0.003**	**0.231**	**0.538**

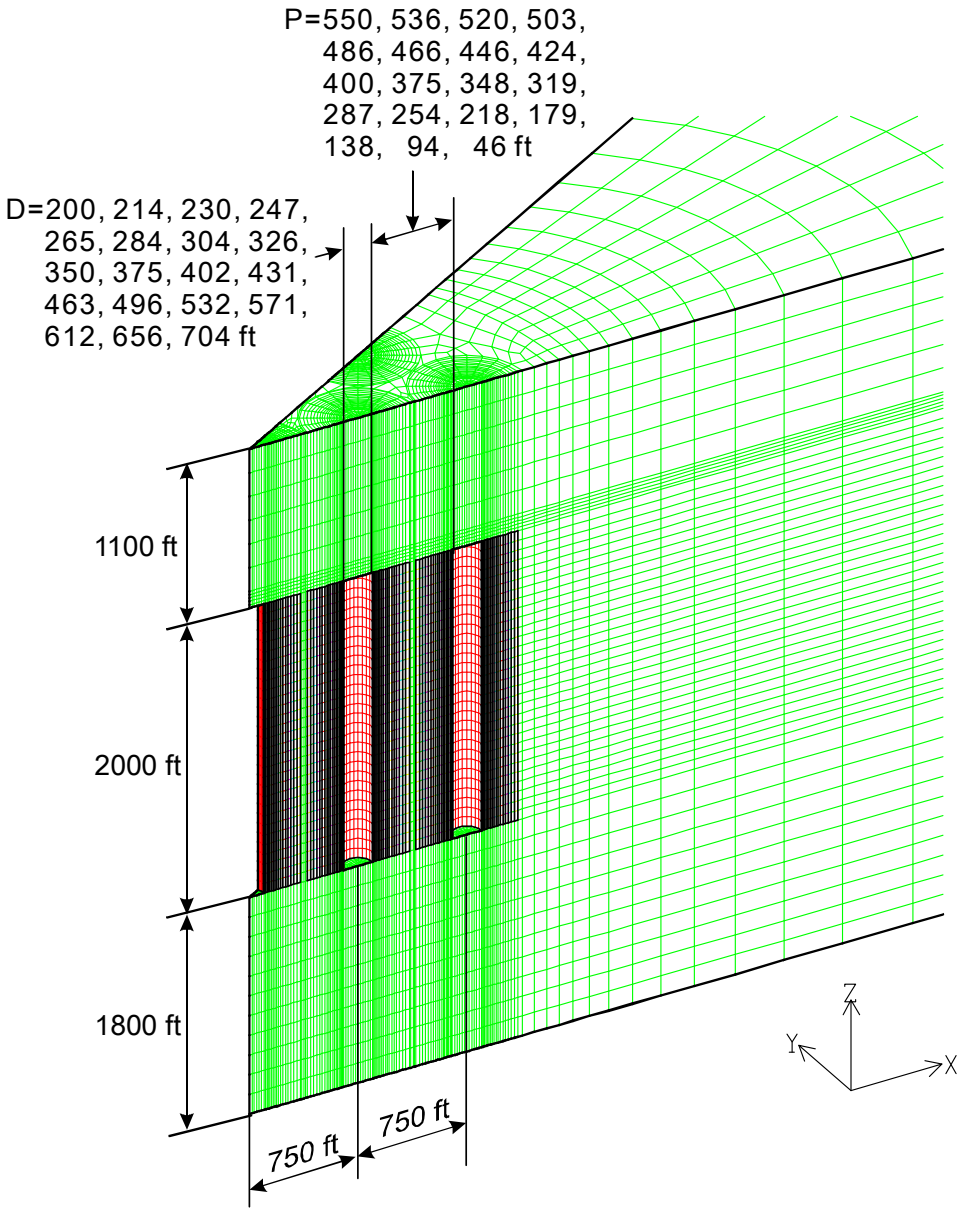

Figure 11: Salt dome mesh of the 19-cavern, 18-drawdown leaches model for the West Hackberry site. Since the cavern diameter (D) increases with each drawdown leach while the pillar size (P) decreases, a smaller P/D indicates more leaches have taken place.

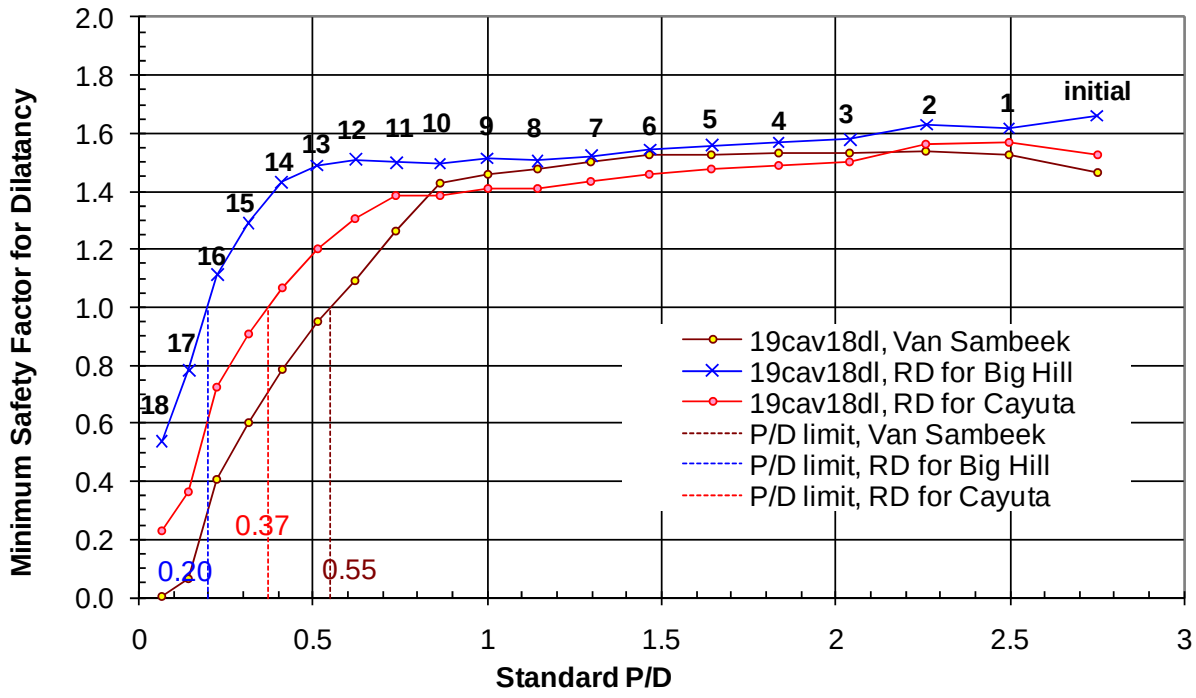

Figure 12: Minimum safety factor for dilatancy as a function of standard P/D. The numbers on the graph indicates the number of drawdown leaches

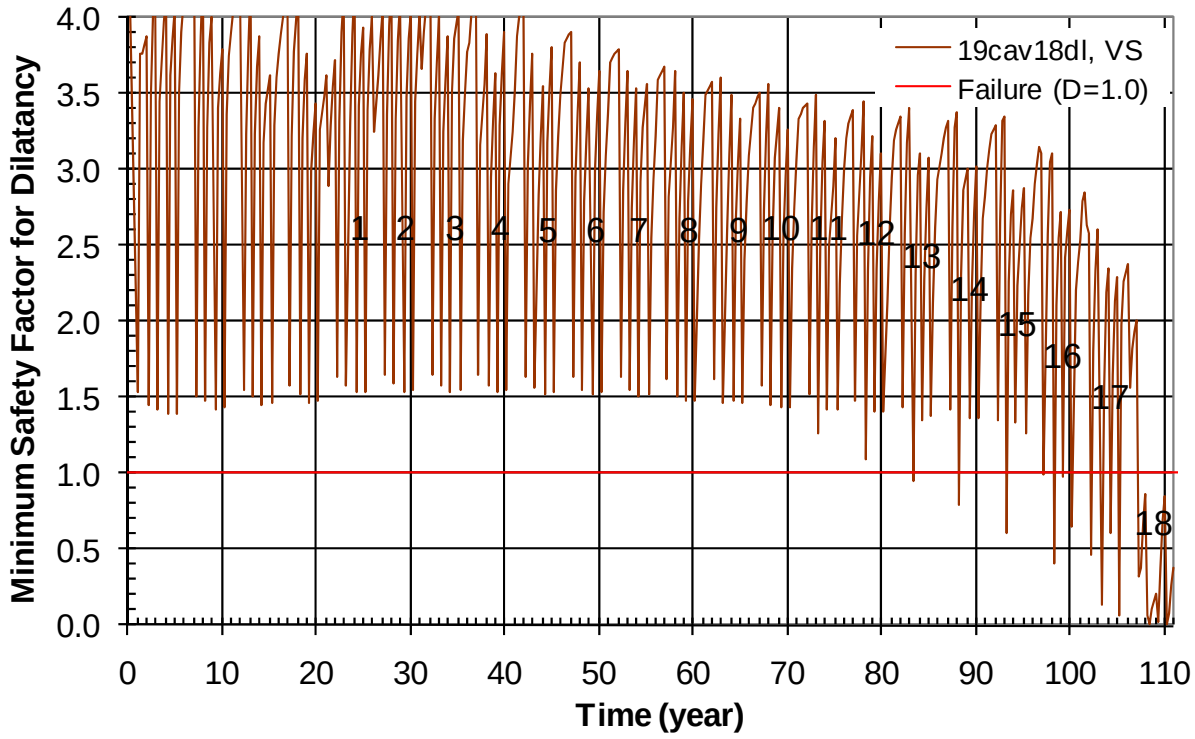

Figure 13: Predicted safety factor history for dilatancy using the Van Sambeek criterion with C=0.18. The numbers on the history line indicates the number of drawdown leaches.

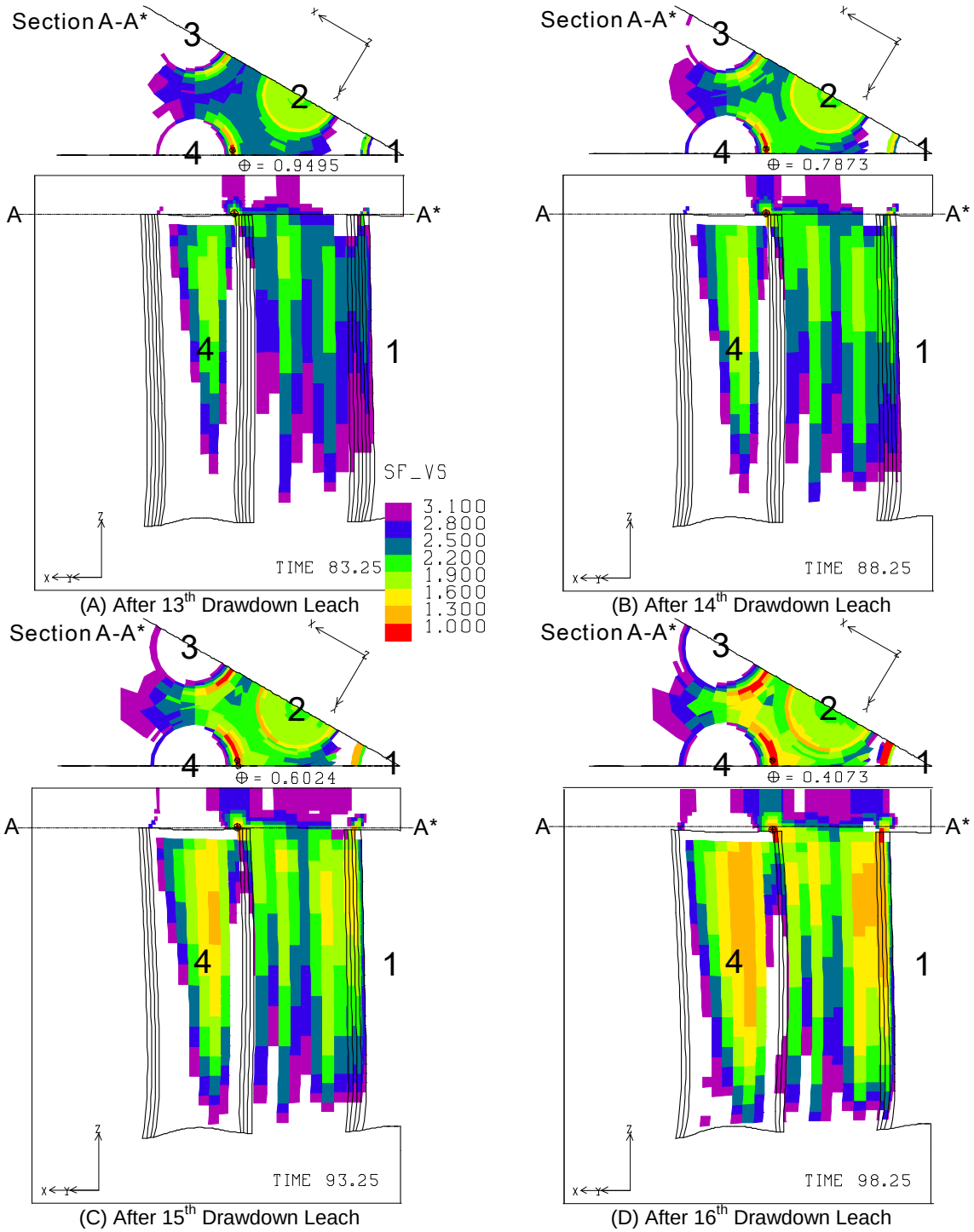

Figure 14: Predicted safety factor contours for dilatancy during workover when the minimum values occur after 13th (A), 14th (B), 15th (C), and 16th (D) drawdown leaches, respectively. Van Sambeek criterion with C=0.18 is used. The vertical cross-section through the centers of caverns and the horizon cross-section at the elevation where the minimum safety factor occurs. The lines A-A* show where the section was cut. Units of time are in years.

4.2. Wedge Symmetry Plane Model for Cavern Shapes

4.2.1. Cylindrical Cavern

Figure 15 (left) shows the computational mesh for the cylindrical caverns. The 19-cavern, 30-degree wedge symmetry planes format is applied to simplify modeling. The diameters of caverns range from 200 ft to 600 ft in 100 ft increments. The webs of salt between the caverns thus range from 550 ft to 150 ft in 100 ft increments. The heights of caverns are 2000 ft. The P/Ds are calculated using the diameters and the web thicknesses and are listed in Table 5. The geology and properties used in the shapes models are very similar to the Big Hill wedge model, however one very important difference exists. In the shape analyses, the cavern sizes do not change over time as oil drawdowns were not simulated. The corresponding values of minimum safety factor for dilatancy in the salt dome from post-processing the EXODUS output provided by Sobolik and Ehgartner [2006] are also listed.

Figure 15 (right) plots the minimum safety factor as a function of standard P/Ds. When the Van Sambeek criterion with C=0.18 is applied to the dilatancy calculation, the onset of dilatant damage is predicted at the standard P/Ds of 1.43. The minimum safety factor value decreases as the P/D value decreases.

Figure 16 shows the predicted safety factor contours for dilatancy during workover of Cavern 2 when the cavern diameters are 600 ft. The Van Sambeek criterion with C=0.18 is applied to calculate the contours. The dilatant damage is predicted to occur at the top of all caverns and middle of Cavern 4.

Table 5: P/D and minimum safety factor for dilatancy in the salt dome for the cylindrical caverns.

Radius (ft)			Standard P/D	Minimum Safety Factor		
At Bottom	At Middle	At Top		Van Sambeek C=0.18	RD for Big Hill salt	RD for Cayuta salt
100	100	100	**2.750**	**1.082**	**1.153**	**1.120**
150	150	150	**1.500**	**1.006**	**1.153**	**1.059**
200	200	200	**0.875**	**0.952**	**1.142**	**1.029**
250	250	250	**0.500**	**0.897**	**1.120**	**0.994**
300	300	300	**0.250**	**0.604**	**0.970**	**0.795**

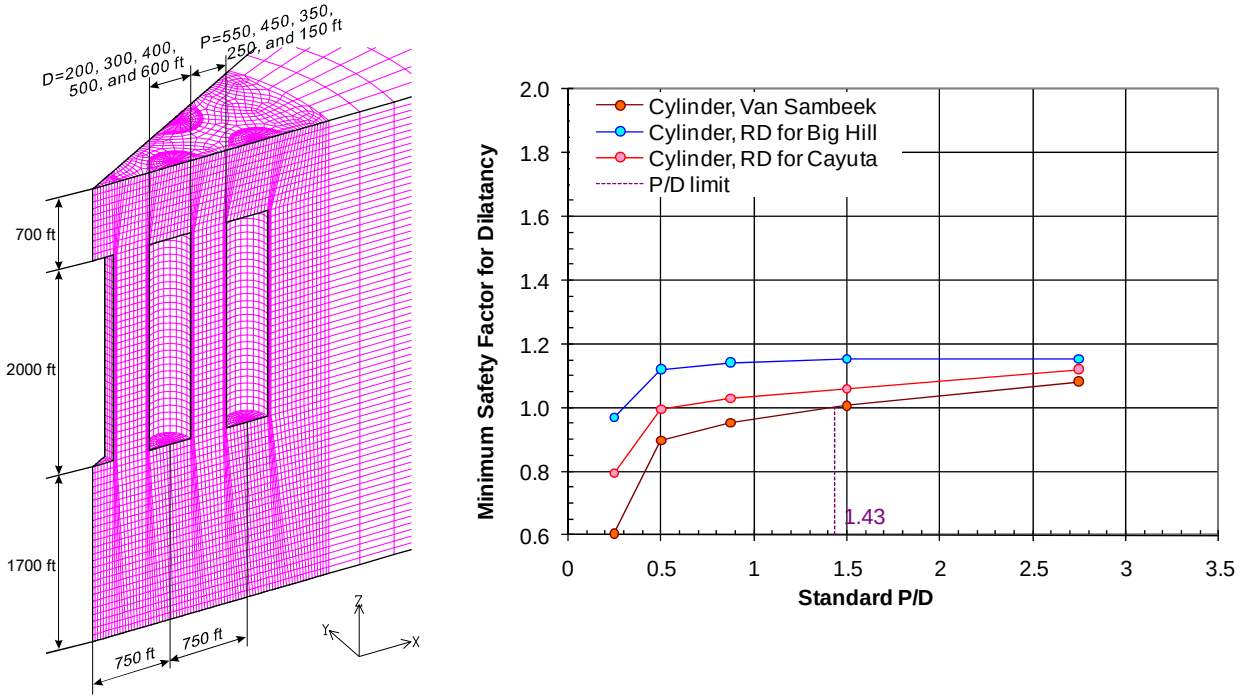

Figure 15: Salt dome mesh with the cylindrical caverns, and safety factor as a function of standard P/D.

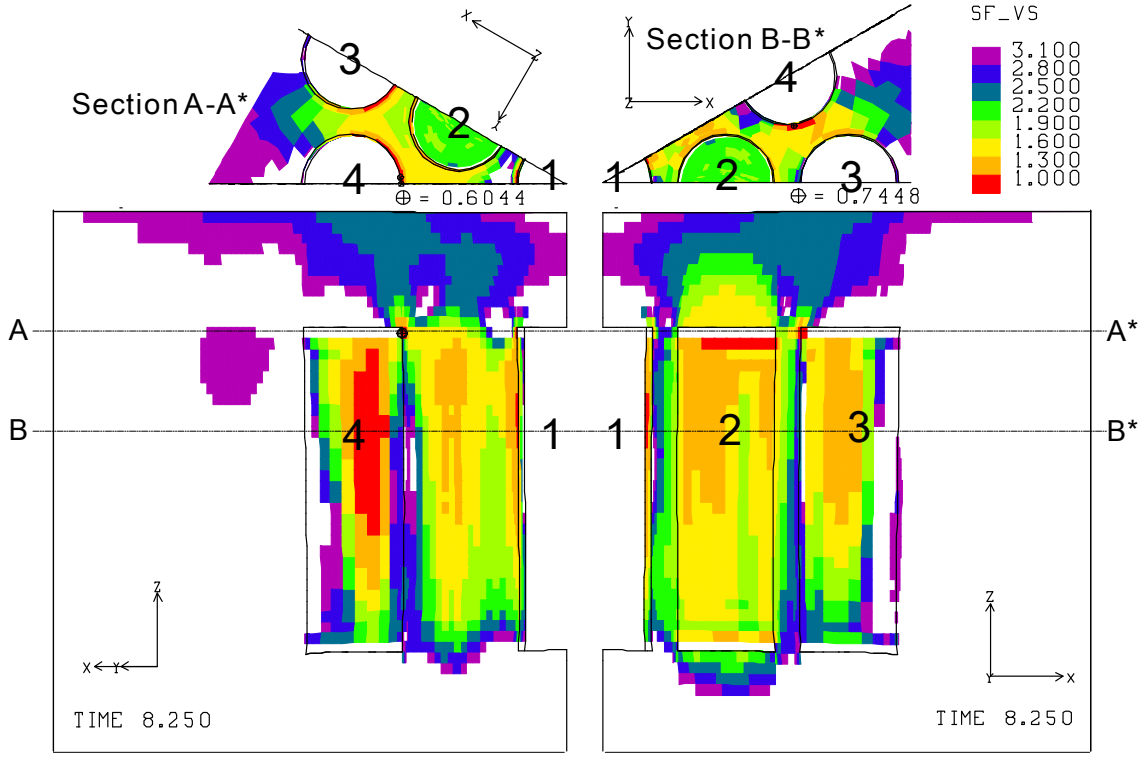

Figure 16: Predicted safety factor contours for dilatancy during workover of Cavern 2 when the minimum values occurs (cavern diameters are 600 ft). Van Sambeek criterion with C=0.18 is used. The vertical cross-section through the centers of caverns and the horizon cross-section at the section A-A* and B-B*. Dash-dot lines show where the section was cut. Time is in years.

4.2.2. Enlarged Bottom Cavern

The left side of Figure 17 shows the computational mesh for the enlarged bottom caverns which taper out towards their tops, the initial diameter at the top is 100 ft and at the bottom is 300 ft. During the simulation the diameters of caverns at the top range from 100 ft to 400 ft in 100 ft increments. The diameters of caverns at the bottom range from 300 ft to 600 ft in 100 ft increments. The webs of salt between the caverns are decreased from 650 ft to 350 ft in 100 ft increments at the cavern tops, and from 450 ft to 150 ft in 100 ft increments at the cavern bottoms. The height of caverns is 2000 ft. The P/Ds are calculated using the diameters and the web thicknesses and listed in Table 6. The corresponding values of minimum safety factor for dilatancy in the salt dome from post-processing the EXODUS output provided by Sobolik and Ehgartner [2006] are also listed.

The graphs on the right side of Figure 17 plot the minimum safety factor as a function of minimum and standard P/Ds, respectively. The onset of dilatant damage is predicted at 0.78 and 1.31 for minimum and standard P/Ds, respectively when the Van Sambeek criterion with C=0.18 is applied to the calculation.

The minimum value of safety factor occurs at the wall near the bottom of the Cavern 4 during workover when the bottom diameter is 600 ft as shown Figure 18.

Table 6: P/D and minimum safety factor for dilatancy in the salt dome for the enlarged bottom caverns.

Radius (ft)			P/D		Minimum Safety Factor		
At Bottom	At Middle	At Top	Minimum	Standard	Van Sambeek C=0.18	RD for Big Hill salt	RD for Cayuta salt
150	100	50	**1.500**	**2.603**	**1.063**	**1.129**	**1.107**
200	150	100	**0.875**	**1.455**	**1.021**	**1.144**	**1.088**
250	200	150	**0.500**	**0.856**	**0.936**	**1.126**	**1.043**
300	250	200	**0.250**	**0.490**	**0.869**	**1.055**	**1.020**

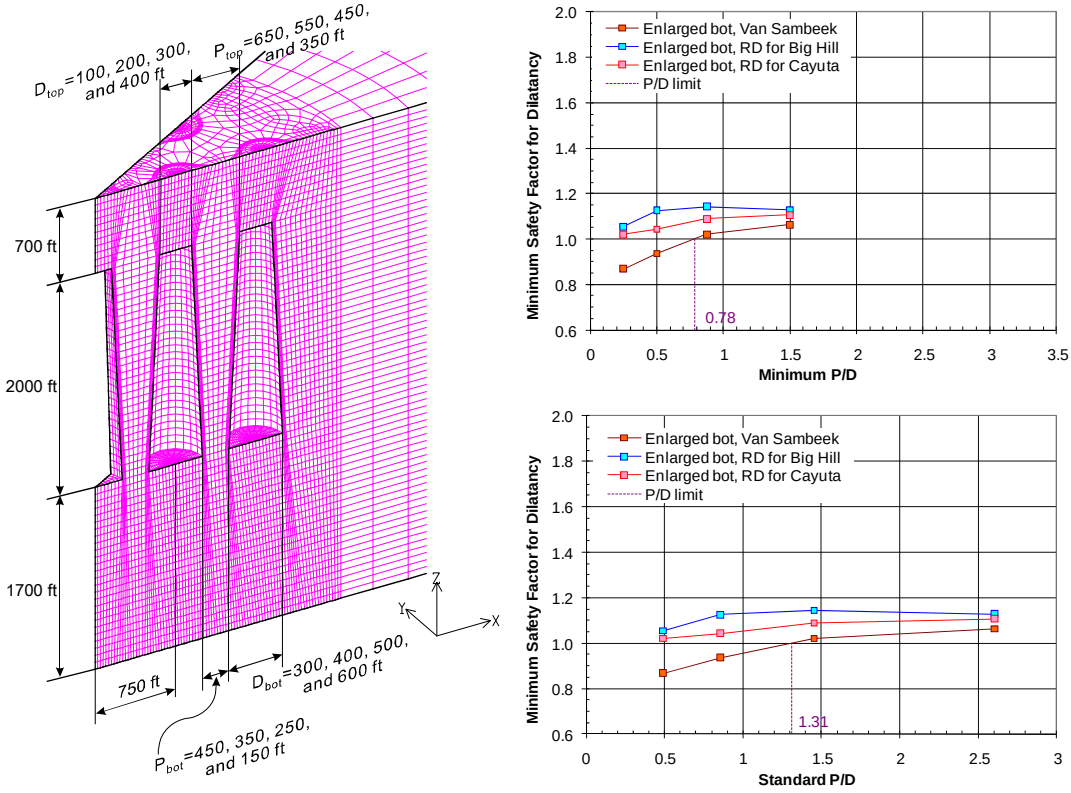

Figure 17: Computational mesh for the enlarged bottom caverns, and safety factor as a function of minimum and standard P/Ds.

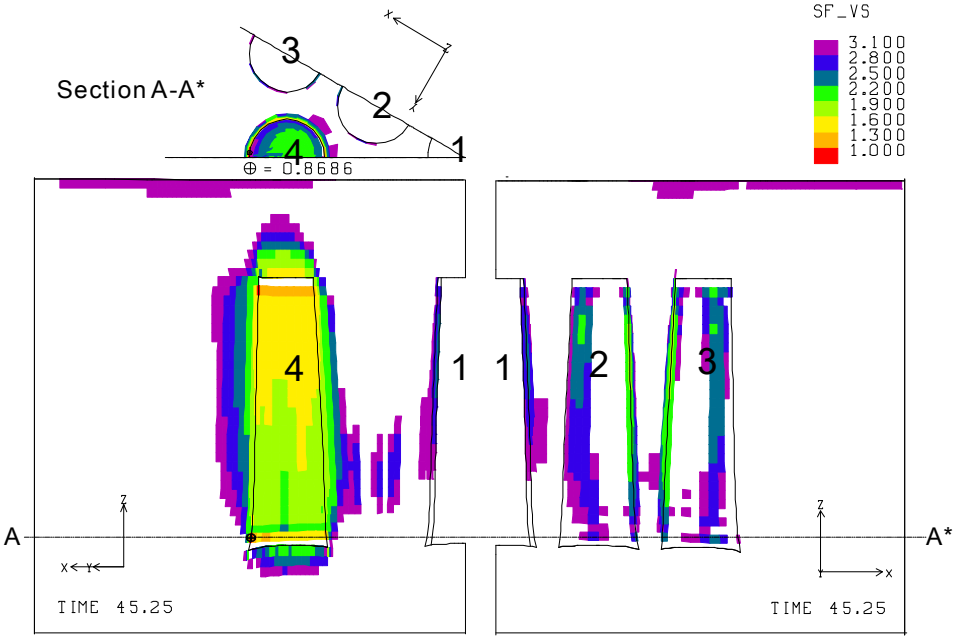

Figure 18: Predicted safety factor contours for dilatancy during workover of Cavern 4 when the minimum safety factor occurs (cavern diameters at bottom are 600 ft). The Van Sambeek criterion with C=0.18 is used. The vertical cross-section through the centers of caverns and the horizon cross-section at the elevation where the minimum safety factor occurs. Dash-dot lines show where the section was cut. Time is in years.

4.2.3. Enlarged Middle Cavern

Figure 19 (left) shows the computational mesh for the caverns which are enlarged in their middles. The caverns are initially 100 ft in diameter at the top, taper smoothly up to 300 ft in diameter at mid-height and then are tapered back down smoothly to 100 ft at their bottoms. The diameters of caverns at the top and bottom are increased from 100 ft to 400 ft in 100 ft increments. The diameter of caverns at the middle is increased from 300 ft to 600 ft in 100 ft increments. The web thicknesses of salt between the caverns are decreased from 650 ft to 350 ft in 100 ft increments at the cavern tops and bottoms, and from 450 ft to 150 ft in 100 ft increments at the caverns mid-heights. The heights of caverns are 2000 ft. The P/Ds are calculated using the diameters and the web thicknesses and are listed in Table 7. The corresponding values of minimum safety factor for dilatancy in the salt dome from post-processing the EXODUS output provided by Sobolik and Ehgartner [2006] are also listed in Table 7.

Figure 19 (right) plots the minimum safety factor as a function of minimum and standard P/Ds, respectively. The onset of dilatant damage is predicted at P/Ds of 0.43 and 0.75 for minimum and standard P/Ds, respectively, when the Van Sambeek criterion with C=0.18 is applied to the calculation. Damage is predicted to occur at smaller P/Ds than for the cylindrical and the enlarged bottom caverns case. In the case of the enlarged middle caverns, a shorter distance between caverns can be allowed than for the cylindrical and enlarged bottom caverns. In other words, the enlarged middle cavern is structurally safer than the cylindrical and enlarged bottom caverns.

The minimum value of safety factor occurs at the wall near the roof of Cavern 4 (Section A-A*) during workover when the middle diameter is 600 ft as shown Figure 20. Damage does not occur at the narrowest pillar (Section B-B*), i.e. the structural interaction between caverns at the Section B-B* is predicted to be safer than at the Section A-A*. In the case of cylindrical caverns, the minimum value occurs at the wall near the roof as shown Figure 16 because the pressure applied on the wall near the roof is smaller than that on the lower areas of the wall due to gravity effects. In a similar manner, the largest damage potential occurs near the roof rather than the pillar at the middle of the caverns.

Table 7: P/D and minimum safety factor for dilatancy in the salt dome for the enlarged middle caverns.

Radius (ft)			P/D		Minimum Safety Factor		
At Bottom	At Middle	At Top	Minimum	Standard	Van Sambeek C=0.18	RD for Big Hill salt	RD for Cayuta salt
50	150	50	**1.500**	**2.603**	**1.142**	**1.176**	**1.146**
100	200	100	**0.875**	**1.455**	**1.073**	**1.154**	**1.090**
150	250	150	**0.500**	**0.856**	**1.010**	**1.142**	**1.049**
200	300	200	**0.250**	**0.490**	**0.975**	**1.069**	**1.027**

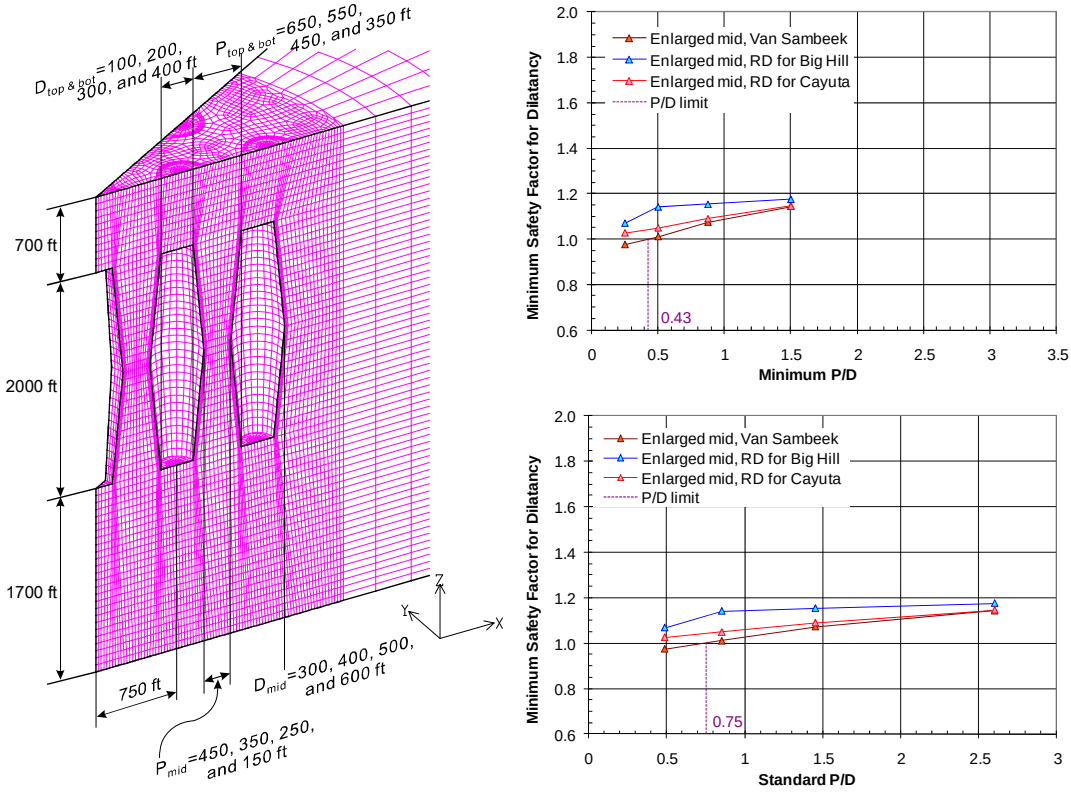

Figure 19: Computational mesh for the enlarged middle caverns (left), and safety factors as a function of minimum and standard P/Ds.

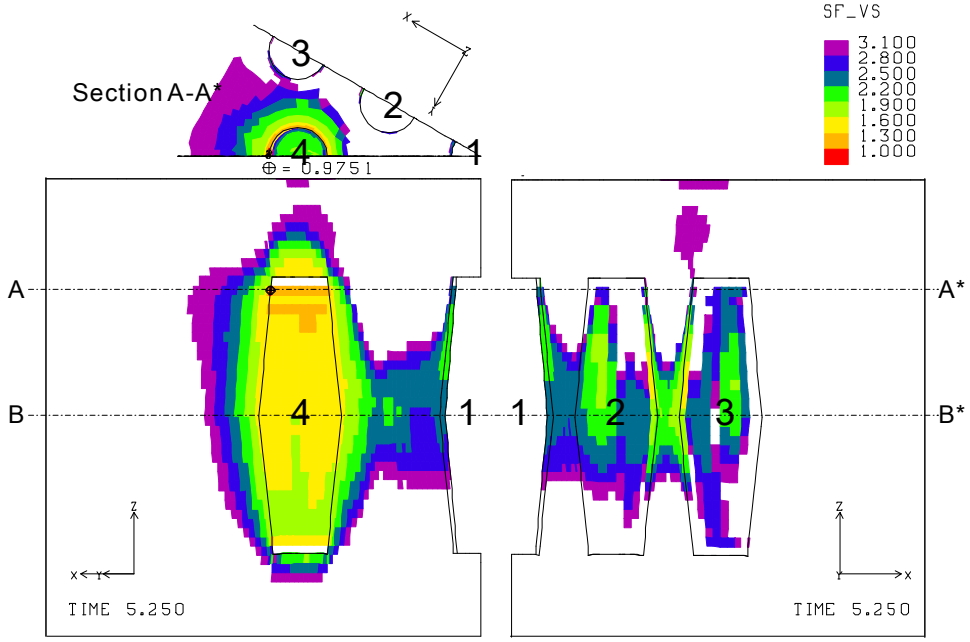

Figure 20: Predicted safety factor contours for dilatancy during workover of Cavern 4 when the minimum safety factor occurs (cavern diameters at middle are 600 ft). Van Sambeek criterion with C=0.18 is used. The vertical cross-section through the centers of caverns and the horizon cross-sections at the elevations where the minimum safety factor occurs (A-A*). Dash-dot lines show where the section was cut. Time is in years.

4.2.4. Enlarged Top Cavern

Figure 21 (left) shows the computational mesh for the caverns in which the tops (300 ft in diameter) are larger than the bottoms (100 ft in diameter). The diameters of caverns at the top range from 300 ft to 600 ft in 100 ft increments. The diameters of caverns at the bottom range from 100 ft to 400 ft in 100 ft increments. The webs of salt between the caverns are decreased from 450 ft to 150 ft in 100 ft increments at the cavern tops, and from 650 ft to 350 ft in 100 ft increments at the cavern bottoms. The heights of caverns are 2000 ft. The P/Ds are calculated using the radii and the web thicknesses and are listed in Table 8. The corresponding values of minimum safety factor for dilatancy in the salt dome from post-processing EXODUS output provided by Sobolik and Ehgartner [2006] are also listed in Table 8.

Figure 21 (right) plots the minimum safety factor as a function of minimum and standard P/Ds, respectively. When the Van Sambeek criterion with C=0.18 is applied to the dilatancy calculation, the onset of dilatant damage is predicted at 1.25 and 2.15 for minimum and standard ratios, respectively.

The minimum value of safety factor occurs at the wall near the roof of Cavern 2 (Section A-A*) during workover of Cavern 2 when the top diameter is 600 ft as shown Figure 22. The minimum values of safety factor for three criteria are smaller than those of other shape caverns because the effect of P/D overlaps with the effect of low internal pressure due to the gravity at the top of the cavern. The enlarged top cavern is structurally less safe than other cavern shapes.

Table 8: P/D and minimum safety factor for dilatancy in the salt dome for the enlarged top caverns.

Radius (ft)			P/D		Minimum Safety Factor		
At Bottom	At Middle	At Top	Minimum	Standard	Van Sambeek C=0.18	RD for Big Hill salt	RD for Cayuta salt
50	100	150	**1.500**	**2.603**	**1.022**	**1.220**	**1.088**
100	150	200	**0.875**	**1.455**	**0.966**	**1.172**	**1.048**
150	200	250	**0.500**	**0.856**	**0.917**	**1.156**	**1.014**
200	250	300	**0.250**	**0.490**	**0.870**	**1.071**	**0.962**

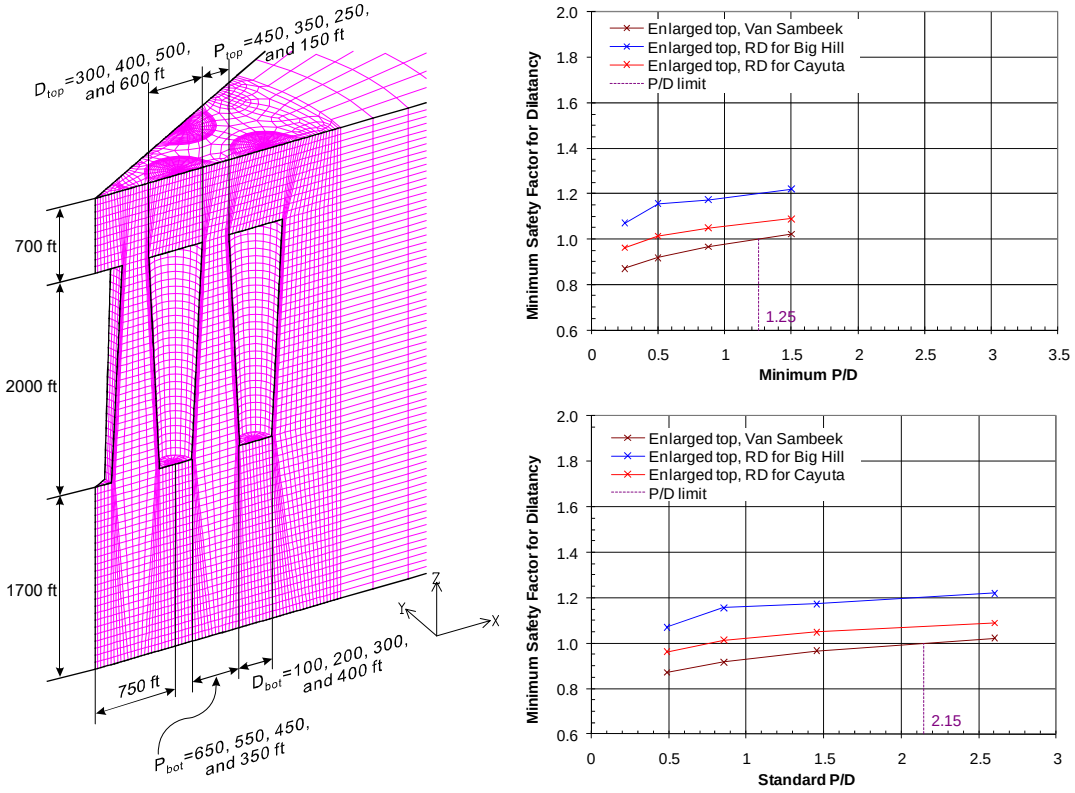

Figure 21: Computational mesh for the enlarged top caverns (left), and safety factor as a function of minimum (right, top) and standard P/D (right, bottom).

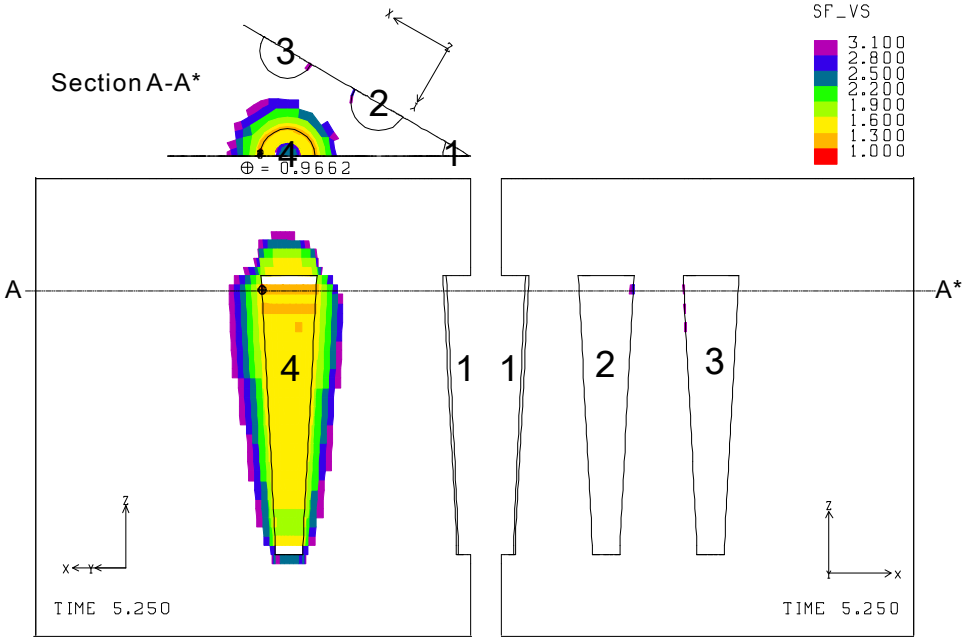

Figure 22: Predicted safety factor contours for dilatancy when the minimum value occurs during workover of Cavern 4 (Cavern radius at top is 200 ft). Van Sambeek criterion with C=0.18 is used. The vertical cross-section through the centers of caverns and the horizon cross-section at the elevation where the minimum safety factor occurs (A-A*). Dash-dot lines show where the section was cut. Time is in years.

4.3. Wedge Symmetry Plane Model for Big Hill

Figure 23 shows the salt dome mesh extracted from the 19-cavern, 15-drawdown leach model (Figure 7). The 19-cavern, 30-degree wedge symmetry planes format was applied to simplify modeling. The diameters of caverns increase from 221 ft to 673 ft in 7.7% increments for the 15 drawdown leaches. The webs of salt between the caverns decrease from 529 ft to 77 ft. The height of caverns is 1890 ft. The P/Ds are calculated using the diameters and the web thicknesses, and are listed in Table 9. The corresponding values of minimum safety factor for dilatancy in the salt dome are also listed in Table 9. The ALGEBRA script for the post-process is provided in Appendix III.

Figure 24 shows the minimum safety factor for dilatancy as a function of standard P/D calculated with three dilation criteria. Note that the caverns in the numerical analyses model for BH was simplified to the cylinder shapes using the volume conserving cylinders. Therefore, "Standard P/D" only was calculated to identify the relationship between P/D and the safety factor for dilatancy. When the Van Sambeek criterion with C=0.18 and RD criteria for the Cayuta and Big Hill salt are applied to the dilatancy calculation, the onsets of dilatant damage are predicted at the P/D values of 0.35, 0.31, and 0.23, respectively. The values of safety factor decreases remarkably after the 11th drawdown leach. The Van Sambeek criterion with C=0.18 yields the largest critical P/D value for the onsets of damage. Therefore, this criterion should be applied to calculate the limit of the P/D in this BH model.

Figure 25 (left) shows the salt dome mesh extracted from the 31-cylindrical cavern model, where a fifth cavern was added to the 19-cavern model. The increment of cavern diameter with drawdown leach is the same as the 19-cavern model. The cavern diameters and web thicknesses are the same as the 19-cavern model, thus the calculated P/Ds are also the same. The corresponding values of minimum safety factor for dilatancy in the salt dome from post-processing the EXODUS output provided by Park, et al. [2006] are listed in Table 9.

Figure 25 (right) plots the minimum safety factor as a function of P/Ds from the 31-cavern model. The values of the safety factors do not decrease as the P/D decreases through the 5th drawdown leach. The lack on sensitivity to P/D may be due to the large stiff caprock in the dome. The dilatant damage does not occur by a P/D of 1.34 for the Van Sambeek and RD criteria.

To investigate the P/D effect between the cavern and the dome perimeter, the minimum safety factor for dilatancy was calculated within the mesh around Cavern 5 as shown in Figure 26 (left and center). The corresponding values of minimum safety factor for dilatancy in the pillar between Cavern 5 and the dome perimeter from post-processing the EXODUS output provided by Park, et al. [2006] are listed in Table 10. When the diameter of Cavern 5 increases from 221 ft to 321 ft, the pillar thickness between the cavern and the surrounding rock decreases from 155 ft to 106 ft. The safety factor for the three criteria does not decrease as the thickness of the pillar decreases as shown Figure 26 (right). The thickness of the pillar between the cavern and the surrounding rock may not affect the safety factor [Park et al., 2006]. The web of salt between the cavern and the surrounding rock behaves structurally stable even though the web thickness decreases because the stiffer surrounding sandstone prevents salt creep closure.

Table 9: P/D and minimum safety factor for dilatancy in the salt dome for the cylindrical caverns.

Drawdowns	Diameter of Caverns (ft)	Pillar Thickness (ft)	Standard P/D	Minimum Safety Factor					
				19-cavern model			31-cavern model		
				Van Sambeek (C=0.18)	RD for Big Hill salt	RD for Cayuta salt	Van Sambeek (C=0.18)	RD for Big Hill salt	RD for Cayuta salt
0	221	529	**2.39**	**1.236**	**1.324**	**1.353**	**1.309**	**1.381**	**1.380**
1	238	512	**2.15**	**1.261**	**1.334**	**1.358**	**1.338**	**1.358**	**1.374**
2	256	494	**1.93**	**1.265**	**1.335**	**1.350**	**1.336**	**1.388**	**1.360**
3	276	474	**1.72**	**1.266**	**1.336**	**1.348**	**1.335**	**1.388**	**1.386**
4	297	453	**1.52**	**1.270**	**1.340**	**1.348**	**1.336**	**1.394**	**1.391**
5	320	430	**1.34**	**1.273**	**1.343**	**1.349**	**1.331**	**1.399**	**1.392**
6	345	405	**1.17**	**1.277**	**1.348**	**1.363**			
7	372	378	**1.02**	**1.284**	**1.356**	**1.382**			
8	400	350	**0.87**	**1.293**	**1.365**	**1.404**			
9	431	319	**0.74**	**1.302**	**1.376**	**1.411**			
10	464	286	**0.62**	**1.297**	**1.391**	**1.410**			
11	500	250	**0.50**	**1.274**	**1.370**	**1.397**			
12	538	212	**0.39**	**1.116**	**1.211**	**1.338**			
13	580	170	**0.29**	**0.844**	**0.972**	**1.172**			
14	625	125	**0.20**	**0.512**	**0.708**	**0.930**			
15	673	77	**0.11**	**0.033**	**0.230**	**0.508**			

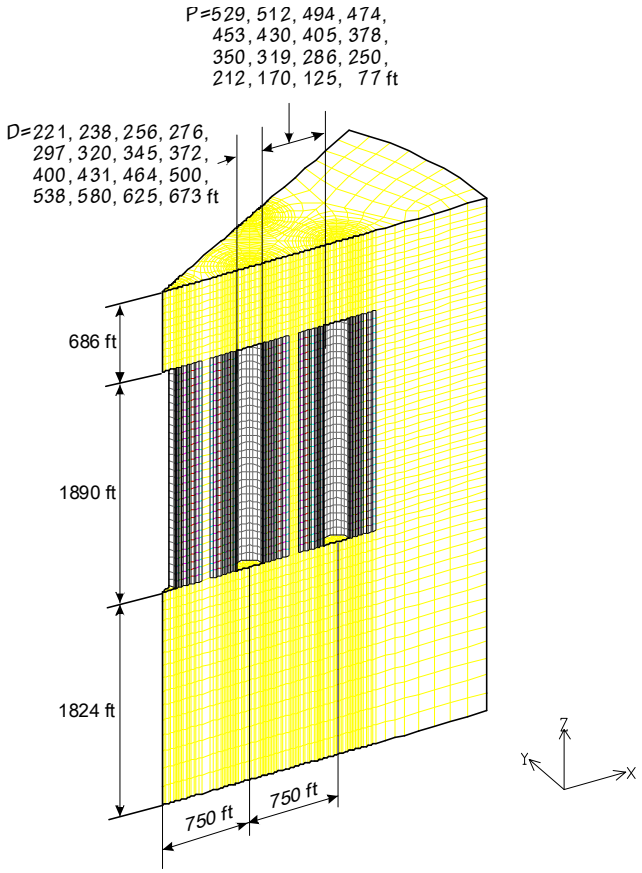

Figure 23: Salt dome mesh of the 19-cavern, 15-drawdown leach model for the Big Hill site. Since the cavern diameter (D) increases with each drawdown leach while the pillar size (P) decreases.

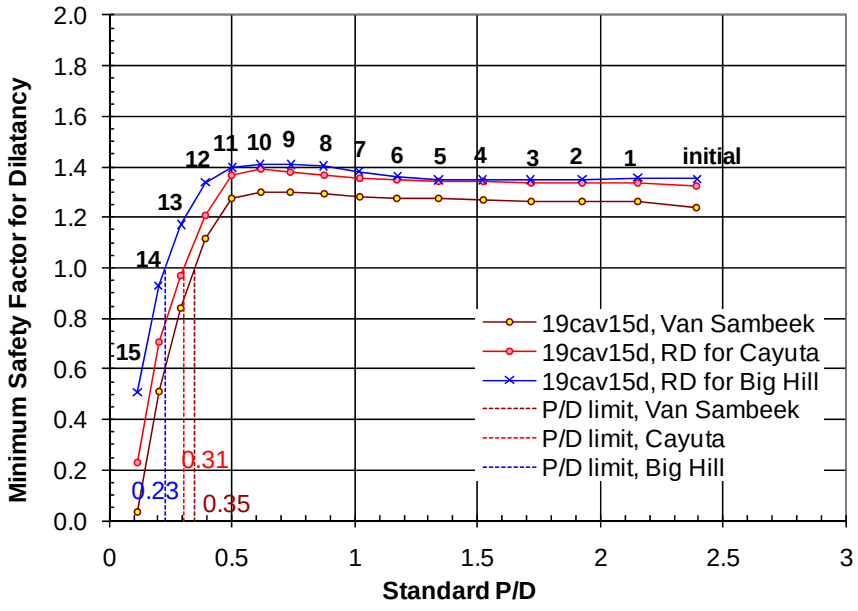

Figure 24: Minimum safety factor for dilatancy as a function of standard P/D. The numbers on the graph indicates the graph indicates the number of drawdown leaches.

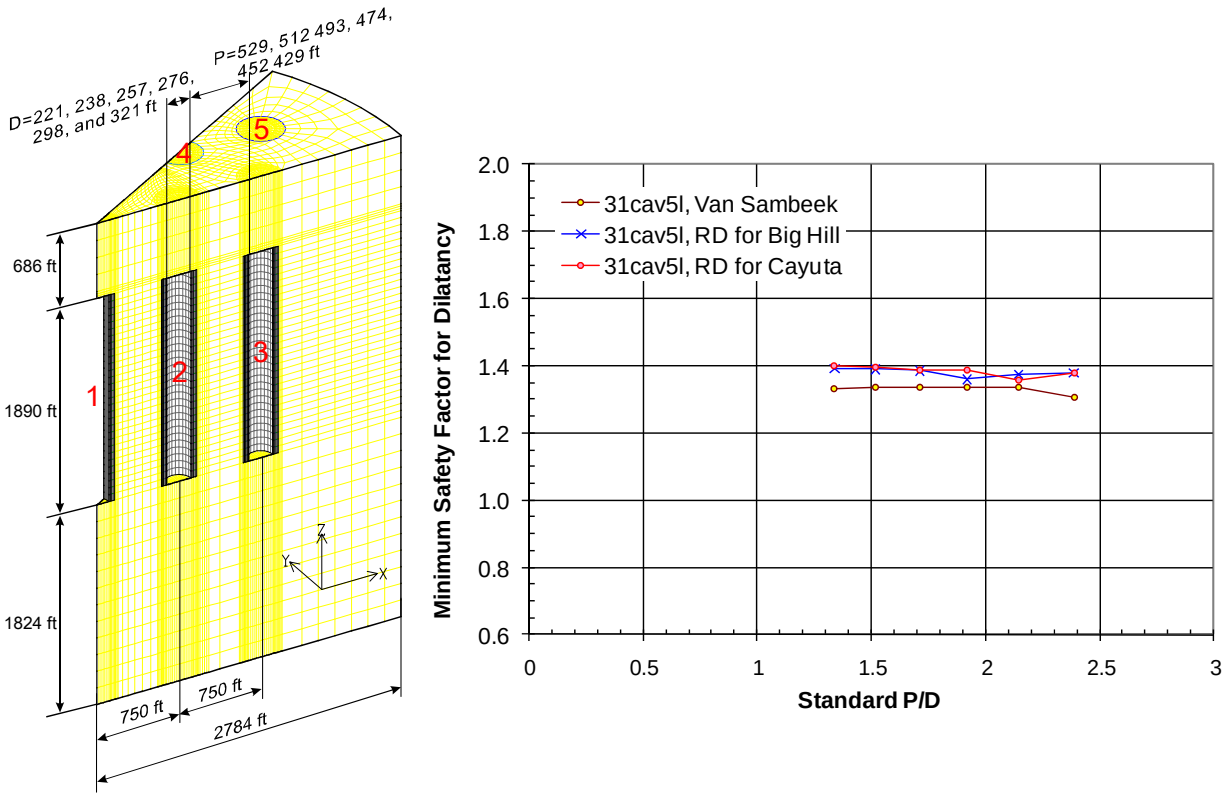

Figure 25: Computational mesh for the 31-cavern model in Big Hill (left), and safety factor as a function of P/D (right).

Table 10: P/D and minimum safety factor for dilatancy in the pillar between Cavern 5 and dome perimeter.

Drawdowns	Diameter of Caverns (ft)	Pillar Thickness (ft)	Standard P/D	Minimum Safety Factor		
				31-cavern model		
				Van Sambeek (C=0.18)	RD for Big Hill salt	RD for Cayuta salt
0	221	155	**0.702**	**1.330**	**1.497**	**1.408**
1	238	147	**0.616**	**1.371**	**1.400**	**1.404**
2	257	138	**0.536**	**1.377**	**1.444**	**1.411**
3	276	128	**0.462**	**1.385**	**1.455**	**1.449**
4	298	117	**0.393**	**1.392**	**1.457**	**1.451**
5	321	106	**0.329**	**1.396**	**1.463**	**1.453**

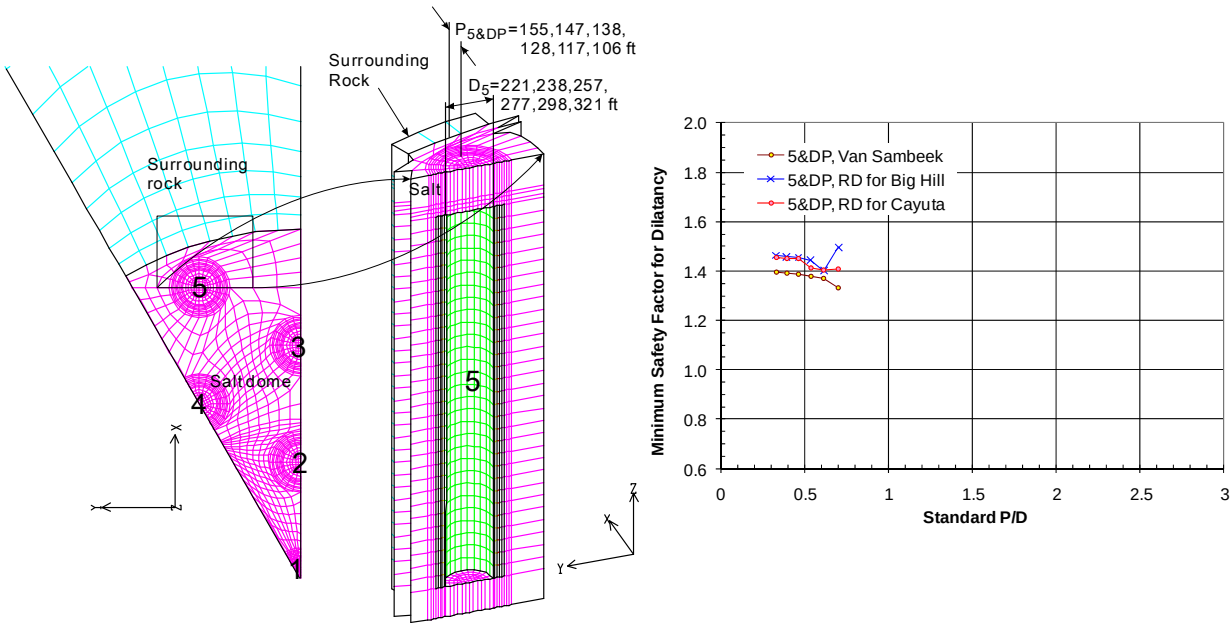

Figure 26: Computational mesh for Cavern 5 and dome perimeter in Big Hill (left and center), and safety factor as a function of P/D (right).

4.4. Salt Dome Model for Bayou Choctaw

To investigate the P/D effect, the EXODUS output, which was obtained from the 3-D finite element analysis [Park et al., 2006], was post-processed using the ALGEBRA scripts in Appendix III.

Figure 27 (left) shows the computational mesh for Caverns 15 and 17 extracted from the BC model as shown Figure 8. The diameter of Cavern 15 increases from 412 ft to 585 ft in 7.24% increments with each of the five drawdown leaches. The diameter of Cavern 17 increases from 247 ft to 351 ft in 7.24% increments. The pillar thickness between Caverns 15 and 17 decreases from 196 ft to 58 ft. The heights of Caverns 15 and 17 are 691 ft and 1423 ft, respectively. The P/Ds are calculated using the diameter and the web thickness, and are listed in Table 11. The corresponding values of minimum safety factor for dilatancy in the salt dome from post-processing are also listed.

Figure 27 (right) plots the minimum safety factor as a function of P/Ds, respectively. When the RD criterion for Cayuta salt is applied to the dilatancy calculation, the onset of dilatant damage is predicted at 0.39 and 0.65 for Caverns 15 and 17, respectively. Whereas the P/D using the Van Sambeek criterion can be as low as 0.15. This illustrates the sensitivity of P/D and hence impact on allowable oil drawdowns to the assumed salt strength. In the previous analyses using the wedge models, the Van Sambeek criterion produced the lowest safety factors. Figure 27 shows that for Bayou Choctaw, the Van Sambeek criterion is not as conservative as the others. This observation will also apply for the remaining analyses, with some exception. It shows that one cannot determine a priori which criterion will be most conservative. As mentioned in Section 2.1, the P/Ds based on Cavern 15 and 17 are not the same because the diameters of Caverns 15 and 17 are not the same. Note that the caverns in the numerical analyses model for BC was simplified to the cylinder shapes using the volume conserving cylinders. Therefore, "Standard P/D" only was calculated to identify the relationship between P/D and the safety factor for dilatancy.

The dilatant damage is predicted to occur at approximately three quarters-height of Cavern 15 in the web salt after the second drawdown leach when the RD criterion for Cayuta salt is applied (Figure 28 (B)). The damaged zone widens through five drawdown leaches. Once dilatant damage occurs on the walls of Caverns 15 and 17 after the second drawdown leach, the damaged zone continues to grow across the pillar. Therefore, the pillar may fail entirely after the second drawdown leach.

Table 11: P/D and minimum safety factor for dilatancy in the web salt between Caverns 15 and 17 in Bayou Choctaw salt dome.

Drawdowns	Avg. Diameter (ft)		Avg. Pillar Thickness (ft)	Standard P/D		Minimum Safety Factor		
	Cav. 15	Cav. 17		For Cav.15	For Cav.17	Van Sambeek (C=0.18)	RD for Cayuta salt	RD for Big Hill salt
0	412	247	196	**0.476**	**0.794**	**1.123**	**1.040**	**1.077**
1	442	265	172	**0.390**	**0.650**	**1.107**	**0.999**	**1.015**
2	474	284	147	**0.309**	**0.516**	**1.082**	**0.973**	**0.973**
3	509	305	119	**0.235**	**0.391**	**1.060**	**0.946**	**0.933**
4	545	327	90	**0.165**	**0.275**	**1.022**	**0.910**	**0.867**
5	585	351	58	**0.100**	**0.166**	**0.825**	**0.837**	**0.768**

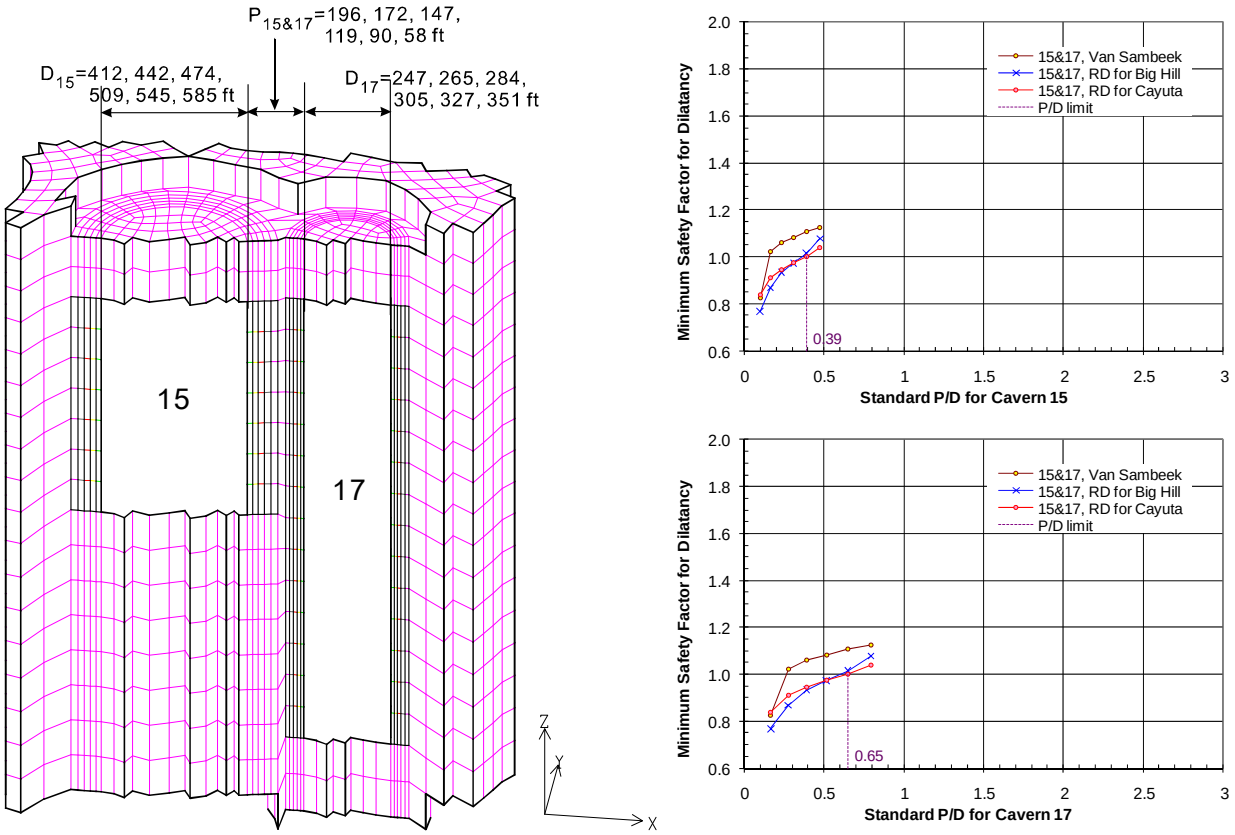

Figure 27: Computational mesh for Caverns 15 and 17 in Bayou Choctaw (left), and safety factor as a function of P/D (right).

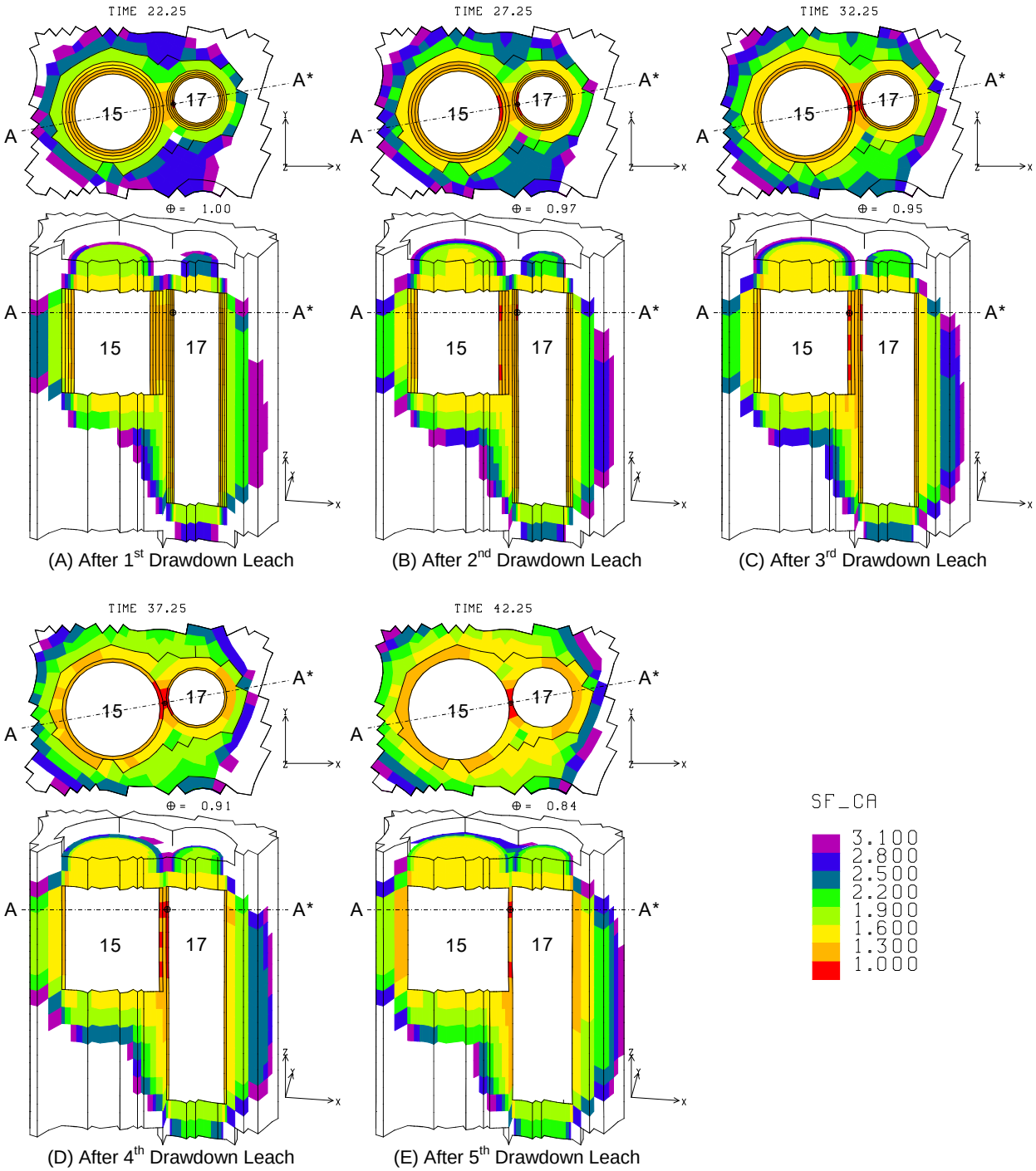

Figure 28: Predicted safety factor contours for dilatancy during workover when the minimum values of safety factor occur after 1st, 2nd, 3rd, 4th, and 5th drawdown leach, respectively. The RD criterion for the Cayuta salt is used. The vertical cross-section through the centers of caverns and the horizon cross-section at the elevation where the minimum safety factor occurs. Dash-dot lines show where the section was cut. Time is given in years.

To investigate the P/D effect between the cavern and the dome perimeter, the mesh around Cavern 20 was extracted (Figure 29 (left)) and the minimum safety factor for dilatancy within the volume calculated. As the diameter of Cavern 20 increases from 407 ft to 578 ft in 7.24% increments, the pillar thickness between the cavern and the surrounding rock decreases from 315 ft to 230 ft. The P/Ds are calculated using the diameters of Cavern 20 and the web thicknesses during drawdown leaches. These are listed in Table 12. The corresponding values of minimum safety factor for dilatancy in the salt dome from post-processing are also listed. The safety factor for three criteria does not decrease as the thickness of the pillar decreases as shown Figure 29 (right). The safety factor of the salt between the cavern and the surrounding rock may not be affected by the web thickness, which is similar to the analysis of Cavern 5 in the Big Hill salt dome as mentioned with Figure 26. The caveat to these analyses is the assumed rock moduli surrounding the dome, which is stiffer than salt. A different result would be expected for a softer rock that may permit loading of the salt web as the pillar width decreases.

Table 12: P/D and minimum safety factor for dilatancy in the web salt between Caverns 20 and the surrounding rock in Bayou Choctaw salt dome.

Drawdowns	Avg. Diameter of Cav. 20 (ft)	Avg. Pillar Thickness (ft)	Standard P/D for Cav.20	Minimum Safety Factor		
				Van Sambeek (C=0.18)	RD for Cayuta salt	RD for Big Hill salt
0	407	315	**0.773**	**1.441**	**1.223**	**1.198**
1	437	300	**0.687**	**1.463**	**1.233**	**1.198**
2	469	284	**0.607**	**1.471**	**1.240**	**1.203**
3	503	267	**0.532**	**1.479**	**1.246**	**1.206**
4	539	249	**0.462**	**1.476**	**1.240**	**1.199**
5	578	230	**0.397**	**1.644**	**1.338**	**1.211**

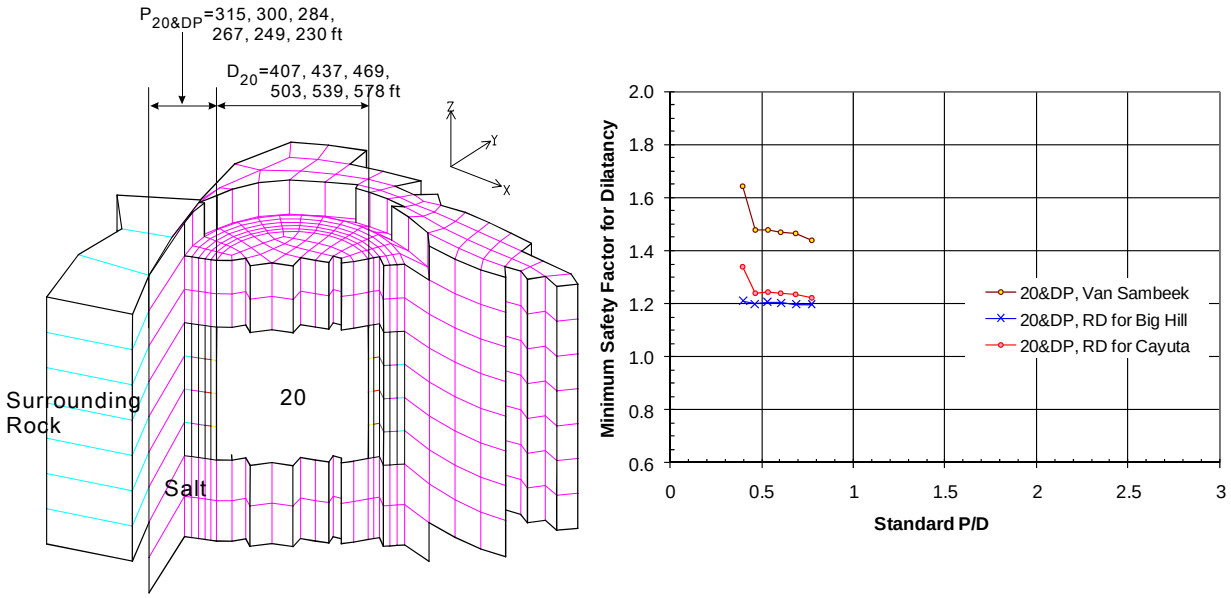

Figure 29: Computational mesh for Cavern 20 and dome perimeter in Bayou Choctaw model (left), and safety factor as a function of P/D (right).

4.5. Salt Dome Model for Bryan Mound

4.5.1. Caverns 103 and 111

Figure 30 shows the mesh used for the web of salt between Caverns 103 and 111 within the Bryan Mound salt dome (Figure 9) to examine the dilatancy damage with P/D. The volumes of Cavern 103 are calculated to be 12.46 MMB, 14.33 MMB, 16.48 MMB, 18.95 MMB, 21.79 MMB, and 25.06 MMB prior to and through the five drawdown leaches, respectively. In this analysis, geometric details are added for the caverns, but they still remain axi-symmetric. The volumes are calculated by Equation (2) in Appendix I. The height of Cavern 103 in the mesh is 1750 ft. Thus the corresponding radii are calculated to be 113 ft, 121 ft, 130 ft, 139 ft, 149 ft, and 160 ft as shown in Figure 30. The volume increases in 15% increments but the diameter does not increase in constant 7.24% increments because the cavern is not a cylindrical shape like the models in the previous sections. The distance between the centers of Caverns 103 and 111 is about 749 ft, thus the corresponding pillar thicknesses are calculated to be 529 ft, 513 ft, 496 ft, 478 ft , 458 ft, and 437 ft as shown in Figure 30. The volumes of Cavern 111 are calculated to be 12.27 MMB, 14.11 MMB, 16.23 MMB, 18.66 MMB, 21.46 MMB, and 24.68 MMB prior to and through the five drawdown leaches, respectively. The height of Cavern 111 in the mesh is 1924 ft. Thus the corresponding radii are calculated to be 107 ft, 115 ft, 123 ft, 132 ft, 141 ft, and 151 ft as shown in Figure 30.

The safety factors are calculated at every element in the mesh. The least value is selected among those as a minimum safety factor at every time step as shown Figure 31, which plots the minimum safety factor history for dilatancy when the RD criterion for the Cayuta salt is used. Five sets of two downward peaks in the graph appear when the well head pressures drop to zero during the workovers at every five years. The first set corresponds to the workover activities after the first drawdown leach. The second, third, fourth and fifth sets correspond to the workover activities after the second, third, fourth, and fifth drawdown leaches, respectively. The first peak and the second peak in each set appear during the workovers of Caverns 103 and 111, respectively. The first peak values are smaller than the second peak values, i.e. the periods for the workovers of Cavern 103 are more critical than those of Cavern 111 for the dilatancy damage.

Figure 32 shows the predicted minimum safety factor for dilatancy as a function of minimum and standard P/D for Cavern 103. When the Van Sambeek criterion with C=0.18 and the RD criteria for Cayuta and Big Hill salts are applied to the dilatancy calculation, the dilatant damage is predicted to occur through five drawdown leaches. The P/D value decreases with drawdown leaches. The value of 0.84, which corresponds to the value indicated by an arrow in Figure 31, indicated by arrows in Figure 32 is the minimum safety factor during the workover of Cavern 103 after the 4^{th} drawdown when the RD criterion for Cayuta salt is applied to the calculation. Figure 31 shows improvement in the safety factor for the lowest P/D. This is attributed to a favorable stress state as leaching removes stressed salt and creates a new surface with slightly improved conditions. It demonstrates an independence to P/D, that may not be representative of the pillar condition. The location of elements where the minimum safety factor occurs is shown as $\oplus$ in Figure 33 and Figure 34.

Figure 33 shows the safety factor contours for dilatancy around Caverns 103 and 111 during the workover of Cavern 103 after the 4^{th} drawdown leach (at 15115 days (5/19/2025) when the minimum safety factor value is predicted) when the RD criteria for Cayuta salt is applied.

Dilatant damage is predicted to occur at the corner of the roof of Cavern 103 (Figure 33, left). The safety factor is calculated to be 0.84 in an element of the corner. The horizontal cross-sections at the elevation, where the damage is expected, are shown in Figure 33 (right-top). These show the damaged area (SF<1) around the perimeters of the roofs is ring-shaped. Also adjacent caverns do not affect the damaged area. This suggests damage is not a function of the P/D. If this damage is caused by the P/D, the contours would expand toward the adjacent cavern as shown in the right bottom diagram in Figure 33. The horizontal cross-sections at the elevation of the minimum P/D (Figure 33 (right-bottom)) show the safety factor contours are affected by the adjacent caverns (Caverns 111 and 102). However, the values of safety factor are larger than 1, so the damage is not predicted to occur at the elevation. These phenomena also occur around cavern 111 after the 4th drawdown leach as shown Figure 34.

This suggests that the top and bottom of the caverns can be excluded to investigate the P/D effect. In the case of the WH model (Figure 11 and Figure 14), the roof and floor elevations of all caverns are the same. Therefore, even though the damage occurs at the roof of a cavern, this damage is caused by P/D. However, the roof and floor elevations of Cavern 103 and 111 are different, and the roof and floor are not flat like the cylinder model. Thus the top and bottom of the cavern will be excluded to investigate an actual P/D effect in the pillar between the caverns.

Figure 35 shows the mesh used for the P/D calculation in the web of salt between Caverns 103 and 111 excluding the roof and floor. Table 13 lists the minimum P/Ds for Caverns 103 and 111 with the maximum diameters of the caverns and the related web thicknesses. The minimum P/Ds for Caverns 103 and 111 are calculated at the elevations of -3380 ft and -3320 ft, respectively. Table 14 lists the standard P/Ds for Caverns 103 and 104 with the average diameters of the caverns and the average thickness of the web between the caverns, and safety factors for the P/Ds. Note that the average diameters and the average pillar thickness are calculated from the volume conserving cylinders as mentioned in Section 2.1.

Figure 36 shows the minimum safety factor for dilatancy as a function of minimum and standard P/D. When the RD criterion for Big Hill salt is applied to the dilatancy calculation, the onset of dilatant damage is predicted at 1.00 and 1.35 for minimum and standard P/Ds based on Cavern 103, respectively. Based on Cavern 111, the onset of dilatant damage is predicted at 1.16 and 1.43 for minimum and standard P/Ds, respectively. Those P/D values are calculated through the extrapolation. The safety factors for the three criteria are greater than one until after the 5th drawdown leach as listed in Table 14. The analysis was conducted only until the 5th drawdown leach [Sobolik and Ehgartner, 2009b]. Thus the extrapolation is needed to find the P/D values corresponding to the safety factors equal to one. The extrapolation may apply to the calculation because the minimum safety factor values during the workover of Cavern 103 after the 5th drawdown leach are close to one.

Figure 37 shows the safety factor contours for dilatancy in the web of salt between Caverns 103 and 110 on 12/30/2031 (17530 days) during workover of Cavern 111 after the 5th drawdown leach. The minimum safety factor value of 1.008 is predicted at the elevation of -3320 ft where the minimum P/D is calculated. We can see the contours expand toward the adjacent cavern; thus the caverns affect the damaged area of each other. In conclusion, the top or bottom of the caverns may locally fail due to the effect of its geometry (caused by stress concentrations) before the web of salt fails due to the P/D effect. Therefore, the failed location (SF<1) due to these geometry influences has to be excluded for examining the actual P/D impacts on pillar stability.

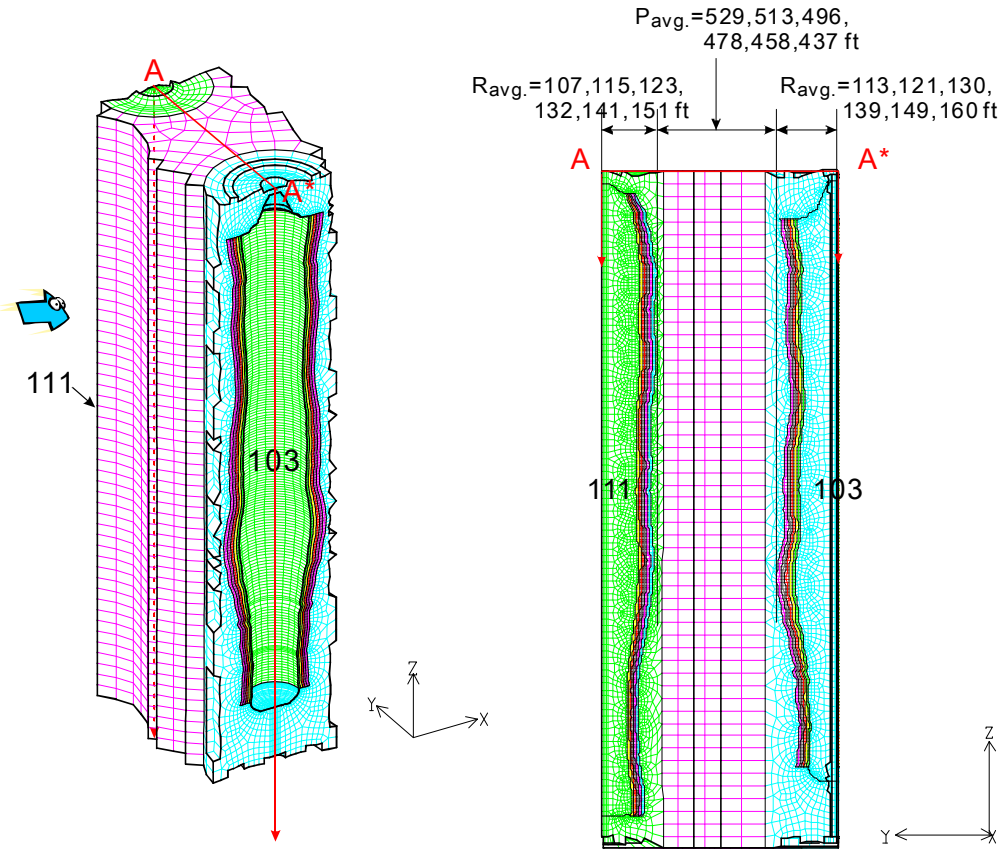

Figure 30: The mesh of web salt between Caverns 103 and 111 in Bryan Mound.

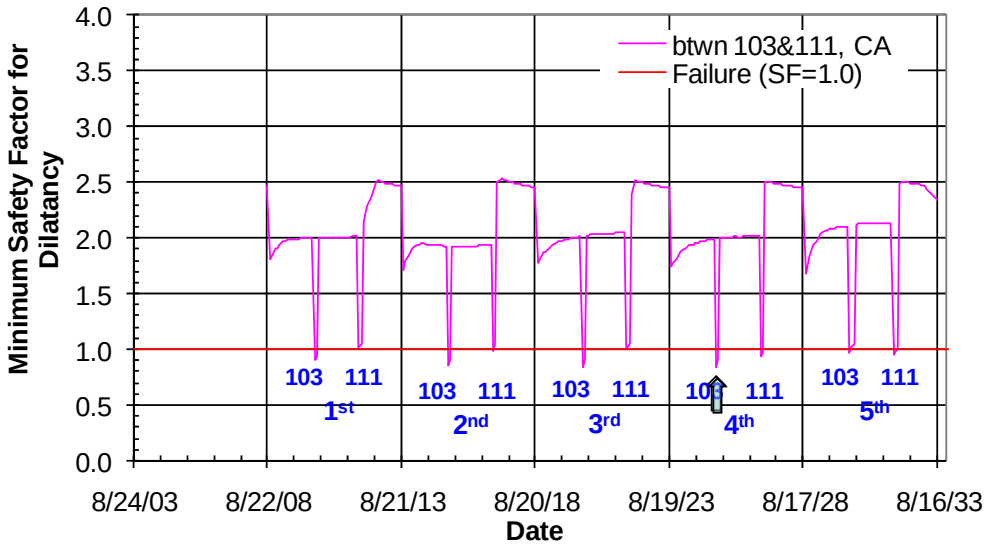

Figure 31: Minimum safety factor for dilatancy using the RD criterion for the Cayuta salt in the web between Caverns 103 and 111 as a function of time.

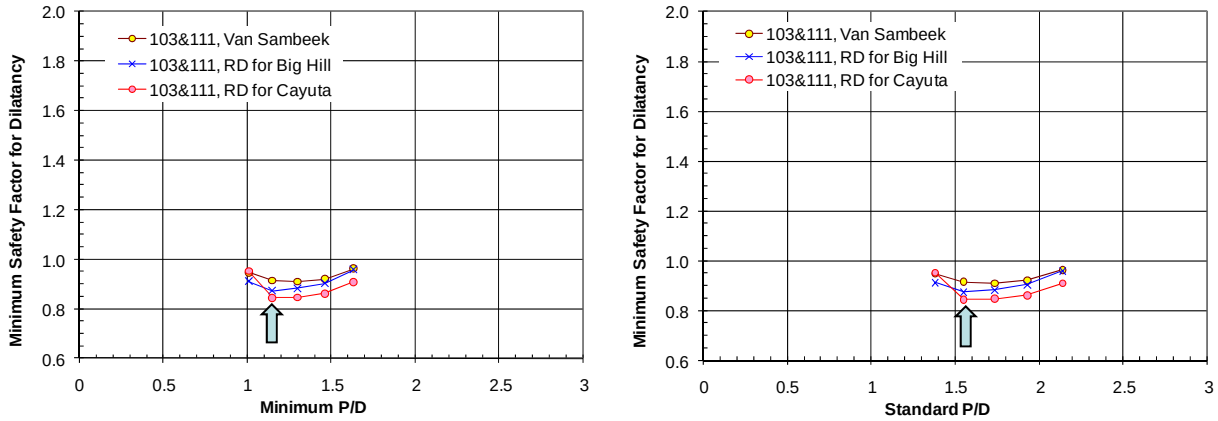

Figure 32: Minimum safety factor of dilatancy as a function of minimum and standard P/D for Cavern 103.

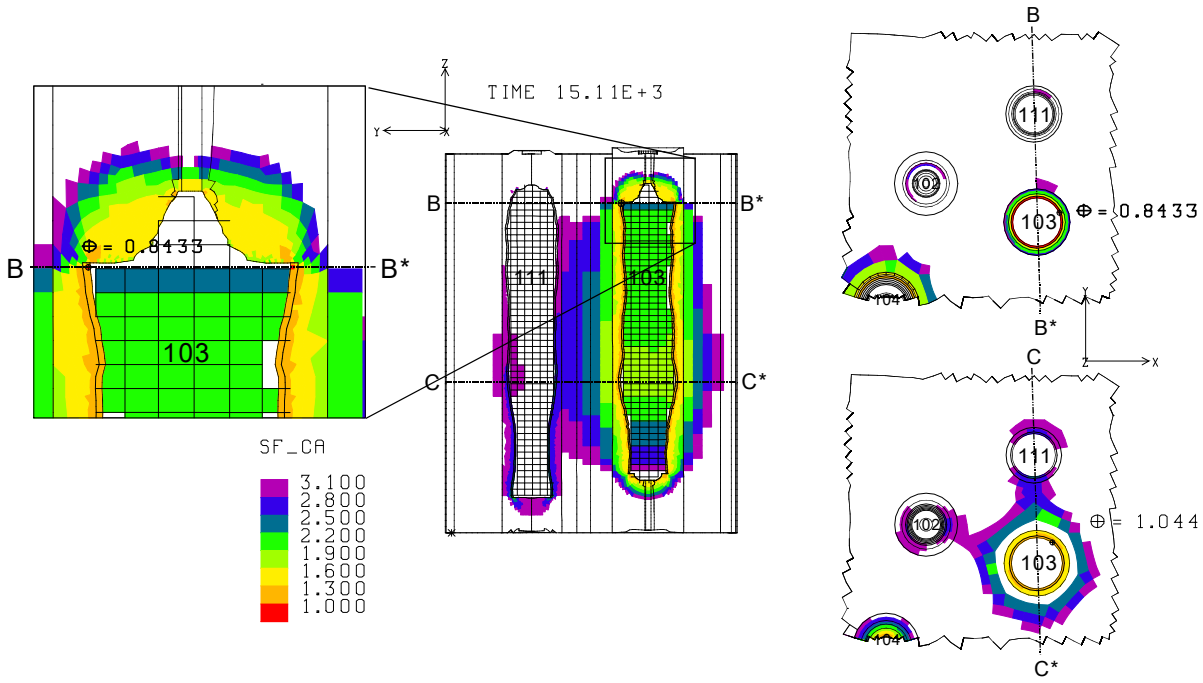

Figure 33: Predicted safety factor contours for dilatancy around Caverns 103 and 111 during workover of Cavern 103 at 5/19/2025 (15115 days) (center) with an enlarged view of the location where the dilatancy damage is predicted in Cavern 103 (left). Horizontal cross-section at the elevation where the damage occurs (right-top). Horizontal cross-section at the elevation where the minimum P/D (right-bottom). Time is given in days.

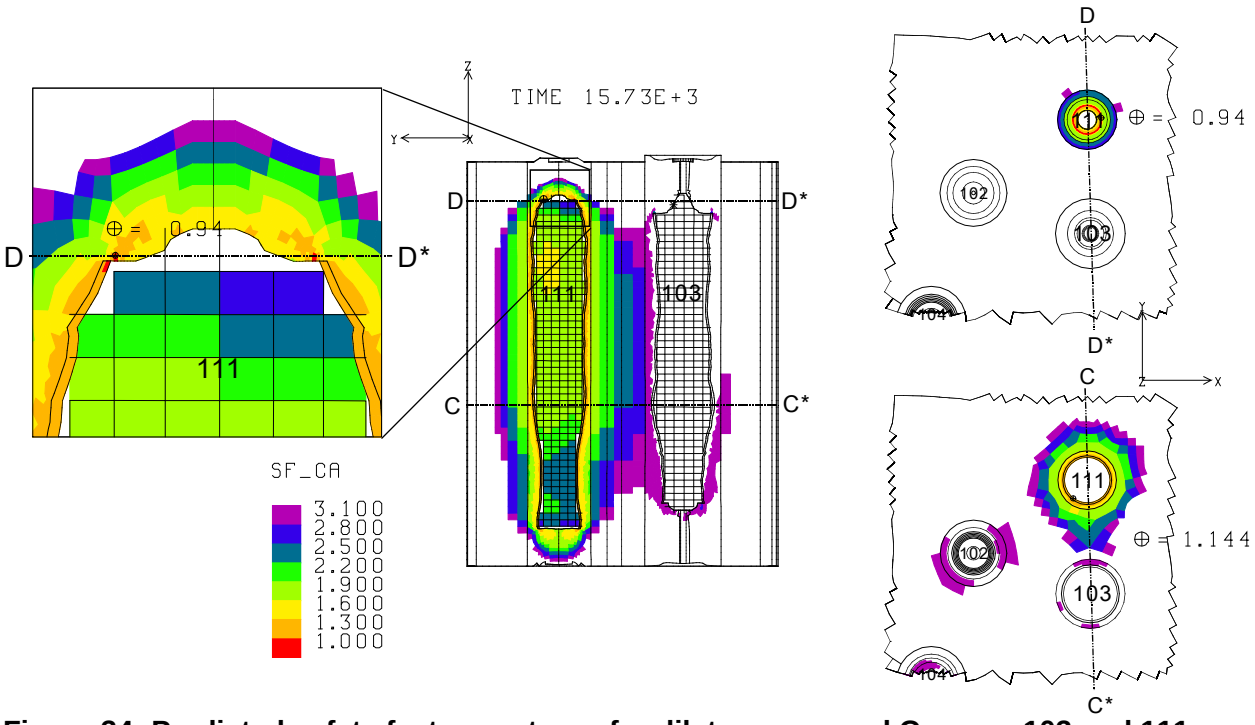

Figure 34: Predicted safety factor contours for dilatancy around Caverns 103 and 111 during workover of Cavern 111 at 1/20/2027 (15725 days) (center) with an enlarged view of the location where the dilatancy damage is predicted in Cavern 111 (left). Horizontal cross-section at the elevation where the damage occurs (right-top). Horizontal cross-section at the elevation where the minimum P/D (right-bottom). Time is given in days.

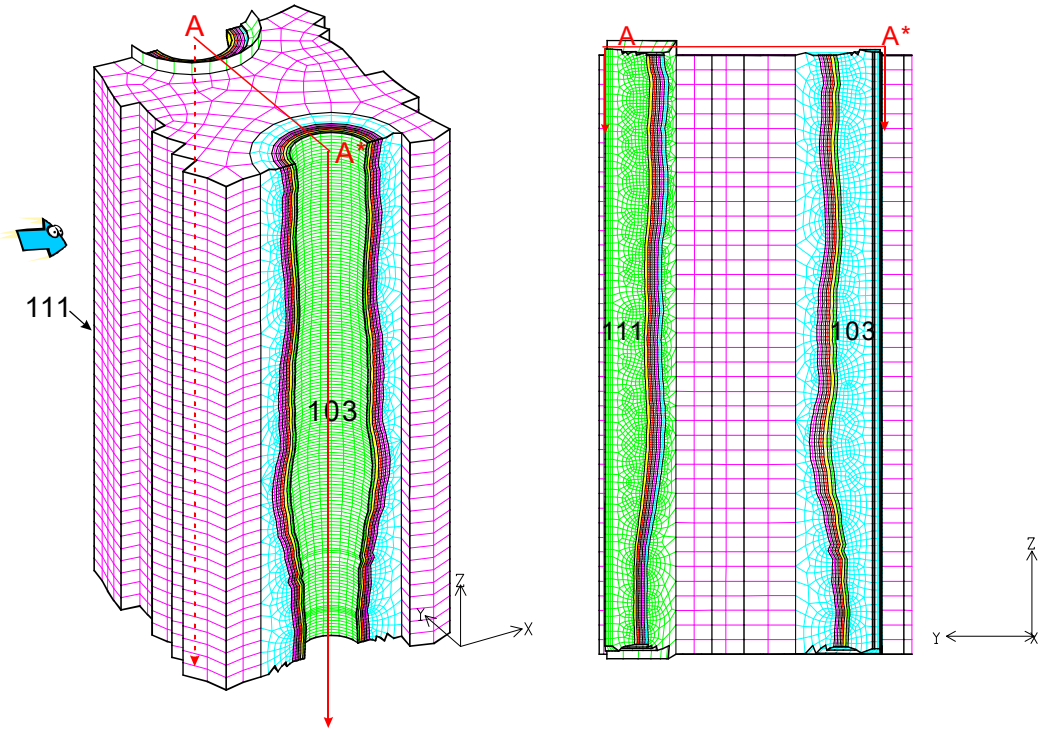

Figure 35. The mesh of web salt between Caverns 103 and 111 excluding the roof and floor in Bryan Mound.

Table 13: Minimum P/Ds in the web salt between Caverns 103 and 111.

Drawdowns	For Cav. 103 (at Ele. -3380 ft)				For Cav. 111 (at Ele. -3320 ft)			
	Maximum Diameter (ft)		Pillar Thickness (ft)	Minimum P/D for Cav.103	Maximum Diameter (ft)		Web Thick (ft)	Minimum P/D for Cav.111
	Cav.103	Cav.111			Cav.103	Cav.111		
0	273	231	496	**1.82**	264	236	499	**2.11**
1	293	248	478	**1.63**	283	253	480	**1.90**
2	314	266	459	**1.46**	304	271	461	**1.70**
3	337	285	438	**1.30**	326	291	440	**1.51**
4	361	306	415	**1.15**	349	312	418	**1.34**
5	387	328	391	**1.01**	374	335	394	**1.18**

Table 14: Standard P/Ds and minimum safety factor for dilatancy in the web salt between Caverns 103 and 111.

Drawdowns	Avg. Diameter (ft)		Avg. Pillar Thickness (ft)	Standard P/D		Minimum Safety Factor		
	Cav. 103	Cav. 111		for Cav.103	for Cav.111	Van Sambeek (C=0.18)	RD for Cayuta salt	RD for Big Hill salt
0	226	214	529	**2.34**	**2.48**			
1	242	229	513	**2.12**	**2.24**	**1.125**	**1.132**	**1.121**
2	259	246	496	**1.91**	**2.02**	**1.098**	**1.104**	**1.115**
3	278	263	478	**1.72**	**1.81**	**1.080**	**1.089**	**1.108**
4	298	282	458	**1.54**	**1.62**	**1.066**	**1.077**	**1.098**
5	320	303	437	**1.37**	**1.44**	**1.046**	**1.014**	**1.008**

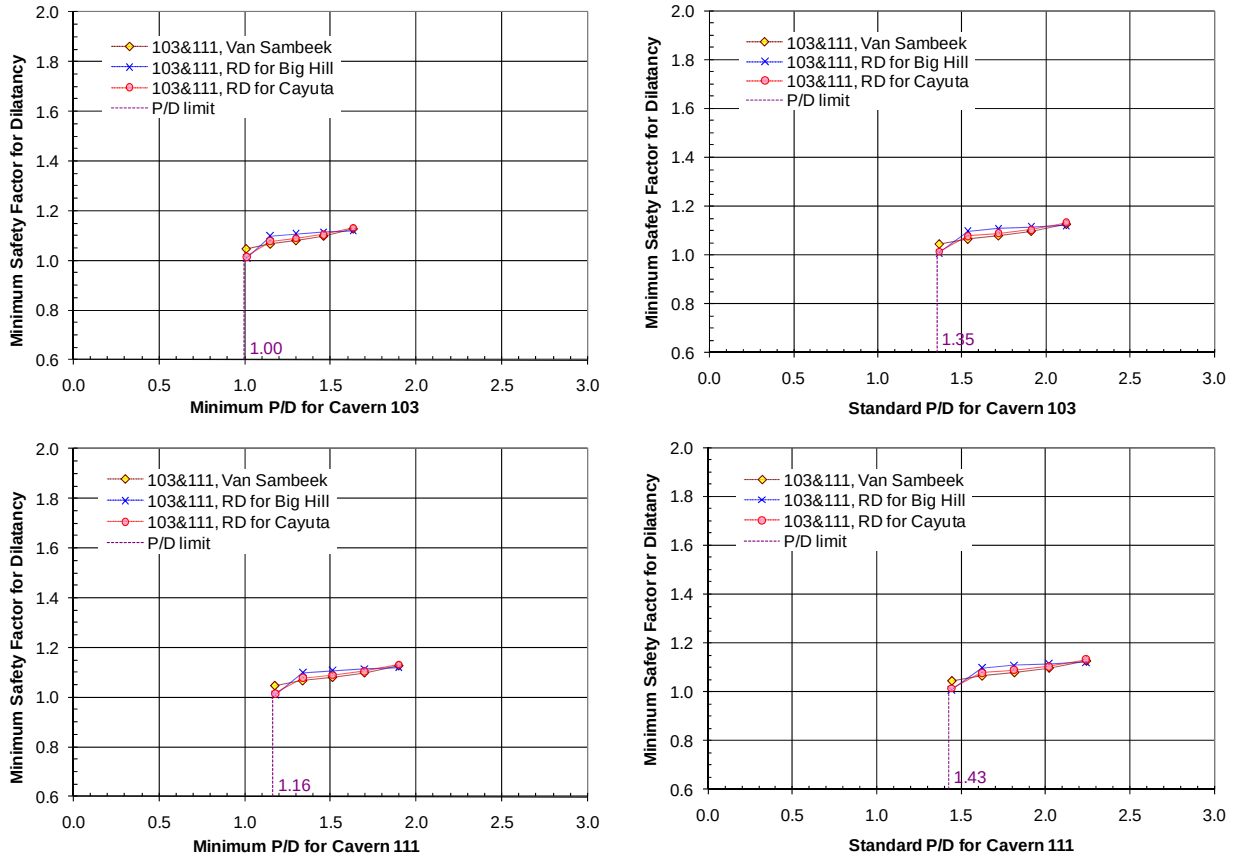

Figure 36: Minimum safety factor for dilatancy as a function of minimum and standard P/D for Caverns 103 and 111.

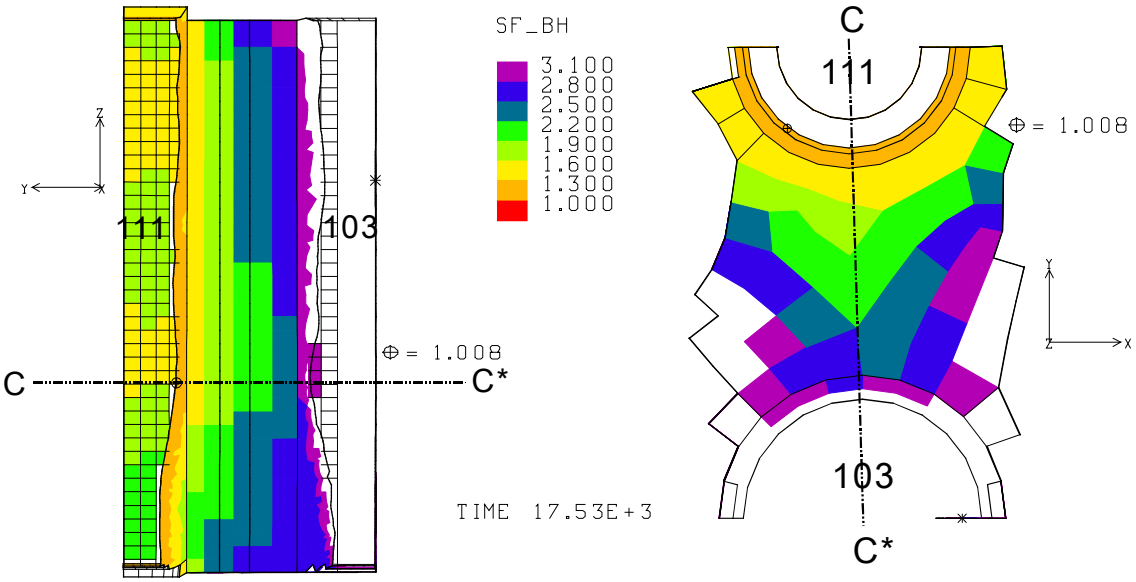

Figure 37: Predicted safety factor contours for dilatancy in the web salt between Caverns 103 and 111 during workover of Cavern 111 at 12/30/2031 (17530 days). The vertical cross-section through the centers of caverns (left) and the horizontal cross-section at the elevation (-3320 ft) where the minimum safety factor value occurs (right). The minimum P/D is calculated at the same elevation. Time is given in days.

4.5.2. Caverns 112 and 114

Figure 38 shows the mesh used to examine the dilatancy damage with P/D for the web of salt between Caverns 112 and 114 in Bryan Mound. The average radius of Cavern 112 increases from 107 ft to 151 ft in 15% increments of volume base for the five drawdown leaches. The average radius of Cavern 114 increases from 84 ft to 119 ft in 15% increments of volume base for the five drawdown leaches. The pillar thickness between two caverns decreases from 523 ft to 444 ft for the five drawdown leaches. Figure 39 shows the predicted minimum safety factor for dilatancy as a function of minimum and standard P/D for Cavern 112. When the Van Sambeek criterion with C=0.18 is applied to the dilatancy calculation, the safety factors are calculated to be more or less than 1.0 with the drawdown leaches. When the RD criterion for Cayuta is applied, the damage occurs since the second drawdown leach. When the RD criterion for Big Hill is applied, the damage occurs since the first drawdown leach.

Figure 40 shows the safety factor contours for dilatancy when the RD criteria for Cayuta salt is applied to the salt in the vicinity of Caverns 112 and 114 during workover of Cavern 112 after the 5th drawdown leach. The dilatant damage is predicted at the corner of the floor of Cavern 112. The horizontal cross-sections at the elevation where the damage occurs in Figure 40 (right-top) shows the damaged area (SF<1) around the perimeter of the floor is ring-shaped; therefore, adjacent caverns do not affect the damaged area. This suggests that damage is not a function of the P/D. This phenomenon also occurs around Cavern 114 after the 5th drawdown leach as shown Figure 41. Thus in order to investigate the P/D effect, the top and bottom of the caverns need to be excluded.

Figure 42 shows the mesh used for the web of salt between Caverns 112 and 114 excluding the roof and floor. Table 15 lists the minimum P/Ds for Caverns 112 and 114 with the maximum diameters of the caverns and the related pillar thicknesses. The minimum P/Ds for Caverns 112 and 114 are calculated at the elevations of -2340 ft and -2280 ft, respectively. Table 16 lists the standard P/Ds for Caverns 112 and 114 with the average diameters of the caverns and the average thickness of the pillar between the caverns, and the minimum safety factors corresponding to the P/Ds. Note again that the average diameters and the average pillar thickness are calculated from the volume conserving cylinders as mentioned in Section 2.1.

Figure 43 shows the minimum safety factor of dilatancy as a function of minimum and standard P/D for Caverns 112 and 114. The safety factors for three criteria are more than one until the 5th drawdown leach. Thus the extrapolation is performed to find the P/D values when the safety factor equals one. When the RD criterion for Big Hill salt is applied to the dilatancy calculation, the onsets of dilatant damage are predicted at 0.95 and 1.42 for minimum and standard P/Ds for Cavern 112, respectively; and at 0.92 and 1.81 for minimum and standard P/Ds for Cavern 114, respectively.

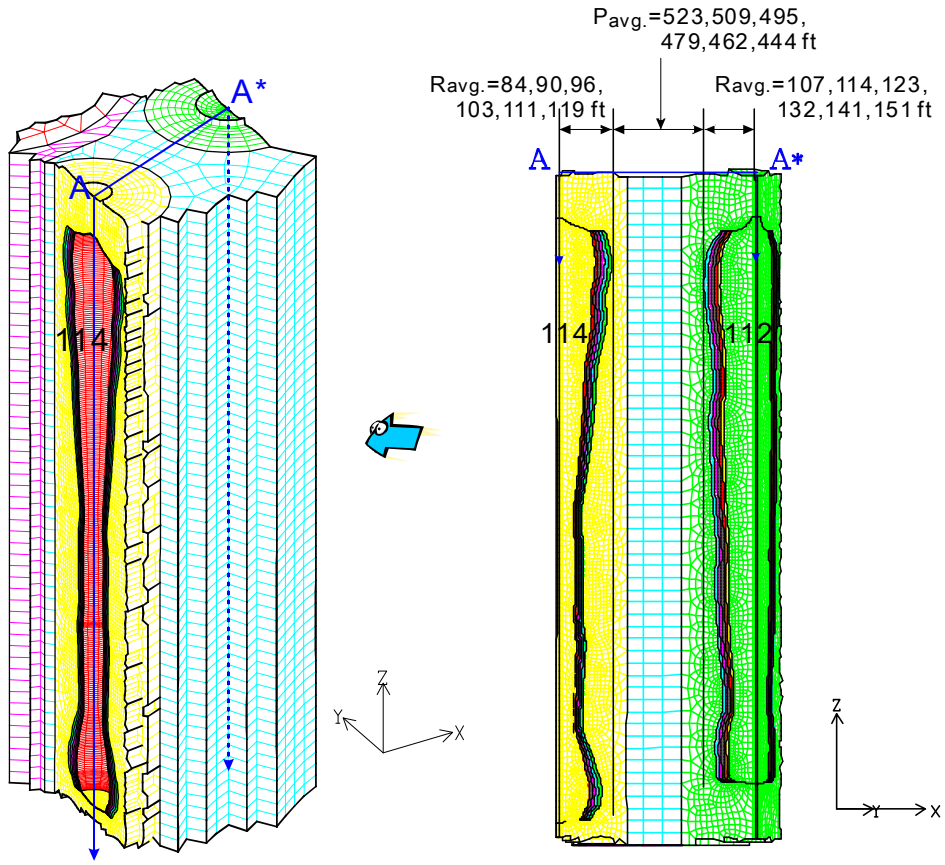

Figure 38: The mesh of web salt between Caverns 112 and 114 in Bryan Mound.

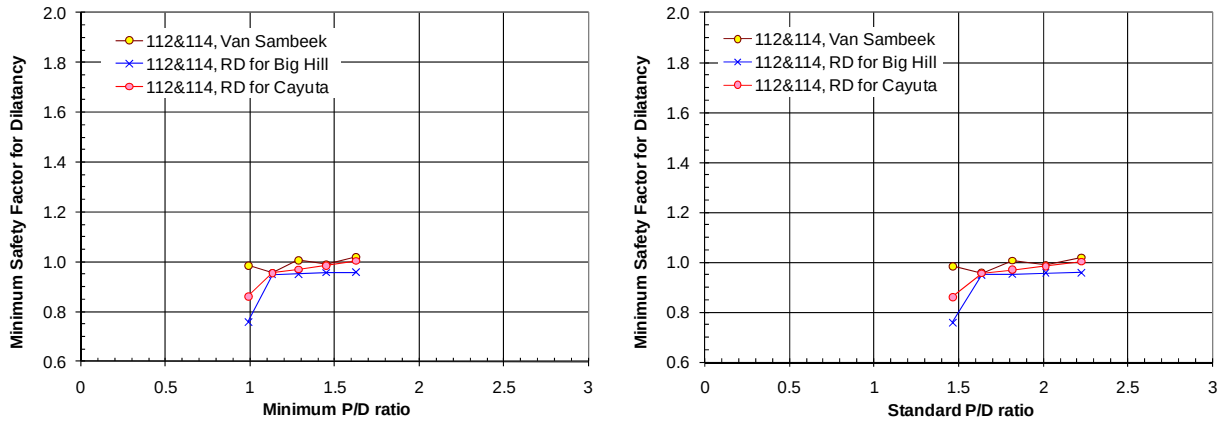

Figure 39: Minimum safety factor of dilatancy as a function of minimum and standard P/D for cavern 112.

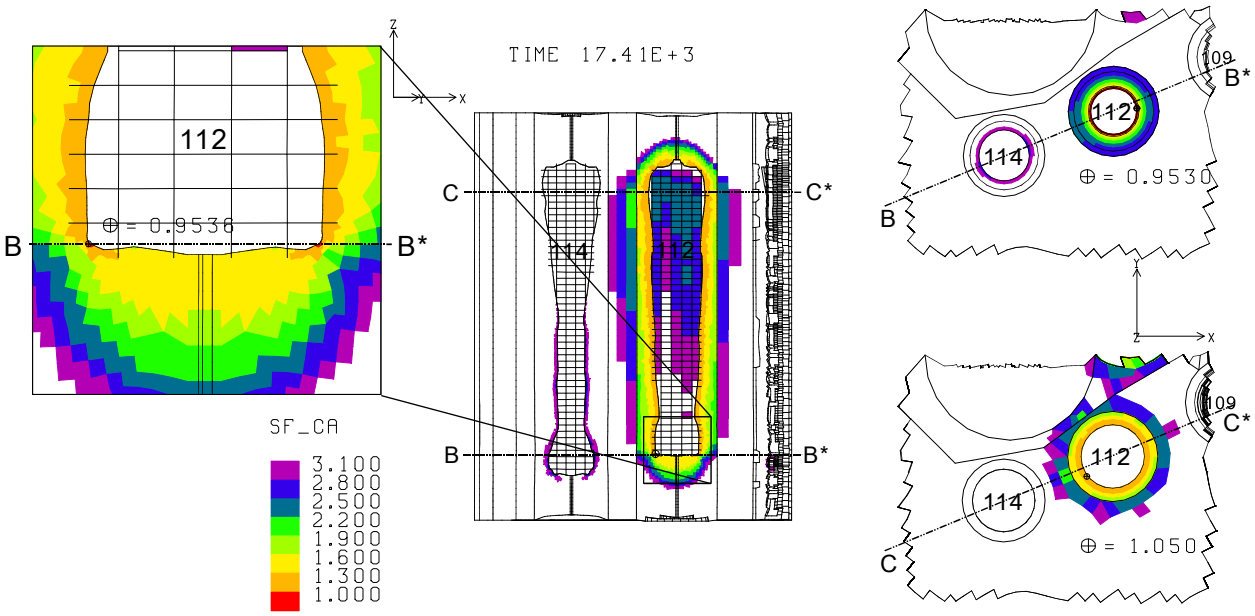

Figure 40: Predicted safety factor contours for dilatancy around Caverns 112 and 114 during workover of Cavern 112 at 9/1/2031 (17410 days) (center) with an enlarged view of the location where the dilatancy damage occurs in Cavern 112 (left). Horizontal cross-section at the elevation where the damage occurs (right-top). Horizontal cross-section at the elevation where the minimum P/D (right-bottom).

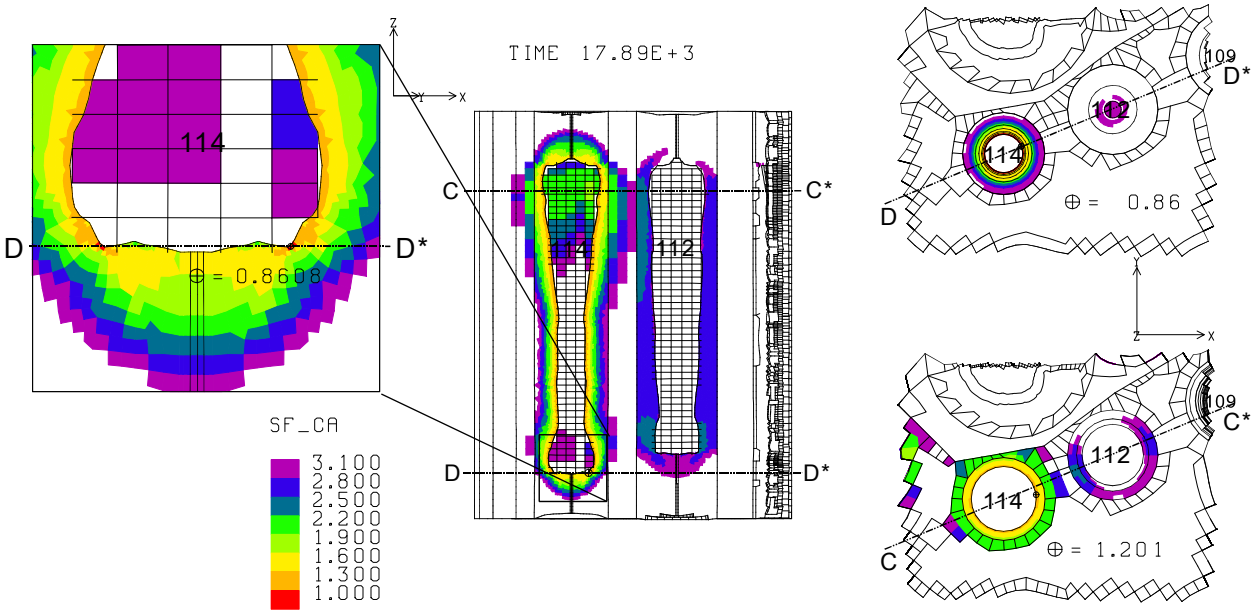

Figure 41: Predicted safety factor contours for dilatancy around Caverns 112 and 114 during workover of Cavern 114 at 12/24/2032 (17890 days) (center) with an enlarged view of the location where the dilatancy damage occurs in Cavern 114 (left). Horizontal cross-section at the elevation where the damage occurs (right-top). Horizontal cross-section at the elevation where the minimum P/D (right-bottom).

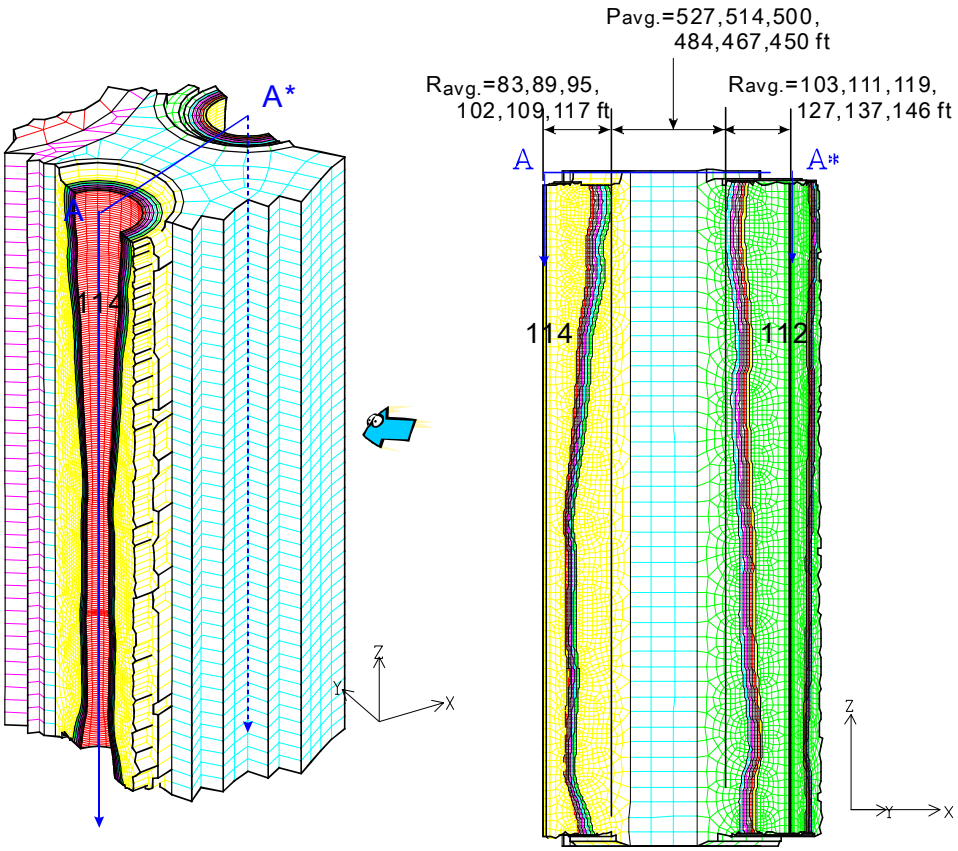

Figure 42: The mesh of web salt between Caverns 112 and 114 excluding the roof and floor in Bryan Mound.

Table 15: Minimum P/Ds for Caverns 112 and 114 in the web salt between Caverns 112 and 114.

Drawdowns	For Cav. 112 (at Ele. -2340 ft)				For Cav. 114 (at Ele. -2280 ft)			
	Maximum Diameter (ft)		Pillar Thickness (ft)	Minimum P/D for Cav.112	Maximum Diameter (ft)		Pillar Thickness (ft)	Minimum P/D for Cav.114
	Cav.112	Cav.114			Cav.112	Cav.114		
0	254	250	461	**1.82**	246	260	460	**1.77**
1	272	269	443	**1.63**	263	279	442	**1.58**
2	292	288	423	**1.45**	282	299	423	**1.41**
3	313	309	402	**1.29**	303	321	401	**1.25**
4	336	331	380	**1.13**	325	344	379	**1.10**
5	360	355	356	**0.99**	348	369	355	**0.96**

Table 16: Standard P/Ds and minimum safety factor for dilatancy in the web salt between Caverns 112 and 114.

Drawdowns	Avg. Diameter (ft)		Avg. Pillar Thickness (ft)	Standard P/D		Minimum Safety Factor		
	Cav. 112	Cav. 114		for Cav.112	for Cav.114	Van Sambeek (C=0.18)	RD for Cayuta salt	RD for Big Hill salt
0	213	167	523	**2.45**	**3.13**			
1	229	179	509	**2.23**	**2.84**	**1.096**	**1.070**	**1.075**
2	245	192	495	**2.02**	**2.57**	**1.086**	**1.057**	**1.063**
3	263	206	479	**1.82**	**2.32**	**1.076**	**1.047**	**1.054**
4	282	221	462	**1.64**	**2.09**	**1.066**	**1.029**	**1.046**
5	303	237	444	**1.47**	**1.87**	**1.036**	**1.009**	**1.010**

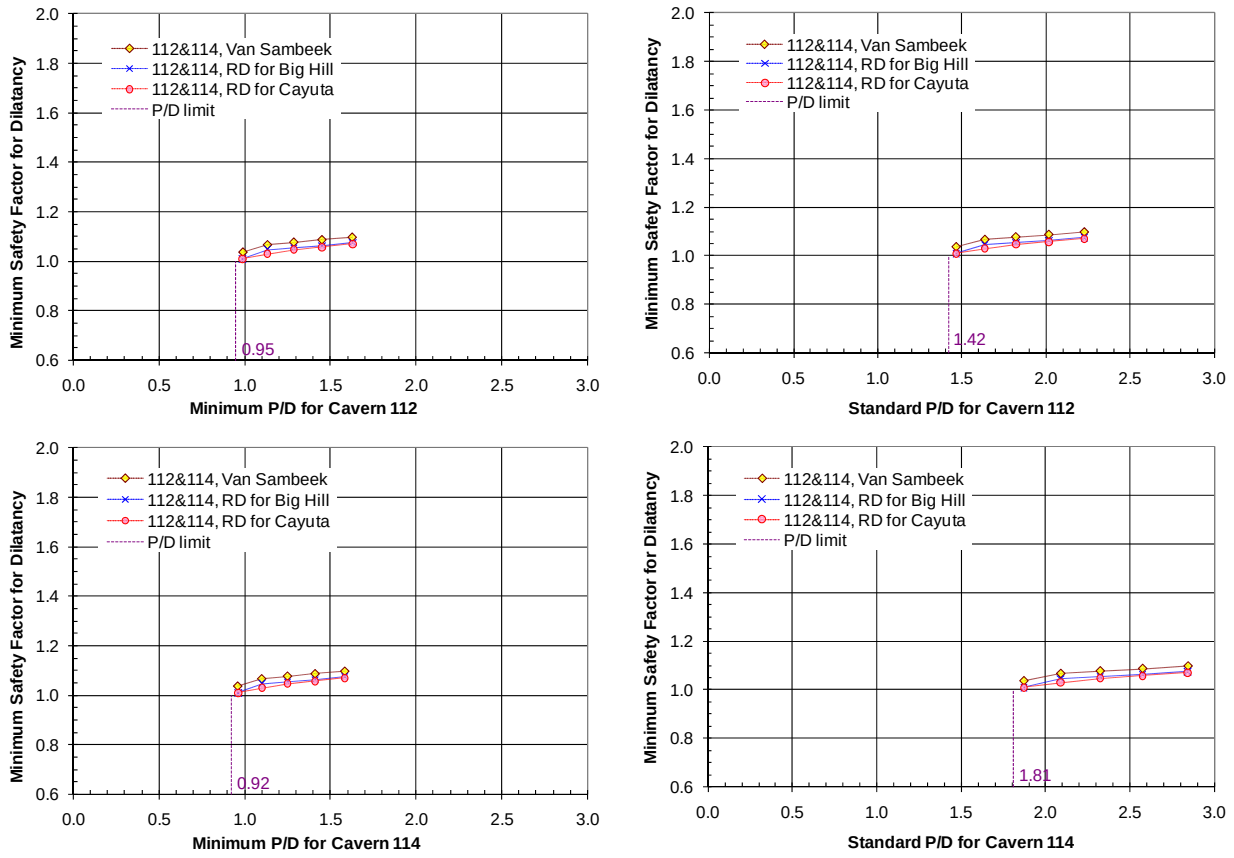

Figure 43: Minimum safety factor for dilatancy as a function of minimum and standard P/D for Caverns 112 and 114.

4.5.3. Caverns 105 and 108

The top and bottom of Caverns 105 and 108 are also excluded in the mesh as shown in Figure 44 to investigate the P/D effect for the same reason as mentioned in Section 4.5.1. The average radius of Cavern 105 increases from 91 ft to 129 ft in 15% increments of volume based on the five drawdown leaches. The average radius of Cavern 108 increases from 103 ft to 146 ft in 15% increments of volume based on the five drawdown leaches. Then the pillar thickness between the caverns decreases from 480 ft to 400 ft.

Figure 45 shows the predicted minimum safety factor for dilatancy as a function of minimum and standard P/D for Caverns 105 in the web of salt between Caverns 105 and 108 excluding the roof and floor. When the RD criterion for BH salt is applied to the dilatancy calculation, the safety factor decreases with the drawdown leaches. However, when the Van Sambeek criterion with C=0.18 and RD criterion for Cayuta salt are applied, the safety factor decreases until the 4th drawdown leach; and the dilatant damage is predicted starting with the initial leach. The safety factors increase abruptly after the 5th drawdown leach. This is an unusual phenomenon. The Cavern 105 has a narrow "waist" as shown in Figure 46 (center). The damage is predicted where the waist abruptly widens similar to the roof, which is enlarged in the leftmost figure. The horizontal cross-section at that elevation (right-top) shows that the damaged area (SF<1) is a ring shape i.e., the adjacent caverns do not affect the damaged zone. This damage is not a function of the P/D effect, because the P/D around this location is larger than that of any elevation. In general, a smaller P/D yields more structural damage in the pillar.

To investigate the P/D effect, this narrowest waist of Cavern 105 should be excluded to calculate the safety factor. Figure 47 shows the web salt between Caverns 105 and 108 above the waist. Table 17 lists the minimum P/Ds for Caverns 105 and 108 with the maximum diameters of the caverns and the related pillar thicknesses. The minimum P/Ds for Caverns 105 and 108 are calculated at the same elevation of -2420 ft. Table 18 lists the standard P/Ds for Caverns 105 and 108 with the average diameters of the caverns and the average thickness of the pillar between the caverns, and the minimum safety factors corresponding to the P/Ds. Note again that the average diameters and the average pillar thickness are calculated from the volume conserving cylinders as mentioned in Section 2.1.

Figure 48 shows the minimum safety factor of dilatancy as a function of minimum and standard P/D for Caverns 105 and 108. The safety factor values decrease with decreasing P/Ds. When the Van Sambeek criterion with C=0.18 is applied to the dilatancy calculation, the onsets of dilatant damage are predicted at 0.74 and 1.43 for minimum and standard P/Ds for Cavern 105, respectively; and at 0.86 and 1.31 for minimum and standard P/Ds for Cavern 108, respectively. The smallest P/D exists above the waist. Therefore, the investigation of P/D effect below the waist is omitted.

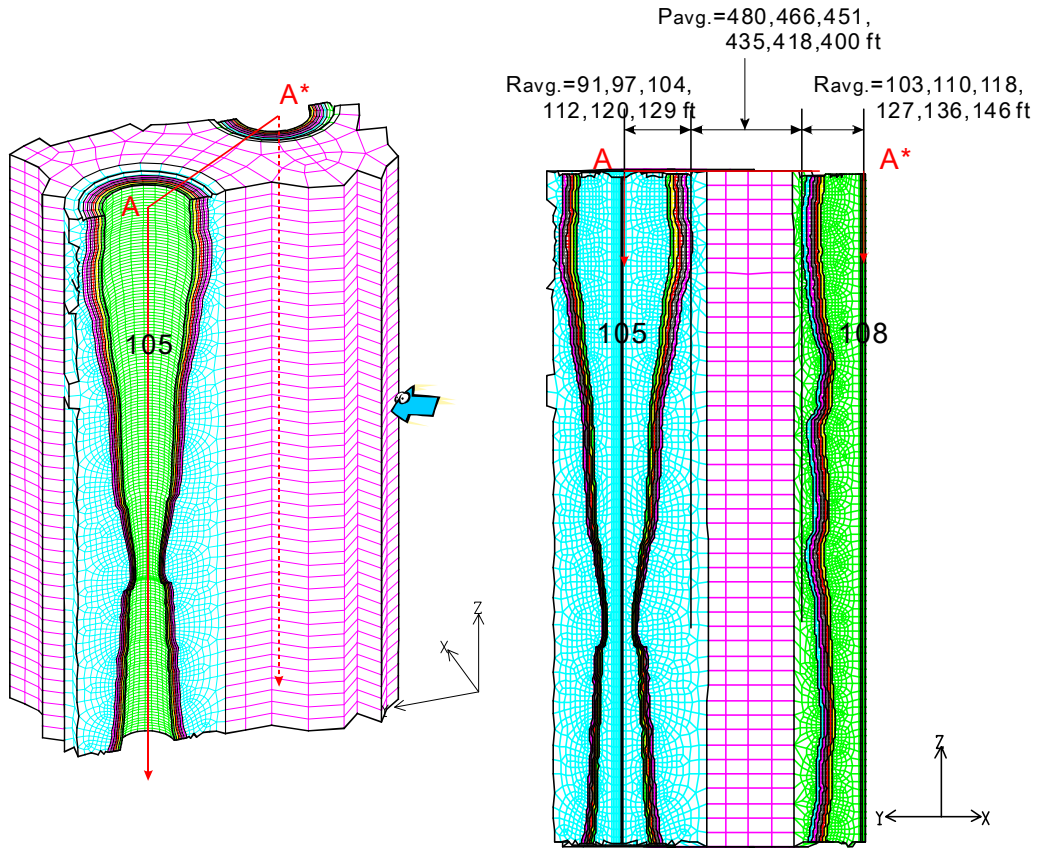

Figure 44: The mesh of web salt between Caverns 105 and 108 excluding the roof and floor in Bryan Mound.

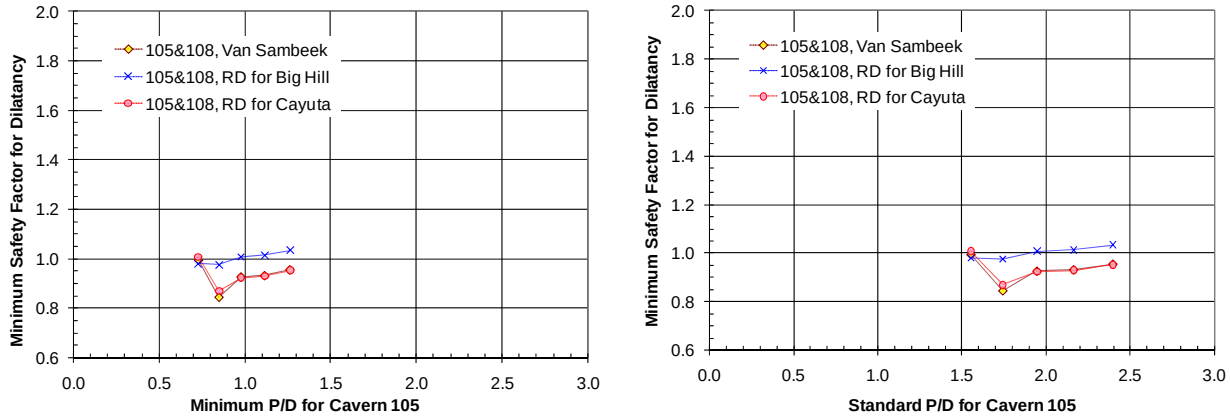

Figure 45: Minimum safety factor for dilatancy as a function of minimum and standard P/D for Cavern 105 in the pillar as shown Figure 44.

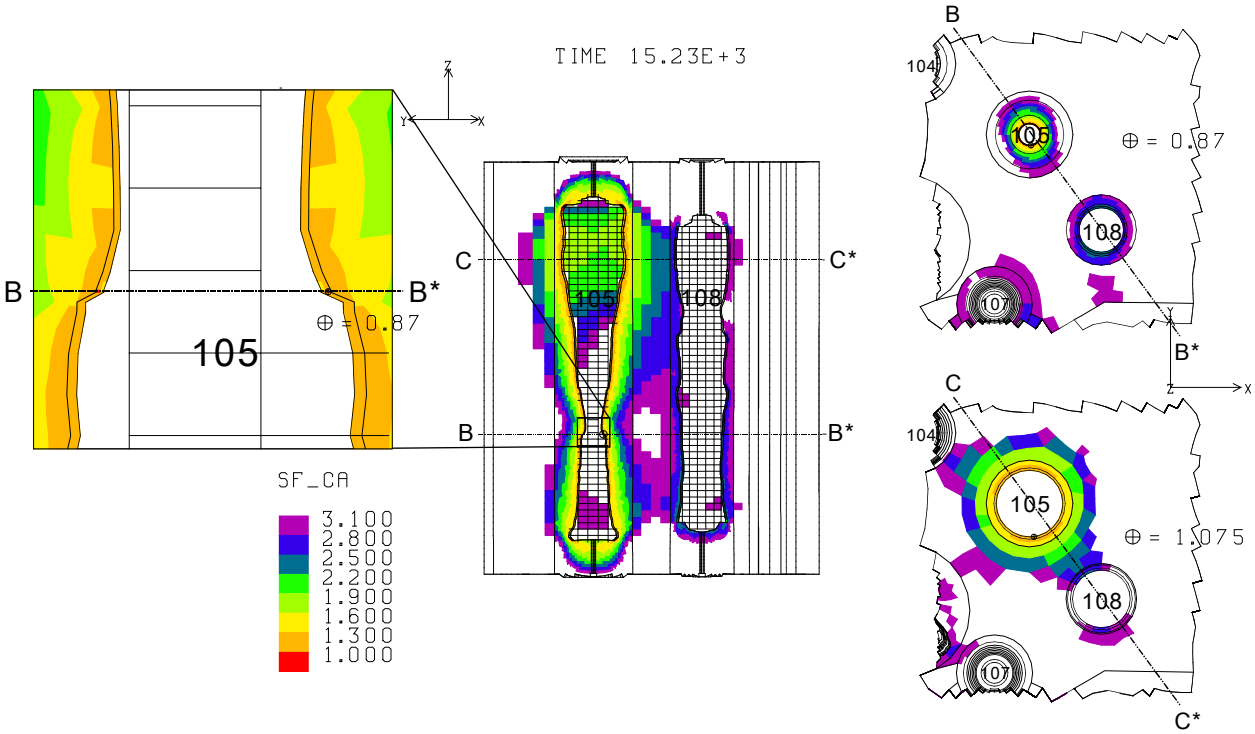

Figure 46: Predicted safety factor contours for dilatancy around Caverns 105 and 108 during workover of Cavern 105 at 15230 days (Center) with an enlarged view at the location where the dilatancy damage occurs in Cavern 105 (left). Horizontal cross-section at the elevation where the damage occurs (right-top). Horizontal cross-section at the elevation where the minimum P/D (right-bottom).

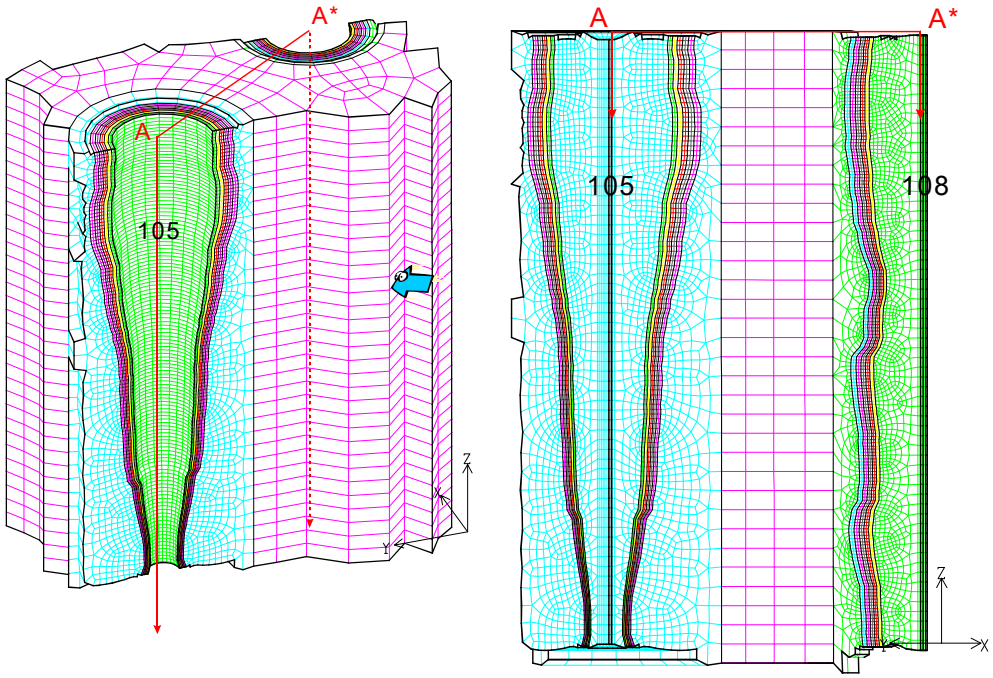

Figure 47: The mesh of web volume and Caverns 105 and 108 above the waist of Cavern 105.

Table 17: Minimum P/Ds in the web salt between Caverns 105 and 108.

Drawdowns	For Cav. 105 (at Ele. -2420 ft)				For Cav. 108 (at Ele. -2420 ft)			
	Maximum Diameter (ft)		Pillar Thickness (ft)	Minimum P/D for Cav.105	Maximum Diameter (ft)		Pillar Thickness (ft)	Minimum P/D for Cav.108
	Cav.105	Cav.108			Cav.105	Cav.108		
0	286	247	407	**1.42**	286	247	407	**1.65**
1	307	265	388	**1.26**	307	265	388	**1.46**
2	329	284	367	**1.12**	329	284	367	**1.29**
3	353	305	345	**0.98**	353	305	345	**1.13**
4	378	327	321	**0.85**	378	327	321	**0.98**
5	406	351	296	**0.73**	406	351	296	**0.84**

Table 18: Standard P/Ds in the web salt between Caverns 105 and 108 as shown Figure 44; and minimum safety factor for dilatancy in the web salt between Caverns 105 and 108 above the waist of Cavern 105.

Drawdowns	Avg. Diameter (ft)		Avg. Pillar Thickness (ft)	Standard P/D		Minimum Safety Factor		
	Cav. 105	Cav. 108		for Cav.105	for Cav.108	Van Sambeek (C=0.18)	RD for Cayuta salt	RD for Big Hill salt
0	193	212	471	**2.44**	**2.23**			
1	207	227	457	**2.20**	**2.01**	**1.079**	**1.086**	**1.082**
2	222	243	441	**1.98**	**1.81**	**1.063**	**1.075**	**1.068**
3	238	261	424	**1.78**	**1.63**	**1.050**	**1.068**	**1.057**
4	256	280	406	**1.59**	**1.45**	**1.038**	**1.057**	**1.046**
5	274	300	387	**1.41**	**1.29**	**0.995**	**1.007**	**1.014**

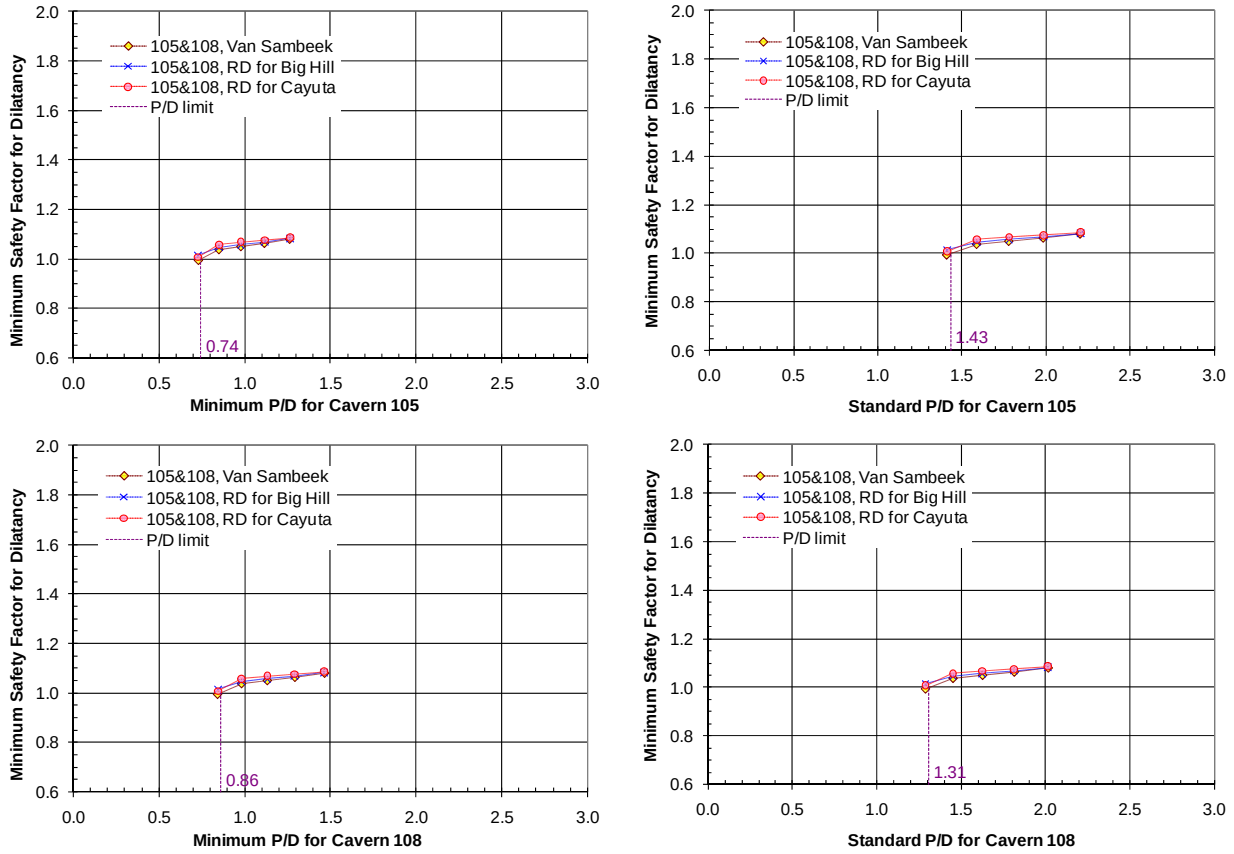

Figure 48: Minimum safety factor for dilatancy as a function of minimum and standard P/D for Caverns 105 and 108.

4.6. Half of Salt Dome Model for West Hackberry

To investigate the P/D effect, the analysis was conducted through ten drawdown leaches as mentioned in Section 3.6. Table 19 lists the radii of bottom, top and average; the minimum and standard P/Ds with ten drawdown leaches for Caverns 101 and 105. Table 20 lists the radii of bottom, top and average; the minimum and standard P/Ds with ten drawdown leaches for Caverns 109 and 110. The volumes of caverns grow approximately 15% for each leach.

Figure 49 shows the mesh used to examine the dilatancy damage with P/D for the web of salt between Caverns 101 and 105 within the West Hackberry salt dome (Figure 10) to examine the dilatancy damage with P/D. Figure 50 shows the minimum safety factor of dilatancy as a function of minimum and standard P/D for Cavern 105. When the RD criteria for Cayuta salt and Big Hill salt are applied, damage is predicted starting with the first drawdown. The safety factor does not decrease as the P/D decreases. Damage may occur at the cavern wall below the mid-height of Cavern 105 as shown in Figure 51 instead of at the roof where the P/D is least. This damage location is a result of local geometric effects rather than the P/D effect.

To investigate the P/D effect, the web volume is analyzed between the roof and 500 ft below the roof as shown Figure 52. The safety factor within this volume decreases as the P/D decreases as shown in Figure 53 because of the P/D effect. However, the dilatant damage is not expected through ten drawdown leaches for any of the criteria. The onset of dilatant damage is predicted at

less than 0.36 and 0.75 for minimum and standard P/Ds for Cavern 101, respectively; and at less than 0.38 and 0.79 for minimum and standard P/Ds for Cavern 105, respectively. The predicted minimum safety factor values with drawdown leaches within the web salt as shown in Figure 52 are listed in Table 21.

In a similar manner, the web volume investigated between Caverns 109 and 110 is also between the roof and 500 ft below the roof as shown Figure 54. The value of the safety factor in this volume decreases slightly with decreasing P/D for three criteria as shown in Figure 55. Again, dilatant damage does not occur through ten drawdown leaches. The safety factor values for Caverns 109 and 110 are larger than those for Caverns 101 and 105 because the pillar thickness of the web between 109 and 110 is larger at the same drawdown leach. The onset of dilatant damage is not predicted to occur through the tenth leach cycle.

Figure 56 shows the computational mesh for the web salt between Caverns 8 and 9 (left). The radius of the cavern at the floor of Cavern 8 is increased from 217 ft to 286 ft in 7.24% increments. The pillar thickness decreases from 86 ft to 16 ft. The minimum value of the safety factor is predicted to occur at the wall right above the floor of Cavern 8 during workover of Cavern 8 after the 5th drawdown leach. The vertical cross-section shows the damage zone in the pillar is caused by the small value of P/D. When the Van Sambeek criterion with C=0.18 and the RD criterion for Cayuta salt are applied to the dilatancy calculation, the onset of dilatant damage is predicted at 0.031 of minimum P/D for Caverns 8 and 9 as shown Figure 57.

Table 19: Minimum and standard P/Ds for Caverns 101 and 105.

Draw-down	Cavern 101 (Height=1800 ft)			Cavern 105 (Height=2000 ft)			Center to Center=750 ft			
	Radius (ft)			Radius (ft)			Minimum P/D		Standard P/D	
	Bottom	Top	Average	Bottom	Top	Average	For 101	For 105	For 101	For 105
0	73.00	139.00	107.70	70.00	133.00	103.12	**1.719**	**1.797**	**2.503**	**2.614**
1	78.28	149.06	115.49	75.07	142.63	110.58	**1.537**	**1.607**	**2.268**	**2.369**
2	83.95	159.85	123.85	80.50	152.95	118.58	**1.368**	**1.429**	**2.049**	**2.140**
3	90.03	171.42	132.82	86.33	164.02	127.17	**1.209**	**1.264**	**1.845**	**1.927**
4	96.54	183.83	142.43	92.58	175.89	136.37	**1.062**	**1.109**	**1.654**	**1.728**
5	103.53	197.13	152.74	99.28	188.62	146.24	**0.924**	**0.966**	**1.476**	**1.542**
6	111.02	211.40	163.80	106.46	202.28	156.83	**0.795**	**0.831**	**1.311**	**1.369**
7	119.06	226.70	175.65	114.17	216.92	168.18	**0.676**	**0.706**	**1.156**	**1.208**
8	127.68	243.11	188.37	122.43	232.62	180.35	**0.564**	**0.590**	**1.012**	**1.057**
9	136.92	260.71	202.00	131.29	249.45	193.41	**0.460**	**0.481**	**0.878**	**0.917**
10	146.83	279.58	216.62	140.80	267.51	207.40	**0.363**	**0.379**	**0.752**	**0.786**

Table 20: Minimum and standard P/Ds for Caverns 109 and 110.

Draw-down	Cavern 109 (Height=2000 ft)			Cavern 110 (Height=2000 ft)			Center to Center=750 ft			
	Radius (ft)			Radius (ft)			Minimum P/D		Standard P/D	
	Bottom	Top	Average	Bottom	Top	Average	For 109	For 110	For 109	For 110
0	84.00	122.00	103.58	78.00	120.00	99.74	**2.082**	**2.117**	**2.639**	**2.741**
1	90.08	130.83	111.08	83.65	128.69	106.96	**1.875**	**1.906**	**2.394**	**2.487**
2	96.60	140.30	119.12	89.70	138.00	114.70	**1.681**	**1.709**	**2.167**	**2.250**
3	103.59	150.45	127.74	96.19	147.99	123.00	**1.501**	**1.526**	**1.954**	**2.029**
4	111.09	161.35	136.99	103.16	158.70	131.91	**1.332**	**1.355**	**1.756**	**1.824**
5	119.13	173.02	146.90	110.62	170.19	141.45	**1.176**	**1.195**	**1.571**	**1.632**
6	127.75	185.55	157.54	118.63	182.51	151.69	**1.029**	**1.046**	**1.399**	**1.453**
7	137.00	198.98	168.94	127.21	195.71	162.67	**0.893**	**0.908**	**1.238**	**1.286**
8	146.92	213.38	181.17	136.42	209.88	174.45	**0.766**	**0.778**	**1.088**	**1.130**
9	157.55	228.82	194.28	146.30	225.07	187.07	**0.647**	**0.658**	**0.949**	**0.985**
10	168.95	245.39	208.34	156.89	241.36	200.61	**0.536**	**0.545**	**0.818**	**0.850**

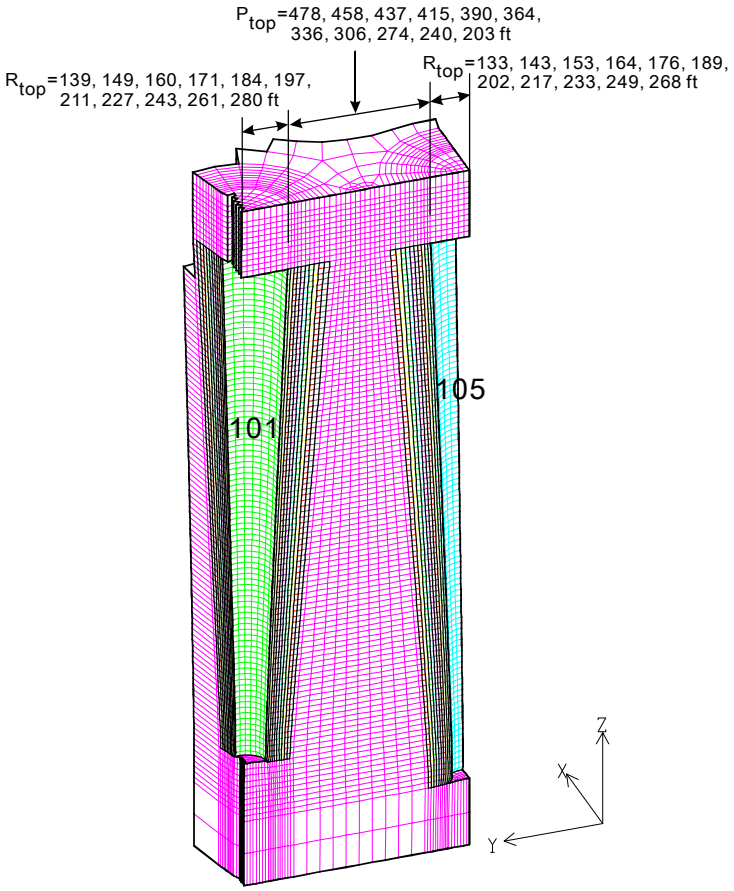

Figure 49: The mesh of web salt modeled between Caverns 101 and 105 within West Hackberry salt dome.

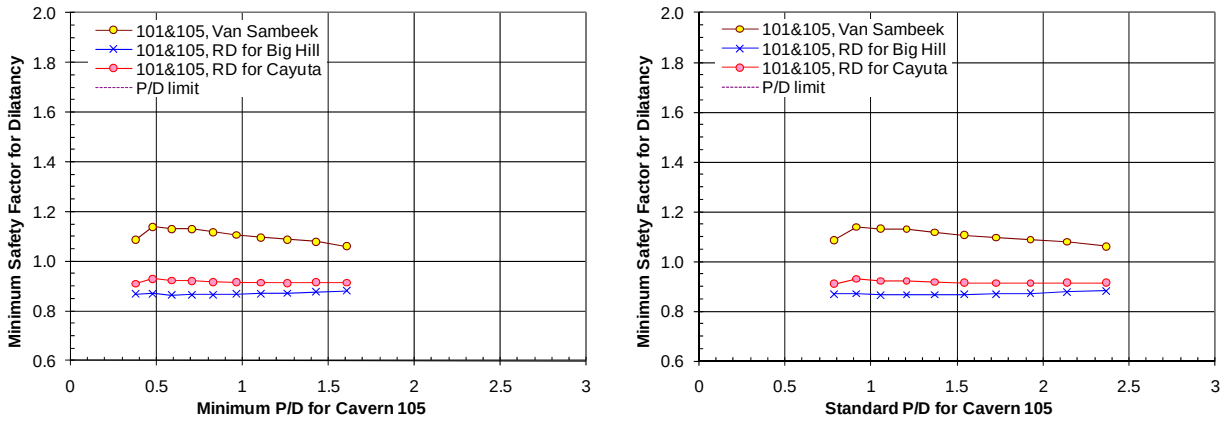

Figure 50: Minimum safety factor for dilatancy as a function of minimum and standard P/D for Cavern 105 in the pillar as shown Figure 49.

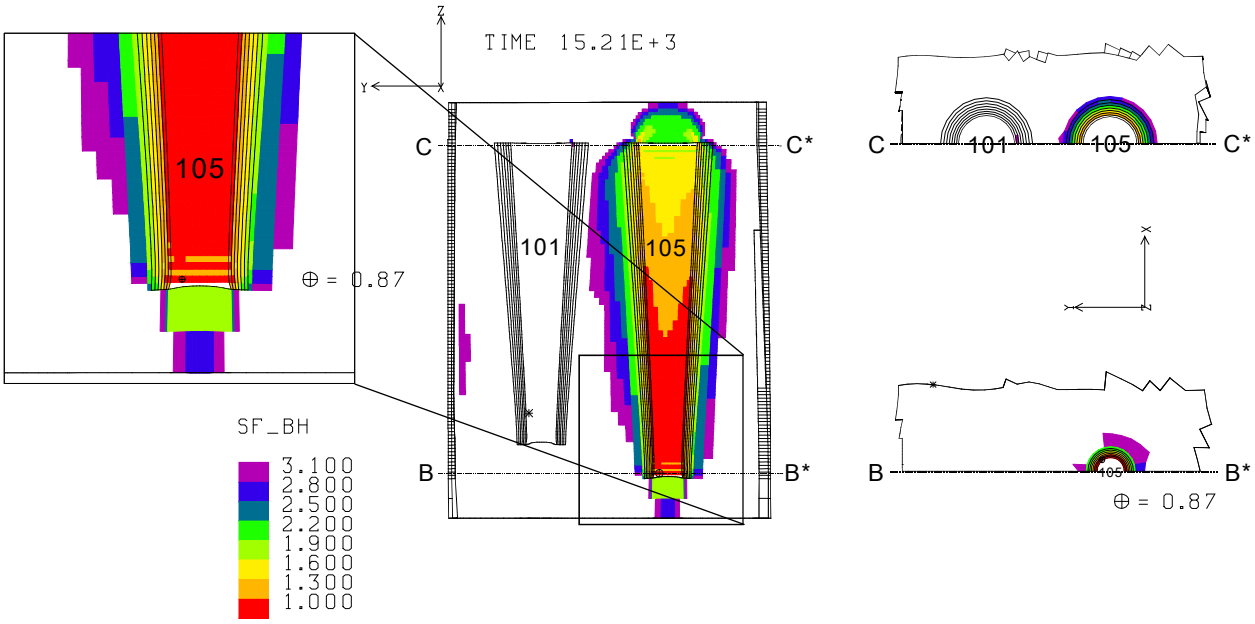

Figure 51: Predicted safety factor contours for dilatancy around Caverns 101 and 105 during workover of Cavern 105 after the 4th drawdown leach (Center) with an enlarged view of the location where the dilatancy damage occurs in Cavern 105 (left). Horizontal cross-section at the elevation where the minimum P/D (right-top). Horizontal cross-section at the elevation where the damage occurs (right-bottom).

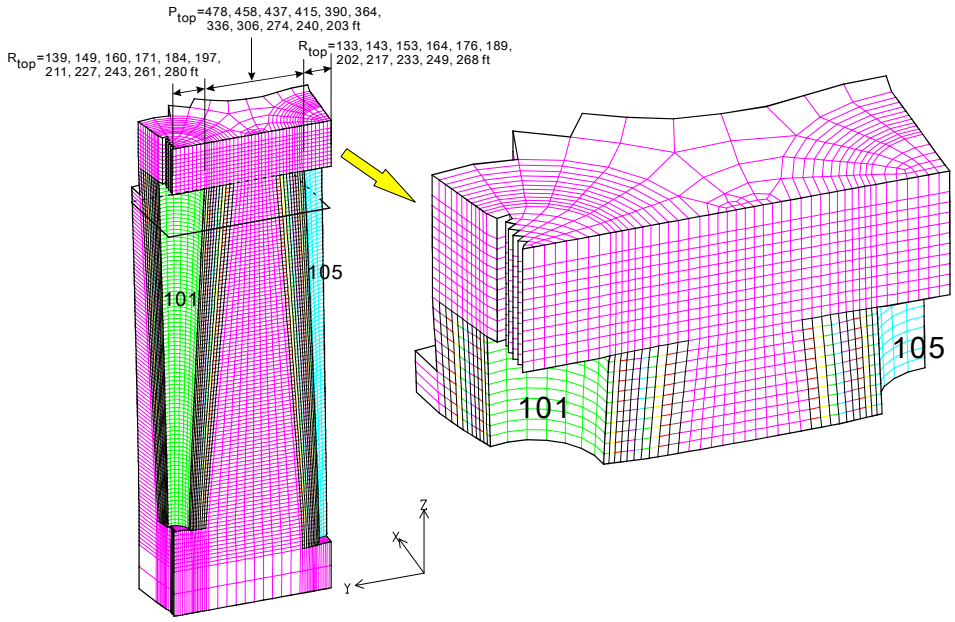

Figure 52: The mesh of web volume between Caverns 101 and 105 (left) and the volume between the roof and 500 ft below the roof (center), and minimum safety factor of dilatancy as a function of minimum (right-top) and standard P/D (right-bottom) in this volume.

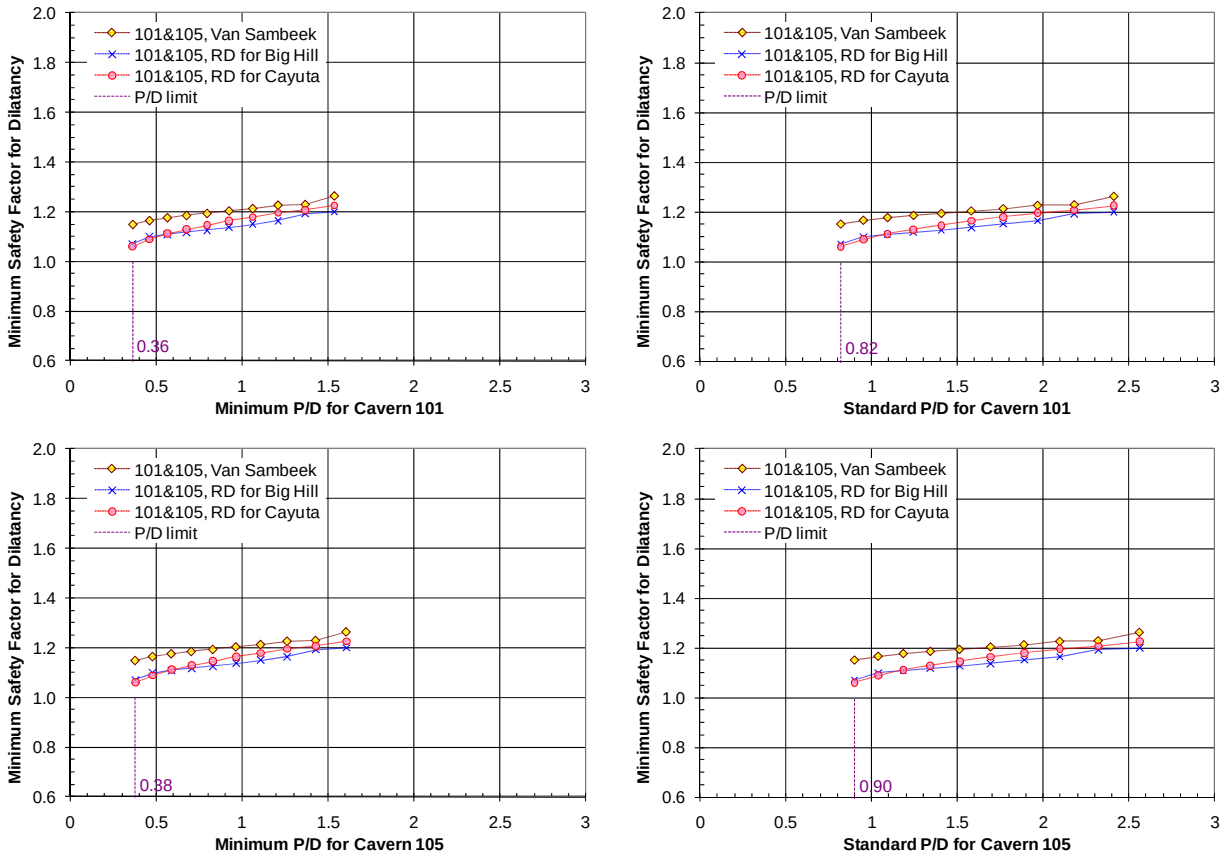

Figure 53: Minimum safety factor for dilatancy as a function of minimum and standard P/D for Caverns 101 and 105.

Table 21: Minimum safety factor for dilatancy within the web salts between Caverns 101 and 105; Caverns 109 and 110.

Drawdown	Web salt between 101 and 105			Web salt between 109 and 110		
	Van Sambeek (C=0.18)	RD for Cayuta salt	RD for Big Hill salt	Van Sambeek (C=0.18)	RD for Cayuta salt	RD for Big Hill salt
0	**1.262**	**1.336**	**1.506**	**1.309**	**1.359**	**1.538**
1	**1.263**	**1.225**	**1.200**	**1.241**	**1.209**	**1.269**
2	**1.229**	**1.207**	**1.192**	**1.226**	**1.200**	**1.254**
3	**1.226**	**1.195**	**1.164**	**1.230**	**1.199**	**1.234**
4	**1.213**	**1.179**	**1.151**	**1.226**	**1.190**	**1.223**
5	**1.203**	**1.164**	**1.137**	**1.223**	**1.182**	**1.211**
6	**1.193**	**1.145**	**1.126**	**1.223**	**1.178**	**1.203**
7	**1.185**	**1.128**	**1.117**	**1.226**	**1.178**	**1.198**
8	**1.176**	**1.111**	**1.108**	**1.230**	**1.178**	**1.193**
9	**1.165**	**1.089**	**1.099**	**1.235**	**1.179**	**1.186**
10	**1.149**	**1.060**	**1.071**	**1.246**	**1.187**	**1.171**

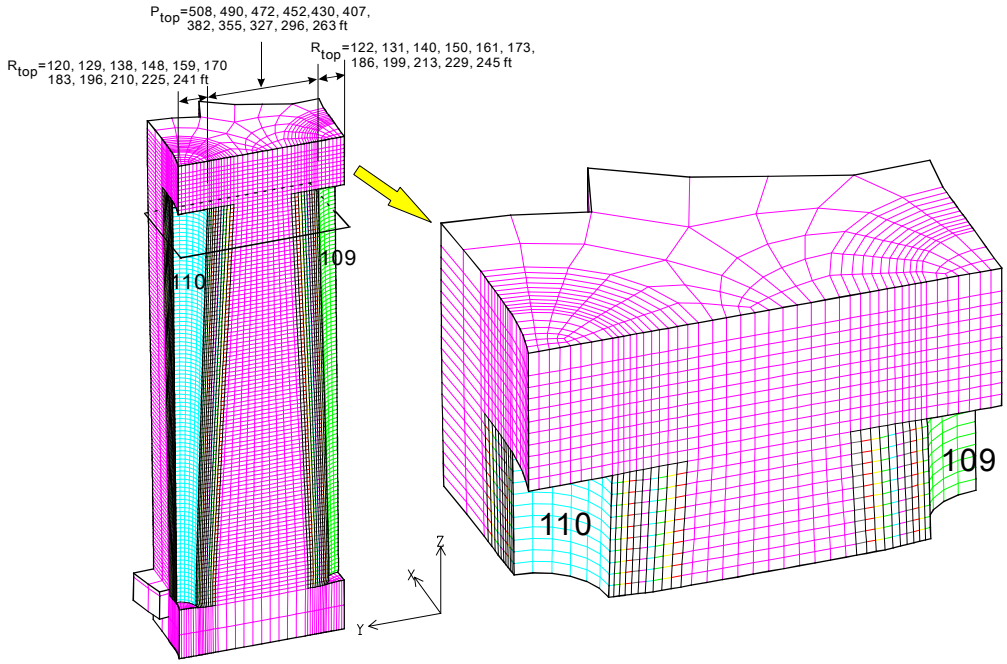

Figure 54: The mesh of web volume between Caverns 109 and 110 (left) and the volume between the roof and 500 ft below the roof.

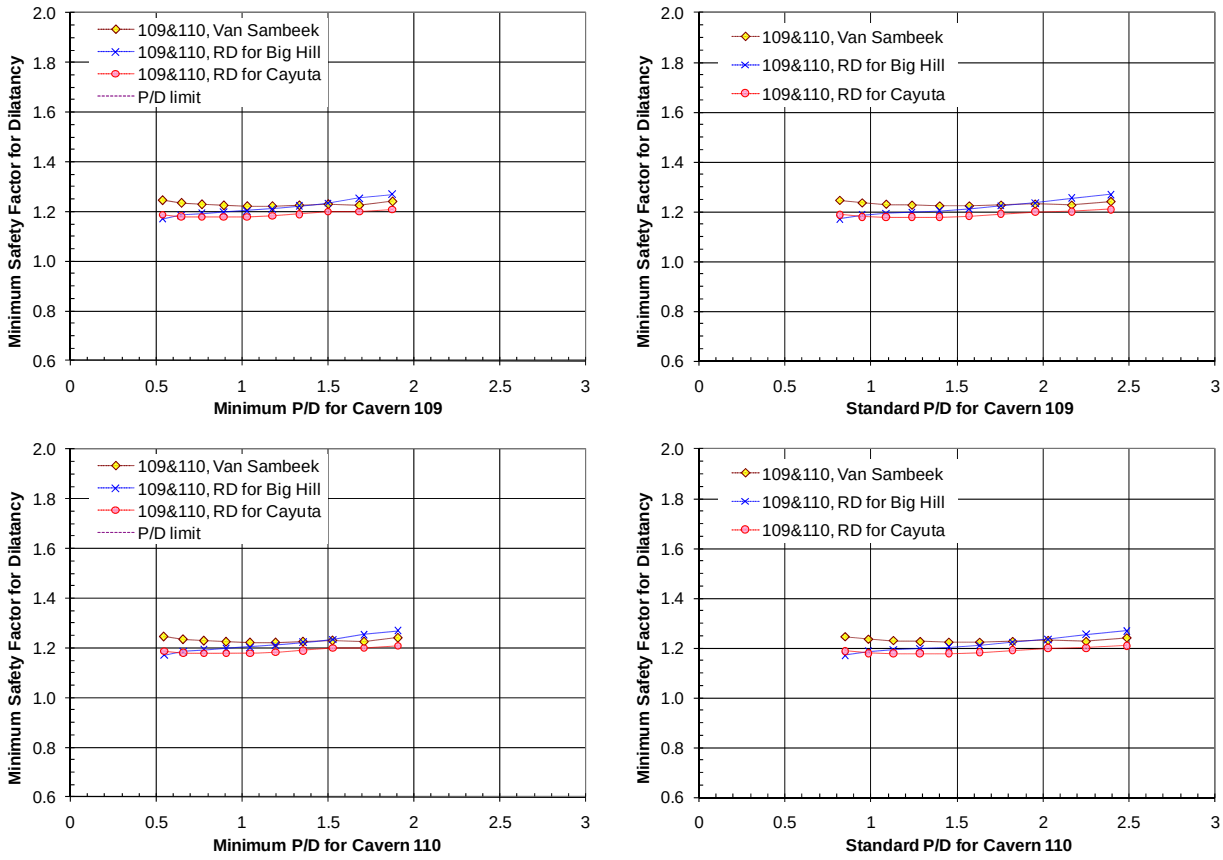

Figure 55: Minimum safety factor for dilatancy as a function of minimum and standard P/D for Caverns 109 and 110 within the web volume as shown in Figure 54.

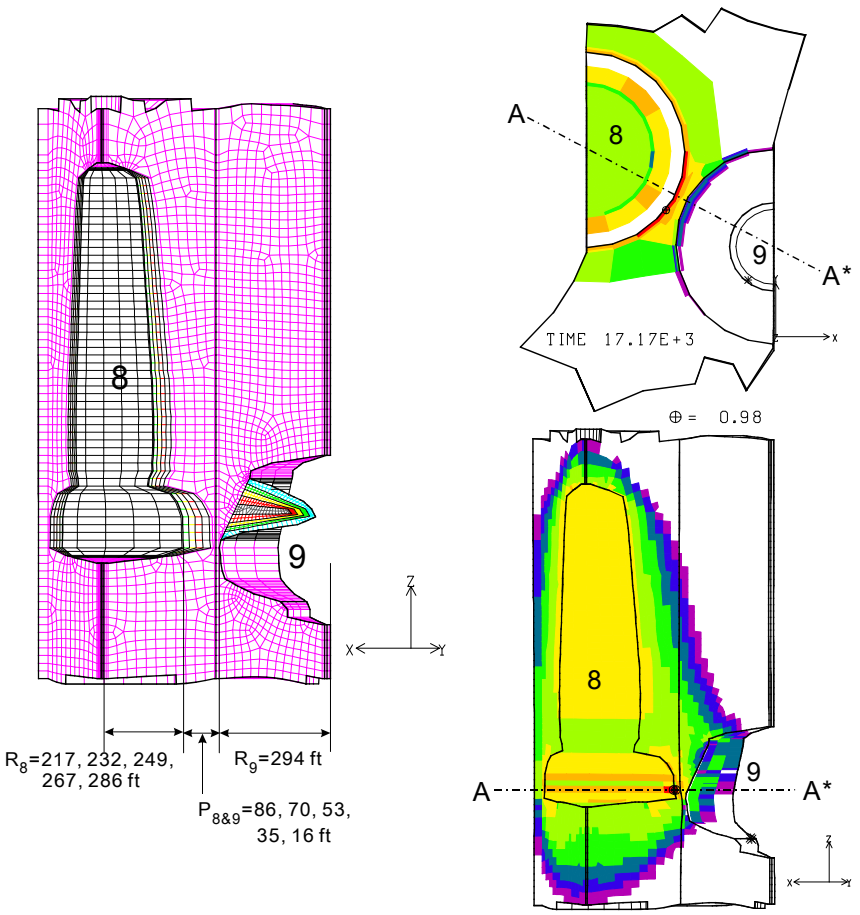

Figure 56: The mesh of web salt between Caverns 8 and 9 in West Hackberry salt dome (left), predicted safety contours for dilatancy during workover of Cavern 8 after the 5th drawdown leach (center, the vertical cross-section through the center of caverns and the horizon cross-section at the elevation where the dilatancy damage occurs).

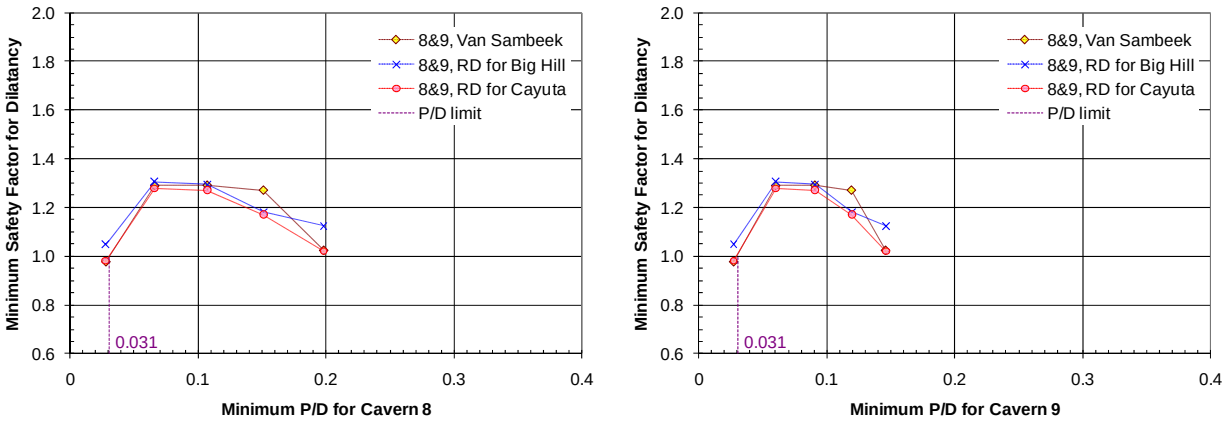

Figure 57: Minimum safety factor for dilatancy as a function of minimum and standard P/D for Caverns 8 and 9.

5. SUMMARY AND CONCLUDING REMARKS

To establish a limit for the spacing between SPR caverns in salt domes, the results from existing geomechanical analyses were post-processed using the Van Sambeek criterion with C=0.18 and RD criterion considering the Lode angle. The webs of salt between the SPR caverns that are relatively close to each other in four salt domes were selected to examine the P/D effect. The P/Ds at the predicted onset of dilatant failure for the various pillars between caverns are summarized in Table 22. Note again that the modeled caverns in the numerical analyses for WH, BH, and BC sites were simplified to the cylindrical shapes using volume conserving cylinders. Therefore, "Standard P/D" only was calculated.

Table 22: P/Ds at the onset of dilatant damage for various webs of salt between caverns.

	Description		Minimum P/D	Standard P/D
Cavern to Cavern	19-cavern 18-drawdown model in WH		N/A	0.55
	Cavern shape study	Cylindrical caverns	N/A	1.43
		Enlarged bottom caverns	0.78	1.31
		Enlarged middle caverns	0.43	0.75
		Enlarged top caverns	**1.25**	2.15
	19-cavern model in BH		N/A	0.35
	31-cavern model in BH		N/A	No decrease through five leaches, less than 1.34
	Caverns 15 and 17 in BC	For Cavern 15	N/A	0.39
		For Cavern 17	N/A	0.65
	Caverns 103 and 111 in BM	For Cavern 103	**1.00**	1.35
		For Cavern 111	**1.16**	1.43
	Caverns 112 and 114 in BM	For Cavern 112	0.95	1.42
		For Cavern 114	0.92	1.81
	Caverns 105 and 108 in BM	For Cavern 105	0.74	1.43
		For Cavern 108	0.86	1.31
	Caverns 101 and 105 in WH	For Cavern 101	Less than 0.36	Less than 0.82
		For Cavern 105	Less than 0.38	Less than 0.90
	Caverns 109 and 110 in WH	For Cavern 109	Less than 0.54	Less than 0.82
		For Cavern 110	Less than 0.55	Less than 0.85
	Caverns 8 and 9 in WH		0.03	0.03
Cavern to Dome Edge	Cavern 5 and dome perimeter in BH		N/A	No decrease through five leaches, less than 0.33
	Cavern 20 and dome perimeter in BC		N/A	No decrease through five leaches, less than 0.40

where, WH is West Hackberry, BH is Big Hill, BC is Bayou Choctaw, and BM is Bryan Mound salt dome. N/A is because of cylindrical cavern geometry.

In general, P/Ds are relative indices, not absolute measures. In solution-mined caverns, P/Ds tend to indicate the extreme and not the average conditions. P/Ds can be evaluated only between pairs of caverns, and even then, the value is not unique because the diameters of the caverns and the thickness of the pillar between them vary as a function of depth and direction. This ambiguity in the P/D is reflected by two different definitions of P/Ds (Eq. (1) and (2)). Regardless of the definition, the P/D for a cavern pair always is based in some sense on extremes (e.g., minimum pillar thickness, maximum cavern diameter, or the minimum ratio between the thickness and diameter) [Osnes, 2010]. Therefore, *the minimum P/D rather than the standard P/D is recommended as an index to assess the structural integrity*.

The Bryan Mound caverns show relatively low safety factors, which yield relatively large P/Ds at the onset of dilatant damage, in part due to the relatively hard salt. Table 23 lists the current minimum P/D obtained from sonar measurement data as described in Appendix I and the predicted minimum safety factors for dilatancy using three different dilation criteria. The current minimum P/Ds of Caverns 1, 2, 4, and 5 are less than 1.0. The corresponding safety factors for these caverns are also predicted to be less than 1. However these caverns are in stable condition according to the field observations. It would appear reasonable to make an exception for the P/D (currently Table 22 constrains the P/D to 1.16) of Cavern 111 in BM to 1.0. Also supportive of this is the relatively low incident of salt falls in the cavern. Cavern 111 has experienced only one salt fall in its 30 year history as compared to a median of three for the site, with some caverns ranging up to ten salt falls historically [Mansure and Ehgartner, 2007].

Table 23: Current minimum P/D and the predicted minimum safety factors for dilatancy using three dilatation criteria for Caverns 1, 2, 3, and 4 in Bryan Mound salt dome.

BM Cavern	Minimum P/D	Minimum Safety Factor		
		Van Sambeek (C=0.18)	RD for Cayuta salt	RD for Big Hill salt
1	**0.52**	**0.44**	**0.71**	**0.85**
2	**0.92**	**0.40**	**0.75**	**0.94**
4	**0.56**	**0.97**	**0.99**	**0.97**
5	**0.61**	**0.44**	**0.72**	**0.90**

The shapes study is different from the other studies in that the caverns were leached to their full size over one year and no further growth occurred. Because large diameter caverns were modeled in the shapes study, it enabled us to compare initially small P/Ds to similar ratios that were derived in other models, particularly the 19-cavern Big Hill model, through progressive leaching over many years associated with oil drawdowns. The comparison of results shows that the shapes study produced adverse conditions. It is believed that the sudden development of large caverns is more restrictive than a program that slowly enlarges caverns over many years. It appears reasonable to make an exception for the P/D of the enlarged top cavern, which currently constrains the P/D to 1.25, to 1.0. In this report, we conclude that the P/D criteria for the existing sites can be safely reduced to a value of 1.0, but the shapes study shows that for new sites, the initial P/D should be larger. The P/D for a new site should be selected based on site specific analyses that include properties derived from testing.

In conclusion, *a minimum P/D of 1.0 is recommended for the existing caverns in the SPR*. The analyses suggest that lower P/Ds may be tolerated for caverns that are leached over time during the infrequent oil drawdowns, in comparison to new cavern fields which currently have a design limitation of 1.78 for the P/D. New cavern fields must be evaluated based in part on their salt

properties and cavern shapes. Factors influencing cavern stability and acceptability of a site are discussed in more detail in Park and Ehgartner [2009]. While site and even cavern specific P/Ds could be established, the DOE prefers to have a single P/D criterion for the entire reserve. As such 1.0 was selected based on the limitations presented with the BM analyses. Arguably, the other sites could have a lower P/D, and with additional detailed cavern modeling, the allowable P/D and hence number of oil drawdowns could be defined for each cavern. The P/D is a relative index and not an absolute reference or measure of the structural integrity of caverns. Other geometrical and geological effects (e.g., stress concentrations associated with surface irregularities and anomalous zones within the salt body) may cause a cavern to fail before pillar failure is indicated by the P/D.

6. REFERENCES

DeVries, K.L., K. D. Mellegard, and G.D. Callahan, 2003. Laboratory Testing in Support of Bedded Salt Failure Criterion, RESPEC, Technical Paper of *Solution Mining Research Institute, Fall 2003 Meeting 5-8 October 2003, Chester, United Kingdom, England*.

DeVries, K.L., 2006. Geomechanical Analyses to Determine the Onset of Dilation around Natural Gas Storage Caverns in Bedded Salt, RESPEC, Technical Conference Paper of *Solution Mining Research Institute, Spring 2006 Conference, 30 April-3 May, Brussels, Belgium*.

DOE (Department of Energy), 2001. *Design Criteria- Level III*, US Department of Energy, Strategic Petroleum Reserve. New Orleans, LA, November, 2001.

Ehgartner, B.L. and Sobolik, S.R., 2002. *3-D Cavern Enlargement Analyses*, SAND2002-0526, Sandia National Laboratories, Albuquerque, NM 87185-0706.

Lord, A.S., D.K. Rudeen, and B.L. Ehgartner, 2009. *List of P/D Ratios of All Caverns and the Allowable Number of Full Drawdowns until P/D ratios of 1.78 and 1.0 are Reached,* Subtask 1.7 (a1), Memorandum to Wayne Elias (DOE) dated January 30, 2009. Sandia National Laboratories, Albuquerque, NM.

Mansure, A.J. and B.L. Ehgartner, 2007. *Update on Hanging String Failures Statistics.* Letter Report to R.E. Myers, April 2. Sandia National Laboratories, Albuquerque, NM.

Osnes, J.D., 2010. *Technical Review of Pillar-to-Diameter Ratio Study Performed by Sandia National Laboratories for the Strategic Petroleum Reserve*, Memorandum to Ms. Lisa Eldredge dated September 21, 2010.

Park, B.Y., B.L. Ehgartner, M.Y. Lee, and S.R. Sobolik, 2005. *Three Dimensional Simulation for Big Hill Strategic Petroleum Reserve (SPR)*, SAND2005-3216, Sandia National Laboratories, Albuquerque, NM.

Park, B.Y., B.L. Ehgartner, and M.Y. Lee, 2006. *Three Dimensional Simulation for Bayou Choctaw Strategic Petroleum Reserve (SPR)*, SAND2006-7589, Sandia National Laboratories, Albuquerque, NM.

Park, B.Y. and B.L. Ehgartner, 2009. *Sensitivity of Storage Field Performance to Geologic and Cavern Design Parameters in Salt Domes*, SAND2009-1278, Sandia National Laboratories, Albuquerque, NM.

Park, B.Y., C.G. Herrick, and D.J. Holcomb, 2008. Prediction of the Extent of the Disturbed Rock Zone around a WIPP Disposal Room, SAND2008-1164C, Paper No. 8057, Session 71, *Proceedings of WM2008 Symposia, Phoenix, AZ, USA, February 24-28, 2008*.

Ratigan, J. L., L. L. Van Sambeek, K. L. DeVries, and J. D. Nieland, 1991. *The Influence of Seal Design on the Development of the Disturbed Rock Zone in the WIPP Alcove Seal Tests*, RSI-0400, prepared by RE/SPEC Inc., Rapid City, SD, for Sandia National Laboratories, Albuquerque, NM.

Sobolik, S.R. and Ehgartner, B.L., 2006. *Analysis of Cavern Shapes for the Strategic Petroleum Reserve*, SAND2006-3002, Sandia National Laboratories, Albuquerque, NM.

Sobolik, S.R. and Ehgartner, B.L., 2009 a. *Analysis of Cavern Stability at the West Hackberry SPR site*, SAND2009-2194, Sandia National Laboratories, Albuquerque, NM

Sobolik, S.R. and Ehgartner, B.L., 2009 b. *Analysis of Cavern Stability at the Bryan Mound SPR site*, SAND2009-1986, Sandia National Laboratories, Albuquerque, NM

Van Sambeek, L., J. Ratigan, and F. Hansen, 1993. *Dilatancy of Rock Salt in Laboratory Tests*, Proc. 34th U.S. Symposium on Rock Mechanics, p.245-248.

APPENDIX I: MEMORANDUM ABOUT PILLAR TO DIAMETER RATIOS OF SPR CAVERNS AND ALLOWABLE NUMBERS OF DRAWDOWNS

Sandia National Laboratories
Operated for the U.S. Department of Energy by
Sandia Corporation

Albuquerque, New Mexico 87185-0706

date: January 30, 2009

to: Wayne Elias, SPRMO

from: Anna S. Lord, 6312
David K. Rudeen, 6711
Brian L. Ehgartner, 6312

subject: List of P/D ratios of all caverns and the allowable number of full drawdowns until P/D ratios of 1.78 and 1.0 are reached, Subtask 1.7 (a1).

DOE held a working meeting August 11, 2008, via videoconference, to discuss pillar to diameter (P/D) ratios. At this meeting Sandia stated that many of the Strategic Petroleum Reserve (SPR) caverns would likely be out of compliance with the SPR Level III Design Criterion, which defines that each cavern should posses a P/D ratio of 1.78 or greater after 5 complete fill and drawdown cycles (DOE, 2001). In response, DOE requested that Sandia define the number of drawdowns for each of the 62 SPR caverns until 1.78 P/D criterion is reached, and a P/D of 1.0 based on previous geomechanics analyses by Ehgartner and Sobolik (2002, 2006). This request is listed as activity (a1) under task 1.7 (Pillar to Diameter Ratio Activity), with a deliverable of a letter report due January 31, 2009.

> Subtask 1.7 (a1): Compile a list of P/D ratios of all caverns and the number of full drawdowns until P/Ds of 1.78 and 1.0 are reached.

To perform this analysis a set of leaching assumptions were determined and modifications were made to Sandia's WinP2D program (Rudeen and Lord, 2007), which is a tool used to monitor P/D ratios by identifying specific regions of each cavern, using the most current sonar survey, that are contributing the most to current P/D values. See the appendix for list of P/D ratios and the number of allowable drawdowns for each cavern at each SPR site.

Background

The pillar to diameter ratio (P/D) is a measure used to establish a limit for the spacing between phase-3 salt caverns used by the Strategic Petroleum Reserve (SPR). This quantity is defined in the Level III Design Criteria for the SPR (2001). "Pillar" refers to the thickness of the web of salt remaining between any two adjacent caverns, or between the cavern and salt dome perimeter. "Diameter" refers to the cavern diameter. However, it is important to mention that the definition for determining P/D ratios is not well defined and is so noted below.

Requirements, Level III Design Criteria for the SPR (2001)

(1) Page 2-9, last paragraph under 2.4.2 "Physical Characteristics",

*The ratio of the web or pillar **average** thickness (P), between two adjacent caverns, to **average** final cavern diameter (D) shall not be less than 1.78.*

(2) Page 2-10, under 2.4.2.2 "Spacing and Proximity Criteria",

*"Pillar" refers to **minimum** thickness of the web of salt remaining between any two adjacent caverns after the last leaching process, or between cavern and salt dome perimeter. . . D **is cavern diameter** after five complete fill and drawdown cycles; P **is pillar width** after five complete fill and drawdown cycles.*

The inconsistencies within the Level III Criteria leave it up to the reader to determine the method for calculating P/D ratios (e.g., define "pillar" as, (1) the minimum web thickness, or (2) the overall average web thickness).

To ensure cavern structural integrity, the Level III criteria mandate that the P/D ratio for each cavern must remain greater than 1.78 after five complete drawdown cycles. The Level III criteria were developed in 1983 to guide design, leaching, and operation of SPR caverns.

Procedure

In order to perform this task several assumptions where decided upon. It was determined that cavern leaching will occur as predicted by Levin (2004), scenario 3. Scenario 3 assumptions are as follows:

- Caverns are refilled to capacity
- Hanging strings are adjusted following each drawdown to maintain a 20 ft distance off the floor
- Volume of salt to be leached will be approximately 15 percent of the cavern volume above the bottom of the hanging string.

A simple leaching function was created from the results presented in Levin (2004) of Sansmic simulations performed on Big Hill caverns. The leaching equation is a function of distance above the hanging string and cavern radius. The following equation is used to determine the change in cavern radius due to leaching:

$$\frac{dr}{\bar{r}} = Ce^{-0.001344h} \qquad (1)$$

C is defined as a tuning coefficient; dr is the change in radius, $\bar{r}$ is the average cavern radius and h is the distance above the bottom of the hanging string, z_{HS}. Note that $\bar{r}$ and dr are functions of elevation z, and $h = z - z_{HS}$

For each leach of each cavern the tuning coefficient, C, is adjusted until the change in cavern volume above the hanging string is 15 percent. An initial value of $C = 0.2433$ was used. The leach function was compared to leaching simulations performed by Levin (2004) for a typical Big Hill Cavern. See Figure 1.

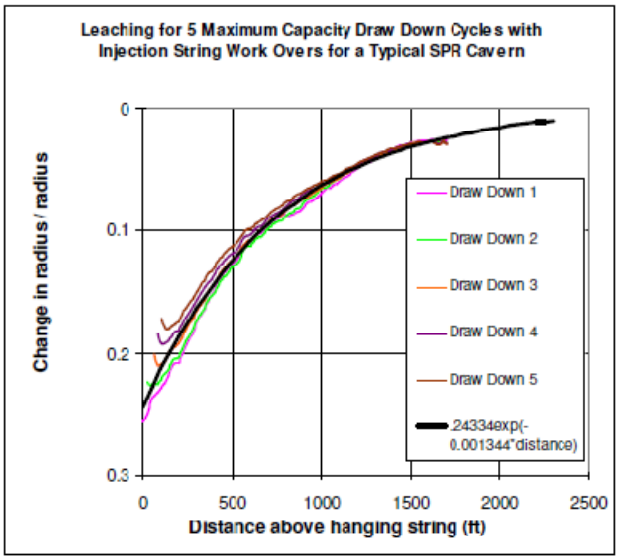

Figure 1. Leaching function compared to Sansmic predictions.

The effect of the leaching equation on typical phase-3 caverns is demonstrated in Figure 2, which shows profiles of Big Hill caverns 101 and 102 using average radius as a function of elevation. Shown in Figure 2 are cavern profiles for no leaching, and after 1, 2, 3, 4 and 5 leaches. Note the bell-shape pattern. Consequences of the leach pattern are discussed in a following section.

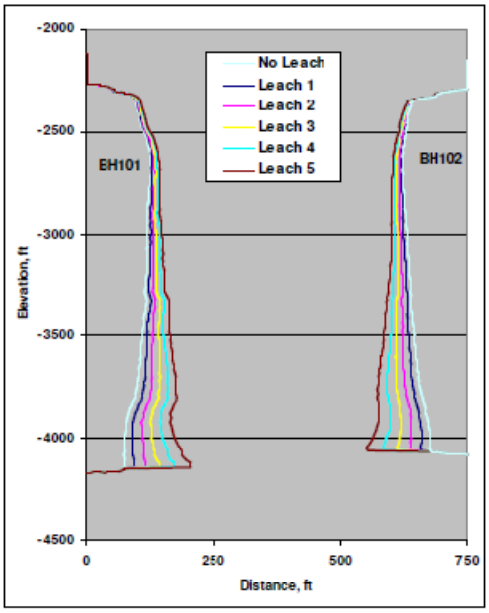

Figure 2. Profiles of Big Hill caverns 101 and 102 using average radius as a function of depth for no leaching, and after 1, 2, 3, 4 and 5 leaches. Distance is measured from center of B-101. X-Scale is exaggerated by ~2. Only one half of each cavern is shown due to symmetry.

WinP2D Modifications

The WinP2D program calculates a P/D ratio for each node or point that defines the 3D surface of the cavern. For each point on a cavern mesh the 3D-P/D ratio is equal to the minimum distance from that point to neighboring caverns divided by the average diameter of the cavern at the elevation of the point. The program calculates the P/D values using the most recent sonar data available. For this task the code was modified to include cavern leaching in order to determine the number of drawdowns that could occur for each cavern before a P/D of both 1.78 and 1.0 is reached.

Modifications made to the WinP2D program are as follows:

1. *A summary table is created* for the UCD version of the sonar files associated with selected caverns during a preprocessor phase of WinP2D. The table includes,
    - cavern volume
    - average radius as a function of elevation
    - volume increments between elevation increments,
    - top-of-cavern elevation (maximum elevation with cavern average radius > 5) and cavern floor (minimum elevation with radius > 5)
    - number of sonar readings per depth station
    - number of depth stations and
    - flags for depths stations with non-horizontal tilt angles

    For non-zero tilt angles, the elevation coordinate of the cavern wall-point will vary with cavern radius. Therefore, an average wall-point elevation is determined for the set of non-horizontal sonar readings at given depth station. This results in a projection of the actual cavern perimeter on to a horizontal plane which greatly simplifies cavern volume calculations. The approximation is good for small tilt angles but can introduce significant errors as tilt angles become large and sonar readings overlap with readings from other depth stations. Typically, non-zero tilt angles are used in small regions near the top and bottom of a cavern and errors introduced by the planar approximations do not affect overall cavern volumes significantly.

    The primary information used from the UCD summary table is the cavern floor elevation from which hanging string elevation is calculated. Currently, hanging string elevation is set to 20 feet above the cavern floor and remains fixed for all drawdown leaches of a cavern. Hanging string elevations are manually input into the WinP2D configuration file and therefore, can be specified as desired.

2. The *calculation of the cavern volume*, or the volume enclosed by the UCD mesh sonar data is an important aspect of the analysis implemented in WinP2D. The accurate volume calculation enclosed by the 3D surface mesh is a complicated numerical problem. If the mesh nodes exist in horizontal planes the problem can be greatly simplified to the summation of volumes of stacked disks. The problem is reduced to areas of complicated bounded planar surfaces, which can be approximated with circles.

    Two methods to address the volume calculations have been programmed into WinP2D – (1) the area of a circle using the average of the radii from a center point to each point on the boundary, and (2) summation of the areas of triangles formed from the surface center point and two consecutive points on the enclosing boundary.

The area determined by method (1) is *dependent* on the location of the center point within the area; method (2) is exact and independent of the center point, if the enclosing points are assumed to be connected by straight lines. The center point is usually the location of the sonar tool. Method (1) can be improved by using a center point actually "centered" within the area. In both cases the cavern volume is calculated as:

$$V_{cav} = \sum dV_i$$
$$dV_i = (z_i - z_{i+1}) * \frac{(A_i + A_{i+1})}{2} \qquad (2)$$

where V_{cav} is cavern volume, dV_i is a volume increment between consecutive elevation points, and A_i is the planar area at depth, z_i.

3. During a second preprocessor phase of WinP2D, the *leach tuning coefficients, $C_{i,j}$ are tabulated* for the specified number of leaches (subscript *i*) for each of the specified caverns (subscript *j*). Note that the coefficients are dependent on the hanging-string depths specified in the configuration file. The set of leach coefficients are also manually input to the WinP2D configuration file.

   The pre-definition of the leaching coefficients simplifies the P/D calculations by eliminating the need to repeatedly determine the tuning coefficient by iteration or the need to store many large mesh files. During the P/D calculations the base UCD file is read and the mesh coordinates are adjusted using equation (1) and the tuning coefficients and hanging string depths read from the configuration file.

4. An *outer drawdown loop was added* to the P/D calculation. This modification allows the user to specify an SPR site, select the caverns of interest, and select the number of drawdowns and subsequent leaches. As an example, WinP2D can generate a tabulation of P/D ratios for Big Hill sweet caverns after three through five drawdowns. The drawdown leach P/D calculation is stopped for a particular cavern when the P/D is below a user specified minimum, in this case 1.0.

5. Finally, a choice of several, more traditional, *single-value P/D ratios* (as opposed to a 3D-P/D) was programmed into the WinP2D program. The program determines the single value ratios by creating a vertical cylindrical equivalent for each cavern from which simple calculations of pillar thickness and cavern diameter are performed. The cylinder center is calculated by one of two methods.

   - Using the average cavern x- and y- coordinates
   - Using a horizontal bounding box created from the maximum and minimum x- and y-coordinates where the center of the box is used as the center of the cylinder.

   The diameter of the cylinder can be calculated in one of four ways by,

   - conserving the relationship between a circle and a bounding square
   - the largest horizontal rectangle dimension
   - the average horizontal rectangle dimension

- a diameter which gives a cylinder volume equal to the cavern volume

The height of the cylinder is the height of the cavern.

To complete the task in a timely manner, the WinP2D program currently requires three executions of the WinP2D program for each SPR site (i.e. twelve runs). The sequence is as follows.

1. The program reads the UCD mesh files and creates a table summarizing the file and lists elevations of cavern top and bottom. Twenty feet is added to the cavern bottom elevation to give the assumed depth of the hanging strings. The tabulated hanging string depths are manually input to the configuration file.
2. WinP2D uses the hanging string depths to calculate leaching coefficients $C_{i,j}$ for 10 drawdowns for each cavern containing oil at a site (i.e., some sites contain abandoned caverns that are not used for storage but are included in P/D calculations). The leaching coefficients are tabulated and manually added to the configuration file.
3. Finally, the program calculates minimum 3D-P/D ratios for each cavern after each specified number of drawdowns. Baseline 3D-P/D ratios are also calculated prior to first draw down to give the current configuration (specified as drawdown 0). Traditional P/D ratios are calculated using cavern average x- and y- coordinates and a diameter that conserves volume, which, in a sense, has generated "average" pillar and diameter values.

The relationship between the minimum 3D-P/D ratio and the standard single-value P/D ratio is shown in Figure 3 using Big Hill caverns 101 and 102 average radius profiles after 5 leaches. Note that the 3D-P/D uses the actual 3D mesh data not the average radius representation to determine the minimum pillar thickness and location. In Figure 3 the 3D-P/D for cavern BH-101is $P_{3D}/ 2R_{3D}$ and the single-value P/D is $P_{L3}/ 2R_{L3}$, where P_{L3} and R_{L3} are determined from the volume conserving cylinders shown as blue boxes. The single-value P/D will always be larger because $P_{L3} > P_{3D}$ and $R_{L3} < R_{3D}$ and can be thought of as an "average" P/D.

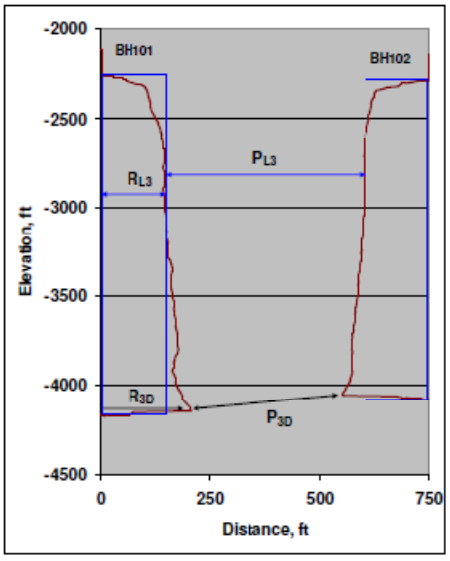

Figure 3. Relationship between 3D-P/D and standard single valued P/D

Results

The output from the WinP2D program is summarized in tables 1 through 4. See the appendix for a complete list of both 3D-P/D and standard P/D values tabulated, along with the number of allowable drawdowns for each cavern until the P/D values fall below both 1.78 and 1.0.

Tables 1 through 4 list the number of drawdowns for each cavern at each site before reaching the P/D criteria of 1.78 and 1.0. In each table the numbers listed in each column are the number of drawdowns before the P/D drops below the criteria of 1.78 and 1.0, which are listed at the top of the table. A "0" indicates the cavern is currently below the criteria or will be after one leach and ">10" indicates that after 10 drawdowns the cavern is still above the criteria. There are two P/D methods – minimum 3D-P/D and standard single-valued P/D.

The explanation of the tables is best understood by using Big Hill cavern 110, highlighted in Table 1, as an example. In Table 1, Big Hill cavern 110 can be drawn down once before the minimum 3D-P/D ratio drops below the 1.78 criterion and the cavern can be drawn down five times before dropping below a P/D of 1.0. Using the standard single-valued P/D ratio the Big Hill cavern 110 has three drawdowns before reaching the 1.78 criterion and nine drawdowns before falling below 1.0 criterion. However, it is *important* to realize that after nine leaches the minimum 3D-P/D ratio is 0.5 (see appendix for actual values), which means that there is a local region on cavern BH-110 that has a relatively small P/D ratio and that region may be problematic.

Table 1. Number Drawdowns before Reaching P/D Criteria at Big Hill

Big Hill Cavern	MIN 3D-P/D		STD P/D	
	<1.78	<1	<1.78	<1
101	0	5	3	8
102	0	5	3	8
103	0	4	2	7
104	0	4	3	9
105	0	4	3	8
106	0	5	2	8
107	0	4	2	8
108	0	4	3	8
109	0	5	3	9
110	1	5	3	9
111	0	3	2	8
112	0	3	2	8
113	0	3	2	8
114	0	4	2	8

Table 2. Number Drawdowns before Reaching P/D Criteria at Bryan Mound.

BM Cavern	MIN 3D-P/D		STD P/D	
	<1.78	<1.0	<1.78	<1.0
101	0	4	4	8
102	2	4	6	>10
103	0	2	2	8
104	0	2	5	>10
105	0	2	3	9
106	0	4	2	8
107	0	0	0	4
108	0	2	2	8
109	0	2	3	9
110	0	4	3	8
111	0	3	3	8
112	0	3	3	9
113	0	3	8	>10
114	0	2	5	>10
115	0	4	6	>10
116	1	4	6	>10
1	0	0	0	1
2	0	0	0	4
4	0	0	0	0
5	0	0	0	1

Table 3. Number Drawdowns before Reaching P/D Criteria at Bayou Choctaw.

BC Cavern	MIN 3D-P/D		STD P/D	
	<1.78	<1.0	<1.78	<1.0
101	0	2	0	3
15	0	0	0	0
17	0	0	0	0
18	0	0	0	5
19	0	1	4	9
20	0	0	0	0

Table 3. Number Drawdowns before Reaching P/D Criteria at West Hackberry.

WH Cavern	MIN 3D-P/D		STD P/D	
	<1.78	<1	<1.78	<1
101	0	4	4	9
102	0	5	8	>10
103	0	3	3	8
104	0	4	4	9
105	2	4	5	>10
106	0	6	4	>10
107	1	3	3	8
108	0	5	3	8
109	0	4	3	7
110	2	4	4	9
111	3	5	5	>10
112	2	4	4	>10
113	1	5	3	9
114	2	4	4	>10
115	2	4	4	>10
116	3	5	5	>10
117	0	5	3	9
6	0	0	0	0
7	0	0	1	5
8	0	0	0	2
9	0	0	0	0
11	0	5	2	7

When reviewing the data presented in the appendix it is crucial to note that both types of P/D values presented (3D and single value) be considered when determining the lifetime of an individual cavern. The single-value P/D value may give the impression that the integrity of cavern is intact, but the corresponding 3D-P/D value may be alarmingly low, indicating a possible problem region on the cavern that should be avoided in subsequent drawdowns. As an example, refer to the Big Hill tables displayed in the appendix. The red box directs the reader to the P/D values calculated for all caverns after seven leaches. The 3D-P/D values are substantially smaller (more than one-half) than the corresponding single-value P/D numbers.

We have also observed that the 3D-P/D values may drop substantially, by possibly more than half after several drawdown cycles (e.g. Big Hill 101 after nine drawdowns). These relatively small values are typically the result of the leaching equation used in this task. Figure 2 demonstrates the effects of leaching on a standard Big Hill cavern. The leaching sequence creates a bell-shaped pattern. The minimum thickness between two standard caverns will be the distance between the two lower protruding lobes, which cause a small P/D value.

Finally, we should mention that the sonar used for West Hackberry cavern 102 P/D calculations was shot in 1983. The volume calculated from the sonar is approximately 6 MMB. The current volume

documented in the West Hackberry daily reports (wh20090101.xls) is 10.5 MMB. It is likely the current P/D ratios are lower than those reported here in the appendix.

References

DOE (Department of Energy). 2001. Design Criteria- Level III, *US Department of Energy, Strategic Petroleum Reserve*. New Orleans, LA, November, 2001.

Ehgartner, B and S. Sobolik, 3-D Cavern Enlargement Analyses. Solution Mining Research Institute, April 2002.

Sobolik, S. and B. Ehgartner, *Analysis of Cavern Shapes for the Strategic Petroleum Reserve*, SAND2006-3002. Sandia National Laboratories, Albuquerque, NM, 2006.

Levin, B. Impact of Big Hill Drawdown Scenarios on Cavern Integrity, Letter report to W. Elias, September 27, 2004.

Rudeen, D. K. and A. S. Lord. A Windows Application for Cavern Three-Dimensional Pillar-to-Diameter Calculations for the U.S. Strategic Petroleum Reserve, letter report to W. Elias, March 21, 2007.

Appendix

The following series of tables list P/D ratios and the number of allowable drawdowns for each cavern at each SPR site. The first table under each site presents 3D-P2D values, whereas the second table presents traditional, single, P/D values for an entire cavern. Columns and rows are color coded and defined as follows.

P/D > 1.78

P/D > 1.0

Big Hill

Example referred to in text.

BIG HILL Minimum 3D-P/D

CavID P/D for leach 0 to 10

	0	1	2	3	4	5	6	7	8	9	10	<1.78	<1
101	1.81	1.73	1.65	1.58	1.42	1.17	0.88	0.65	0.50	0.46	0.15	0	5
102	1.81	1.72	1.65	1.57	1.44	1.14	0.85	0.62	0.52	0.48	0.14	0	5
103	1.78	1.70	1.61	1.44	1.20	0.99	0.81	0.63	0.48	0.39	0.30	0	4
104	1.73	1.66	1.59	1.53	1.25	0.94	0.69	0.49	0.40	0.40	0.05	0	4
105	1.67	1.60	1.53	1.47	1.32	0.99	0.72	0.53	0.43	0.41	0.11	0	4
106	1.41	1.34	1.28	1.22	1.17	1.00	0.74	0.57	0.43	0.39	0.11	0	5
107	1.71	1.63	1.57	1.49	1.22	0.91	0.65	0.48	0.41	0.37	0.14	0	4
108	1.67	1.60	1.53	1.47	1.31	0.97	0.70	0.50	0.41	0.36	0.11	0	4
109	1.68	1.60	1.53	1.47	1.40	1.04	0.76	0.60	0.50	0.20	0.14	0	5
110	1.87	1.79	1.72	1.66	1.55	1.19	0.89	0.65	0.49	0.49	0.13	1	5
111	1.40	1.34	1.29	1.23	0.94	0.67	0.46	0.28	0.21	0.17	0.11	0	3
112	1.60	1.53	1.47	1.20	0.90	0.66	0.47	0.32	0.16	0.10	0.07	0	3
113	1.56	1.49	1.42	1.23	0.92	0.67	0.46	0.34	0.22	0.07	0.06	0	3
114	1.52	1.45	1.38	1.32	1.21	0.90	0.65	0.47	0.42	0.38	0.10	0	4

BIG HILL Standard-P/D (cylinder conserves volume)

CavID P/D for leach 0 to 10

	0	1	2	3	4	5	6	7	8	9	10	<1.78	<1
101	2.41	2.21	2.02	1.84	1.67	1.52	1.37	1.24	1.11	0.99	0.88	3	8
102	2.37	2.16	1.97	1.80	1.63	1.48	1.33	1.20	1.07	0.95	0.84	3	8
103	2.22	2.03	1.85	1.69	1.53	1.38	1.25	1.12	1.00	0.89	0.78	2	7
104	2.42	2.21	2.03	1.85	1.68	1.53	1.39	1.26	1.13	1.01	0.89	3	9
105	2.39	2.19	2.00	1.83	1.67	1.52	1.37	1.24	1.12	1.00	0.89	3	8
106	2.30	2.08	1.90	1.73	1.57	1.42	1.28	1.16	1.03	0.92	0.81	2	8
107	2.28	2.08	1.90	1.73	1.57	1.42	1.28	1.15	1.03	0.92	0.81	2	8
108	2.43	2.23	2.03	1.85	1.69	1.53	1.38	1.24	1.11	0.99	0.88	3	8
109	2.46	2.25	2.06	1.89	1.72	1.57	1.43	1.29	1.16	1.04	0.93	3	9
110	2.48	2.27	2.08	1.90	1.73	1.58	1.43	1.29	1.17	1.05	0.93	3	9
111	2.32	2.12	1.94	1.76	1.60	1.45	1.31	1.19	1.06	0.95	0.84	2	8
112	2.26	2.07	1.89	1.73	1.57	1.43	1.29	1.17	1.05	0.93	0.83	2	8
113	2.32	2.13	1.94	1.78	1.62	1.47	1.33	1.20	1.08	0.96	0.85	2	8
114	2.27	2.08	1.90	1.73	1.58	1.43	1.30	1.17	1.05	0.93	0.83	2	8

Bryan Mound

BRYAN MOUND Minimun 3D P/D

CavID	P/D for leach 0 to 10												
	0	1	2	3	4	5	6	7	8	9	10	<1.78	<1.0
101	1.67	1.53	1.39	1.25	1.01	0.75	0.54	0.48	0.42	0.13	0.12	0	4
102	2.46	2.36	1.81	1.39	1.06	0.79	0.56	0.46	0.26	0.12	0.10	2	4
103	1.44	1.28	1.13	1.00	0.88	0.70	0.50	0.37	0.32	0.32	0.05	0	2
104	1.47	1.40	1.33	0.98	0.67	0.45	0.39	0.20	0.11	0.07	0.05	0	2
105	1.26	1.20	1.16	0.86	0.59	0.42	0.22	0.12	0.06	0.02	0.02	0	2
106	1.54	1.39	1.26	1.13	1.02	0.91	0.74	0.56	0.41	0.33	0.31	0	4
107	0.85	0.77	0.69	0.64	0.61	0.54	0.49	0.39	0.28	0.25	0.02	0	0
108	1.57	1.52	1.22	0.92	0.68	0.54	0.35	0.26	0.22	0.20	0.15	0	2
109	1.37	1.33	1.06	0.80	0.60	0.43	0.30	0.19	0.13	0.07	0.06	0	2
110	1.71	1.52	1.35	1.22	1.10	0.87	0.60	0.48	0.20	0.06	0.03	0	4
111	1.59	1.41	1.26	1.12	0.85	0.63	0.47	0.43	0.19	0.11	0.07	0	3
112	1.90	1.77	1.36	1.03	0.77	0.55	0.47	0.46	0.42	0.18	0.09	0	3
113	1.70	1.66	1.61	1.28	1.00	0.76	0.56	0.39	0.28	0.25	0.22	0	3
114	1.68	1.46	1.20	0.99	0.81	0.67	0.52	0.37	0.25	0.21	0.09	0	2
115	1.71	1.66	1.63	1.45	1.15	0.90	0.68	0.50	0.38	0.32	0.10	0	4
116	1.86	1.79	1.72	1.66	1.30	0.99	0.74	0.55	0.50	0.49	0.16	1	4
1	0.52	0.45	0.40	0.35	0.35	0.30	0.24	0.16	0.09	0.03	0.00	0	0
2	0.92	0.83	0.75	0.67	0.59	0.53	0.46	0.40	0.34	0.29	0.24	0	0
3	0.49	0.49	0.49	0.47	0.45	0.43	0.41	0.39	0.36	0.36	0.37	0	0
4	0.56	0.51	0.45	0.40	0.34	0.28	0.21	0.16	0.15	0.14	0.15	0	0
5	0.61	0.53	0.46	0.37	0.29	0.22	0.16	0.11	0.07	0.05	0.01	0	0

BRYAN MOUND Standard-P/D (cylinder conserves cavern volume)

CavID	P/D for leach 0 to 10												
	0	1	2	3	4	5	6	7	8	9	10	<1.78	<1.0
101	2.71	2.49	2.25	2.02	1.81	1.61	1.42	1.25	1.08	0.92	0.77	4	8
102	3.08	2.85	2.61	2.40	2.21	2.03	1.85	1.69	1.54	1.40	1.27	6	10
103	2.27	2.08	1.90	1.73	1.57	1.42	1.29	1.16	1.04	0.92	0.82	2	8
104	2.77	2.55	2.35	2.16	1.99	1.83	1.68	1.53	1.40	1.27	1.15	5	10
105	2.47	2.27	2.09	1.92	1.77	1.62	1.48	1.35	1.22	1.10	0.99	3	9
106	2.26	2.07	1.89	1.71	1.56	1.41	1.27	1.14	1.01	0.90	0.79	2	8
107	1.74	1.57	1.40	1.25	1.11	0.97	0.84	0.72	0.60	0.49	0.39	0	4
108	2.23	2.05	1.88	1.72	1.57	1.43	1.30	1.17	1.06	0.95	0.85	2	8
109	2.37	2.18	2.01	1.85	1.69	1.55	1.42	1.29	1.17	1.05	0.95	3	9
110	2.61	2.38	2.14	1.94	1.75	1.57	1.40	1.24	1.09	0.95	0.82	3	8
111	2.38	2.17	1.99	1.81	1.65	1.50	1.36	1.22	1.09	0.98	0.86	3	8
112	2.35	2.18	2.02	1.87	1.72	1.58	1.45	1.32	1.20	1.09	0.98	3	9
113	3.51	3.24	2.99	2.75	2.54	2.33	2.13	1.95	1.78	1.62	1.46	8	10
114	2.83	2.61	2.43	2.23	2.04	1.87	1.70	1.55	1.40	1.26	1.15	5	10
115	2.98	2.74	2.53	2.32	2.13	1.95	1.78	1.63	1.48	1.34	1.21	6	10
116	3.01	2.78	2.56	2.35	2.16	1.99	1.82	1.67	1.52	1.38	1.25	6	10
1	1.20	1.08	0.96	0.86	0.75	0.66	0.57	0.48	0.40	0.33	0.25	0	1
2	1.50	1.38	1.27	1.16	1.06	0.96	0.87	0.79	0.71	0.63	0.56	0	4
3	1.22	1.20	1.17	1.14	1.11	1.07	1.04	1.00	0.96	0.91	0.86	0	6
4	1.10	0.98	0.87	0.76	0.66	0.57	0.47	0.38	0.30	0.22	0.14	0	0
5	1.13	1.00	0.88	0.77	0.66	0.56	0.47	0.38	0.29	0.21	0.14	0	1

Bayou Choctaw

Boxes enclose the SPR owned caverns that contain oil. The remaining caverns listed are either abandoned or not owned by the SPR and were not drawn down, but were used in P/D calculations with their nearest neighbors.

BAYOU CHOCTAW Minimun 3D P/D

CavID P/D for leach 0 to 10

	0	1	2	3	4	5	6	7	8	9	10	<1.78	<1.0
101	1.33	1.23	1.04	0.84	0.79	0.76	0.64	0.51	0.39	0.30	0.22	0	2
UTP102	1.58	1.58	1.57	1.56	1.55	1.55	1.54	1.54	1.53	1.53	1.52	0	10
10	1.04	1.04	1.04	1.04	1.04	1.04	1.04	1.04	1.04	1.04	1.04	0	10
15	0.33	0.29	0.27	0.22	0.20	0.20	0.18	0.14	0.10	0.07	0.06	0	0
17	0.55	0.54	0.56	0.55	0.44	0.35	0.31	0.32	0.29	0.28	0.05	0	0
18	0.47	0.35	0.27	0.22	0.19	0.17	0.15	0.12	0.09	0.08	0.06	0	0
19	1.33	1.15	0.98	0.81	0.66	0.53	0.41	0.33	0.30	0.26	0.23	0	1
20	0.49	0.41	0.34	0.27	0.21	0.17	0.16	0.16	0.17	0.16	0.16	0	0
UTP25	1.78	1.78	1.77	1.77	1.77	1.76	1.76	1.76	1.76	1.75	1.75	0	10
1	0.89	0.89	0.89	0.89	0.89	0.89	0.89	0.89	0.89	0.89	0.89	0	0
2	0.52	0.52	0.52	0.52	0.52	0.52	0.52	0.52	0.52	0.52	0.52	0	0
4	1.87	1.87	1.87	1.87	1.87	1.87	1.87	1.87	1.87	1.87	1.87	10	10
8	2.00	2.00	2.00	2.00	2.00	2.00	2.00	2.00	2.00	2.00	2.00	10	10

BAYOU CHOCTAW Standard-P/D (cylinder conserves cavern volume)

CavID P/D for leach 0 to 10

	0	1	2	3	4	5	6	7	8	9	10	<1.78	<1.0
101	1.68	1.49	1.31	1.14	0.99	0.84	0.71	0.58	0.45	0.34	0.23	0	3
UTP102	3.14	3.10	3.05	3.01	2.96	2.91	2.85	2.80	2.74	2.67	2.61	10	10
10	2.28	2.28	2.28	2.28	2.28	2.28	2.28	2.28	2.28	2.28	2.28	10	10
15	0.47	0.39	0.32	0.25	0.19	0.13	0.07	0.02	-0.03	-0.08	-0.12	0	0
17	0.84	0.70	0.57	0.45	0.34	0.23	0.13	0.03	-0.05	-0.14	-0.22	0	0
18	1.76	1.59	1.44	1.30	1.16	1.03	0.89	0.75	0.62	0.50	0.39	0	5
19	2.74	2.54	2.36	2.15	1.94	1.75	1.56	1.39	1.23	1.08	0.93	4	9
20	0.85	0.75	0.66	0.58	0.50	0.42	0.35	0.29	0.22	0.17	0.11	0	0
UTP25	4.48	4.42	4.37	4.31	4.24	4.17	4.10	4.02	3.94	3.85	3.75	10	10
1	1.48	1.48	1.48	1.48	1.48	1.48	1.48	1.48	1.48	1.48	1.48	0	10
2	0.62	0.62	0.62	0.62	0.62	0.62	0.62	0.62	0.62	0.62	0.62	0	0
4	2.81	2.81	2.81	2.81	2.81	2.81	2.81	2.81	2.81	2.81	2.81	10	10
8	2.23	2.23	2.23	2.23	2.23	2.23	2.23	2.23	2.23	2.23	2.23	10	10

West Hackberry

Note that WH-102 P/D values were calculated using a 1983 sonar survey. We expect current P/D values are actually lower than reported in the tables below.

WEST HACKBERRY Minimum 3D-P/D

CavID P/D for leach 0 to 10

	0	1	2	3	4	5	6	7	8	9	10	<1.78	<1
101	1.58	1.53	1.49	1.34	1.04	0.79	0.58	0.47	0.37	0.13	0.13	0	4
102	1.49	1.45	1.41	1.37	1.34	1.24	0.95	0.73	0.62	0.61	0.23	0	5
103	1.30	1.26	1.22	1.19	0.96	0.72	0.57	0.43	0.37	0.13	0.11	0	3
104	1.57	1.53	1.49	1.44	1.11	0.84	0.61	0.43	0.40	0.23	0.15	0	4
105	2.02	1.96	1.91	1.50	1.15	0.86	0.62	0.47	0.45	0.42	0.11	2	4
106	1.76	1.71	1.66	1.61	1.57	1.30	1.03	0.81	0.63	0.48	0.37	0	6
107	1.97	1.91	1.54	1.21	0.93	0.71	0.52	0.39	0.26	0.11	0.07	1	3
108	1.76	1.69	1.63	1.58	1.39	1.07	0.80	0.58	0.49	0.46	0.42	0	5
109	1.72	1.53	1.34	1.17	1.01	0.85	0.65	0.50	0.40	0.14	0.11	0	4
110	2.12	2.05	1.89	1.50	1.18	0.91	0.69	0.50	0.39	0.32	0.13	2	4
111	2.09	2.02	1.97	1.92	1.62	1.26	0.96	0.72	0.56	0.49	0.20	3	5
112	2.11	2.05	1.83	1.45	1.14	0.88	0.67	0.49	0.45	0.47	0.14	2	4
113	1.96	1.83	1.69	1.56	1.44	1.11	0.85	0.65	0.57	0.33	0.20	1	5
114	2.15	2.08	1.97	1.57	1.24	0.97	0.75	0.56	0.40	0.32	0.29	2	4
115	2.09	2.04	1.99	1.65	1.27	0.96	0.71	0.57	0.44	0.18	0.13	2	4
116	2.12	2.04	1.97	1.84	1.48	1.15	0.88	0.70	0.68	0.37	0.24	3	5
117	1.54	1.49	1.45	1.41	1.29	1.01	0.77	0.58	0.49	0.45	0.22	0	5
6	0.23	0.18	0.13	0.08	0.04	0.00	0.00	0.00	0.00	0.00	0.00	0	0
7	1.15	0.97	0.84	0.77	0.68	0.62	0.53	0.48	0.43	0.32	0.22	0	0
8	0.42	0.29	0.18	0.09	0.01	0.00	0.00	0.00	0.01	0.00	0.00	0	0
9	0.40	0.27	0.26	0.27	0.29	0.29	0.15	0.16	0.15	0.14	0.11	0	0
11	1.84	1.68	1.53	1.38	1.23	1.05	0.89	0.75	0.62	0.51	0.40	0	5

WEST HACKBERRY Standard-P/D (cylinder conserves volume)

CavID P/D for leach 0 to 10

	0	1	2	3	4	5	6	7	8	9	10	<1.78	<1
101	2.58	2.36	2.16	1.98	1.80	1.64	1.49	1.34	1.21	1.08	0.96	4	9
102	3.77	3.48	3.21	2.95	2.73	2.51	2.30	2.10	1.91	1.73	1.57	8	10
103	2.42	2.21	2.02	1.84	1.67	1.52	1.37	1.23	1.11	0.99	0.87	3	8
104	2.63	2.41	2.21	2.02	1.84	1.68	1.52	1.38	1.24	1.12	1.00	4	9
105	2.92	2.65	2.43	2.23	2.03	1.85	1.69	1.53	1.38	1.24	1.12	5	10
106	2.62	2.41	2.21	2.02	1.84	1.68	1.53	1.39	1.25	1.13	1.01	4	10
107	2.41	2.21	2.02	1.84	1.68	1.52	1.38	1.25	1.12	1.00	0.88	3	8
108	2.38	2.18	1.99	1.82	1.65	1.50	1.35	1.22	1.09	0.98	0.87	3	8
109	2.47	2.23	2.01	1.80	1.60	1.41	1.24	1.07	0.91	0.77	0.63	3	7
110	2.64	2.42	2.23	2.04	1.86	1.70	1.55	1.40	1.27	1.08	0.90	4	9
111	2.97	2.73	2.51	2.30	2.11	1.92	1.75	1.60	1.44	1.30	1.17	5	10
112	2.70	2.47	2.26	2.07	1.89	1.72	1.56	1.41	1.26	1.13	1.01	4	10
113	2.45	2.24	2.05	1.87	1.70	1.55	1.40	1.27	1.14	1.02	0.91	3	9
114	2.66	2.44	2.23	2.04	1.86	1.69	1.53	1.40	1.26	1.13	1.01	4	10
115	2.74	2.52	2.31	2.12	1.94	1.77	1.61	1.46	1.32	1.19	1.06	4	10
116	2.82	2.60	2.39	2.20	2.01	1.84	1.68	1.54	1.40	1.27	1.14	5	10
117	2.51	2.31	2.11	1.93	1.76	1.60	1.45	1.31	1.18	1.05	0.94	3	9
6	0.56	0.47	0.39	0.31	0.24	0.17	0.11	0.05	0.00	-0.06	-0.11	0	0
7	2.14	1.91	1.71	1.51	1.32	1.15	0.99	0.83	0.69	0.55	0.43	1	5
8	1.36	1.20	1.06	0.91	0.78	0.65	0.53	0.42	0.31	0.21	0.12	0	2
9	0.83	0.70	0.58	0.47	0.36	0.26	0.17	0.08	-0.01	-0.08	-0.16	0	0
11	2.20	2.00	1.82	1.66	1.50	1.35	1.21	1.09	0.97	0.85	0.75	2	7

APPENDIX II: SPR SITE SPECIFIC DILATION AND STRENGTH DATA

There is an uncertainty in test data, modeling, and interpreting results that is typically handled by applying an appropriate safety factor to the results. This appendix will recommend a safety factor for SPR 3D geomechanics analyses based on the inherent uncertainties of modeling.

The SPR is unique and fortunate to have a long history of operational data and metrics on subsidence and underground closure. This enables the analyst to calibrate the creep properties based on laboratory testing to match both subsidence and closure measurements for a given pressure history. Since creep strain is very sensitive to stress, matching the time dependent deformations of the cavern and ground surface implies the stress field is correct and evolves properly with time. Uncertainty arises when the predicted stresses are post-processed using a damage criterion.

The SPR has tested all of its salts for strength. The results are found in a number of publications and will be compiled in this appendix from the following sources:

1. Acres American Inc., 1977. Weeks Island Geotechnical Study. Prepared for U.S. Federal Energy Administration under contract FEA-1251-75, November.
2. PB-KBB Inc., 1978. Strategic Petroleum Reserve Program, Salt Dome Geology and Cavern Stability Analysis, Bayou Choctaw Dome, Louisiana, Final Report, Appendix, Prepared for U.S. Department of Energy, Houston, Texas.
3. Wawersik, W.R., D.W. Hannum and H.S. Lauson, 1980. Compression and Extension Data for Dome Salt from West Hackberry, Louisiana, SAND79-0668, Sandia National Laboratories, Albuquerque, NM.
4. Wawersik, W.R., D.J. Holcomb, D.W. Hannum and H.S. Lauson, 1980. Quasi-Static and Creep Data for Dome Salt from Bryan Mound, Texas" SAND80-1434, Sandia National Laboratories, Albuquerque, NM.
5. Price, R.H., W.R. Wawersik, O.W. Hannum, and J.A. Zirzow, 1981. Quasi-Static Rock Mechanics Data for Rocksalt from Three Strategic Petroleum Reserve Domes, SAND81-2521, Sandia National Laboratories, Albuquerque, NM.
6. Mellegard, K.D. and T.W. Pfeifle, 1994. Laboratory Testing of Dome Salt from Weeks Island, Louisiana. RSI-0552, prepared by RE/SPEC Inc. for DynMcDermott Petroleum Operations Company, New Orleans, LA.
7. Lee, M.Y., Ehgartner, B.L., and Bronowski, D.R., 2004. Laboratory Evaluation of Damage Criteria and Permeability of Big Hill Salt, SAND2004-6004, Sandia National Laboratories, Albuquerque, NM.
8. Broome, S.T., S.J. Bauer, D. Dunn, J.H. Hofer, and D.R. Bronowski, 2009. Geomechanical Testing of MRIG-9 Core for the Potential SPR Siting at the Richton Salt Dome, SAND2009-0852, Sandia National Laboratories, Albuquerque, NM.

With the exceptions of the most recent 3 reports, the earlier reports did not determine the stress state for the onset of dilatants damage [Van Sambeek, 1993]. However, in most cases the data was available to derive the onset of dilation by examining the change in volumetric strain [Tavares, 1994 and Ehgartner, 1994]. The stress invariants (I_1 and $\sqrt{J_2}$) for the onset of dilation

and failure states are listed in Table 1. The data is plotted in Figure 1 along with criteria that have been used in past analyses. For dilation, the ratio between the stress tensors is 0.27, and 0.45 for failure.

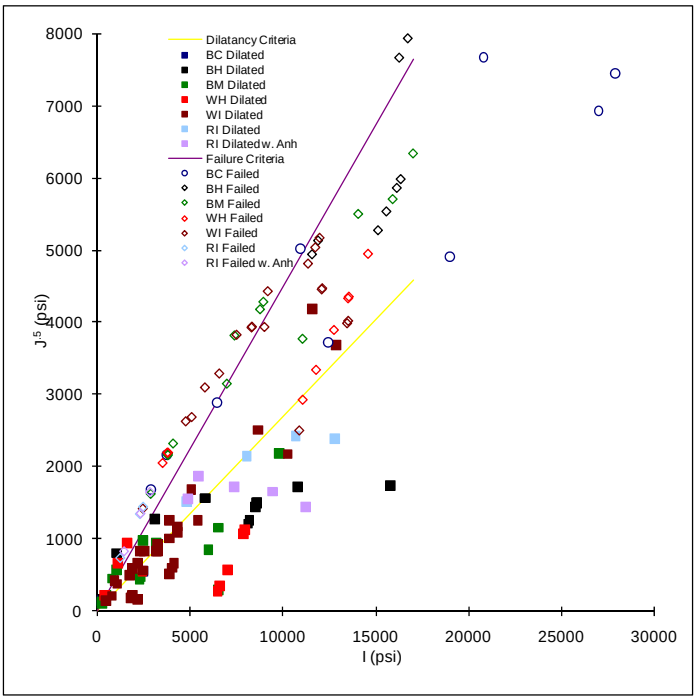

Figure II-1: Stress states of SPR core at dilation and failure.

As one can see, there is considerable variation in the measurements. The coefficient of variation is 0.25 and 0.57 for the failed and dilated samples about the criteria. The true variation for the dilated samples is probably closer to that of the failed ones as it is more difficult to measure changes in volume, as opposed to ultimate stresses. Never the less, the lower bound of the measured failure strengths may be defined by the dilation criterion. This would define the absolute minimum acceptable stress state since failure is an unacceptable condition. However, the use of the dilation criterion, without applying any safety factor to it, results in a 50% chance of dilation occurring. If a safety factor of 1.5 is used, the probability of dilatants damage is 5% and failure is less than 1%. These appear to be reasonable probabilities.

In evaluating an analysis result, the allowable deviatoric stress ($\sqrt{J_2}$) is a function of the dilation ratio (0.27), mean stress ($I_1/3$), and safety factor.

$$\sqrt{J_2} < \frac{0.27}{Safety\ \ Factor} \cdot I_1$$

Recently, a dilational criterion has been developed for extensile stress states which can occur around caverns [Devries, 2002]. Test results on Gulf Coast salt [Nieland, 2006] and bedded salt [DeVries, 2003] show that extensile dilation occurs at 63% and 70% of the compressive stress at dilation. This suggests that a safety factor of about 1/.67 or 1.5 needs to be applied to the compressive criterion to cover this condition. The reduction in dilational strength associated with extension has been disputed [Rokar and Durup, 2009]. Test results by Hunsche [1996] do not support the reduction.

SPR salt was also tested in both modes. The results of 5 split core tests are compared in Figures 2 and 3 for dilation and failure.

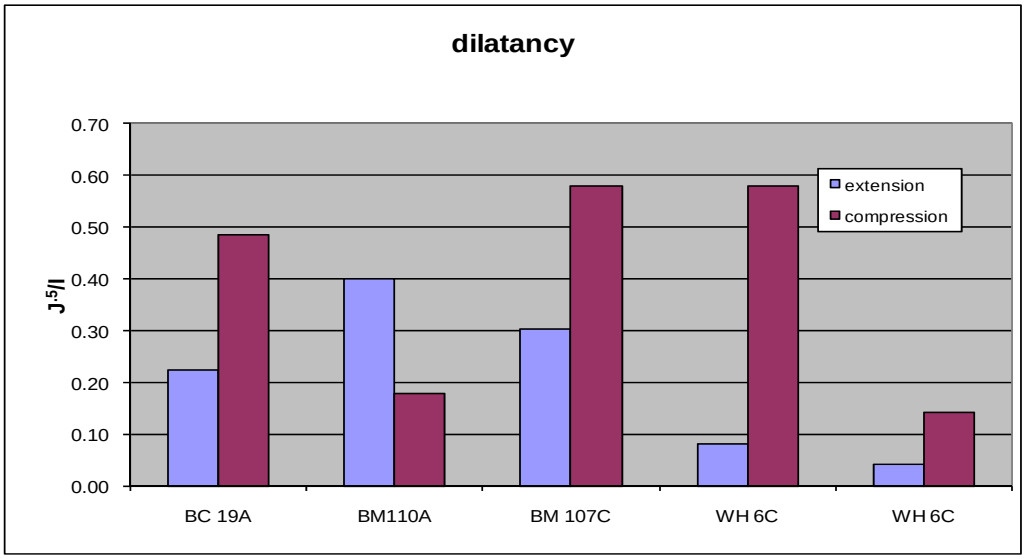

Figure II-2: Comparison of dilatant strength in extension and compression.

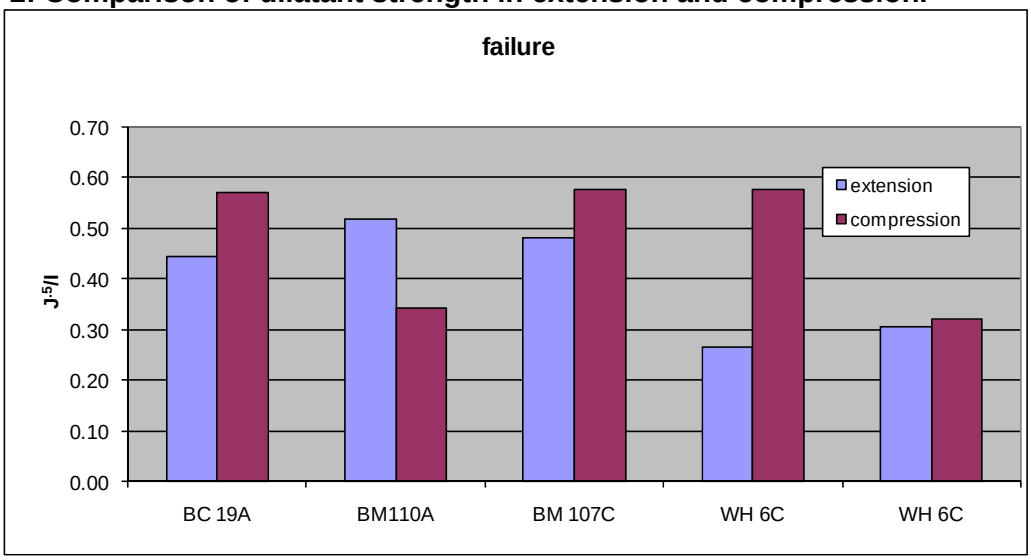

Figure II-3: Comparison of ultimate strength in extension and compression.

In 4 of the 5 tests, the exception is BM110A salt, the salt tested weaker in extensile mode. On average, the extensile strength was 74% and 91% of the compressive strength at dilation and failure.

In conclusion, a safety factor of 1.5 applied to the compressive dilational criterion appears to be reasonable. A safety factor of 1.5 is typically used by RE/SPEC [Devries, 2006] and a safety factor of 1.6 was interpreted in LOOP cavern analyses by PB Energy Storage Services [Ratigan, 2006] as acceptable of the lifetime of the facility. In some cases, predicted damage or safety factors less than 1 have been acceptable, such as cases where it occurs near the bottom of the cavern [Thoms, 2004], is of short duration [Eickemeier, BGR, 2005]), or localized [Bruno, Terralog, 2005].

When the extensile stress state is considered in the Lode angle dependent criterion, a safety factor of 1 may be reasonable for that stress state until such time the salt mechanics community comes to consensus about its influence on damage or additional SPR testing resolves the criteria.

In the future, analyses may use more sophisticated damage models that may simulate damage accumulation and healing. Once validated, damage may be permitted in cavern design [DeVries, 2003], provided those analyses do not show damage evolution to progress to problematic conditions, such as loss of containment or extensive salt falls.

Table II-1: SPR salt strength and dilatant data

Site	Ultimate Strength		Onset of Dilation	
	I_1 (psi)	$\sqrt{J_2}$ (psi)	I_1 (psi)	$\sqrt{J_2}$ (psi)
BC	3784	2159	274	133
	6492	2882	2450	548
	2900	1674	N/A	N/A
	20800	7679	N/A	N/A
	19000	4907	N/A	N/A
	27900	7448	N/A	N/A
	10950	5023	N/A	N/A
	27000	6928	N/A	N/A
	12440	3718	N/A	N/A
BH	16290	7673	1000	806
	15142	5278	3073	1282
	11893	5134	5782	1561
	16370	5987	10782	1712
	16754	7941	15782	1740
	16160	5866	5782	1561
	11565	4945	8593	1497
	15595	5540	8500	1443
	N/A	N/A	8592	1496
	N/A	N/A	8097	1211
	N/A	N/A	8188	1263
	N/A	N/A	8600	1501
	N/A	N/A	290	167
BM	2854	1622	1034	572
	3770	2177	770	445
	3780	2182	220	127
	3784	2159	419	217
	4064	2321	214	98
	6960	3152	2250	433
	7370	3822	2450	981
	8750	4186	2300	462
	8930	4290	3140	947
	11040	3776	6500	1155
	14044	5510	5975	852
	15900	5716	6500	289
	17000	6351	9800	2194
WH	3540	2044	1150	664
	3790	2188	1625	938
	3834	2188	424	219

Site	Ultimate Strength		Onset of Dilation	
	I_1 (psi)	$\sqrt{J_2}$ (psi)	I_1 (psi)	$\sqrt{J_2}$ (psi)
	11060	2921	7000	577
	11780	3337	2450	548
	12740	3891	6480	277
	13500	4330	6600	346
	13540	4353	7950	1126
	14570	4948	7850	1068
WI	8300	3926	2475	563
	8320	3938	1825	188
	9170	4428	1900	231
	11330	4809	4040	600
	11720	5034	4160	670
	11950	5167	3900	520
	N/A	N/A	464	142
	N/A	N/A	798	209
	N/A	N/A	1088	377
	N/A	N/A	1740	502
	N/A	N/A	1885	586
	N/A	N/A	3915	1005
	N/A	N/A	11600	4191
	N/A	N/A	8700	2509
	N/A	N/A	10295	2175
	N/A	N/A	12905	3683
	2465	1423	2175	670
	4771	2629	2175	167
	5090	2687	3263	921
	5800	3097	3263	837
	7497	3826	4350	1172
	6569	3290	4350	1089
	8990	3935	2538	837
	12093	4470	5438	1256
	12064	4454	3915	1256
	13485	4018	5075	1682
	13427	3985	943	419
	10861	2503	3190	837
			2320	837
Richton	N/A	N/A	5415	1869
	N/A	N/A	7349	1725
	N/A	N/A	9401	1657
	N/A	N/A	11204	1440
	N/A	N/A	4857	1547
	N/A	N/A	4819	1523
	N/A	N/A	8071	2143
	N/A	N/A	10722	2421
	N/A	N/A	12836	2383
	2845	1643	1456	841
	1423	822	1289	744
	2334	1348	1768	1020
	2324	1342	984	568

Site	Ultimate Strength		Onset of Dilation	
	I_1 (psi)	$\sqrt{J_2}$ (psi)	I_1 (psi)	$\sqrt{J_2}$ (psi)
	1275	736	1042	602
	2497	1442	1741	1005

References:

Bruno, M., L. Dorfmann, L. Khang, H. Gang, and J. Young, 2005. 3-D Geomechanical Analysis of Multiple Caverns in Bedded Salt. Fall Conference Solution Mining Research Institute, Nancy, France.

DeVries, K.L., 2003. Improved Modeling Increases Salt Cavern Storage Working Gas. GasTIPS, Winter Ed.

DeVries, K.L, K.D. Mellegard, and G.D. Callahan, 2002. Proof-of-Concept Research on a Salt Damage Criterion for Cavern Design: a Project Status Report. Spring Conference Solution Mining Research Institute, Banff, Alberta.

DeVries, K.L, K.D. Mellegard, and G.D. Callahan, 2003. Laboratory Testing in Support of a Bedded Salt Failure Criterion. Fall Conference Solution Mining Research Institute, Chester, U.K., England.

DeVries, K.L. 2006. Geomechanical Analyses to Determine the Onset of Dilation Around natural Gas Storage Caverns in Bedded Salt. Spring Conference Solution Mining Research Institute, Brussels, Belgium.

Ehgartner, B.L., 1994. Dilatancy Criterion for Weeks Island Salt. Internal memo to J.K. Linn, Sandia National Laboratories, February 21, 1994.

Eickemeier, R. S. Heuserman, and W. Paar, 2005. Hengelo Brine Field: FE Analysis of Stability and Integrity of Inline Pillars. Spring Conference Solution Mining Research Institute, Syracuse, NY.

Hunsche, U., 1996. Determination of Dilatancy Boundary and Damage up to Failure for Four Types of Rock Salt at Different Stress Geometries. 4th Conference on the Mechanical Behavior of Salt.

Nieland, J. D. and J.L. Ratigan, 2006. Geomechanical Evaluations of Two Gulf Coast Natural Gas Storage Caverns. Spring Conference Solution Mining Research Institute, Brussels, Belgium.

Ratigan, J.L., J.D. Nieland, and T.V. McCauley, 2006. Geomechanical Assessment of the LOOP LLC Crude Oil Storage Facility in the Clovelly Salt Dome, Louisiana. Fall Conference Solution Mining Research Institute,Rapid City, S.D.

Rokar, R. and G. Durup, 2009. Over 40 Years of Development of Design Criteria for Salt Caverns. Spring Conference Solution Mining Research Institute, Krakow, Poland.

Tavares, M.P., 1994. Dilatancy and Failure Criteria for SPR Rock Salt, Internal Report to J.K. Linn, August 9, Sandia National Laboratories, Albuquerque, NM,.

Thoms, R.L., 2004. Geomechanics Report for Pine Prairie Energy Center. S.G Resources, Louisiana. Report available to public through FERC.

Van Sambeek, L., J. Ratigan, and F. Hansen, 1993. *Dilatancy of Rock Salt in Laboratory Tests*, Proc. 34th U.S. Symposium on Rock Mechanics, p.245-248.

APPENDIX III: ALGEBRA SCRIPTS FOR POST-PROCESS

III-A. Units.txt

```
'Unit conversion:
'
'Angular:
' rad  = {rad_deg  =180/3.1415926536} deg
' deg  = {deg_rad  =1/rad_deg} rad
'
'Length:
' ft   = {ft_m=0.3048} m
' m    = {m_ft=1/ft_m} ft
'
'Pressure:
' MPa  = {MPa_Pa  = 1E6} Pa
' Pa   = {Pa_MPa  = 1/MPa_Pa} MPa
' psi  = {psi_Pa=6894.757} Pa
' Pa   = {Pa_psi=1/psi_Pa} psi
' Pa   = {Pa_psf=0.0208854} psf
' psf  = {psf_Pa=1/Pa_psf} Pa
' MPa  = {MPa_psf=MPa_Pa*Pa_psf} psf
'
'Time:
' min  = {min_s   = 60           } s
' h    = {h_min   = 60           } min
' d    = {d_h     = 24           } h
' mon  = {mon_d   = 30.4166666667} d
' yr   = {yr_d    = 365          } d
' dec  = {dec_yr  = 10           } yr
' cen  = {cen_dec = 10           } dec
' mil  = {mil_cen = 10           } cen
' h    = {h_s     = h_min*min_s  } s
' d    = {d_s     = d_h*h_s      } s
' mon  = {mon_s   = mon_d*d_s    } s
' yr   = {yr_s    = yr_d*d_s     } s
' dec  = {dec_s   = dec_yr*yr_s  } s
' cen  = {cen_s   = cen_dec*dec_s} s
' mil  = {mil_s   = mil_cen*cen_s} s
'
```

III-B. An example for wedge symmetry plane model

```
'
' Dilation Criteria
' Journalized by B.Y.Park on August 4, 2010
' Consider safety factor of 1.5 for Van Sambeek criterion
'
save displx disply displz     'To see deformed mesh
'
{include("units.txt")}
'
' Time selection
tmin {d_s}     '1 day
'
' Define time in term of year
TIME=TIME/{yr_s}
'
' Select Salt Dome
blocks delete 2 3             'exclude caprock overburden farfield
'
' Compute I1 and SJ2
I1T=sigxx+sigyy+sigzz         'I1 (Pa), Positive for tension
I1C=-I1T                              'I1 (Pa), Positive for compression
SJ2=VONMISES/SQRT(3.0)                'Sqrt(J2) (Pa)
'
' Compute Lode angle
'
sig1=pmax(sigxx,sigyy,sigzz,sigxy,sigyz,sigzx) 'Maximum principal stress (Pa)
sig3=pmin(sigxx,sigyy,sigzz,sigxy,sigyz,sigzx) 'Minimum principal stress (Pa)
sig2=I1T-sig1-sig3                    'Intermediate principal stress (Pa)
                              'because I1T=sig1+sig2+sig3=sigxx+sigyy+sigzz
Deno=sig1-sig3                        'Denominator
Denom=ABS(sig1-sig3)-1.E-6            'Screen out when -1.E-6<Deno<1.E-6
Denomi=IFLZ(Denom,1.E-6,Deno)         'If Denom<0, Denomi=1.E-6; Otherwise Denomi=Deno
Psi=atan((2*sig2-sig1-sig3)/Denomi/sqrt(3)) 'Lode angle (rad)
```

```
APsi=ABS(Psi)-1.E-6                  'Screen out when -1.E-6<Psi<1.E-6
Lode=IFLZ(APsi,1.E-6,Psi)            'If APsi<0, Lode=1.E-6; Otherwise Lode=Psi (rad)
'
' Compute Maximum sig1 (Pa)
'
Maxsig1=smax(sig1)
'
' Compute Minimum Safety Factor for Dilatancy
' Based on dilatant damage criteria for WIPP
' Sqrt(J2)=0.27*I1
' [Van Sambeek et al., 1993]
'
F_VS=0.27*I1C/1.5              'Consider safety factor of 1.5 (App.II) (Pa)
DPOT_VS=SJ2/F_VS                     'Dilatant damage potential
CUT=0.01                             'Screen out when DPOT<0.01 i.e. SF>100
DIL_VS=IFLZ(DPOT_VS-CUT,CUT,DPOT_VS) 'If DPOT<CUT then DIL=CUT, if DPOT>CUT then DIL=DPOT
SF_VS=IFEZ(STATUS,1/DIL_VS,100) 'Safety factor against dilatancy (SF=1/DPOT)
' If STATUS=0, elements are active. STATUS=1, elements are inactive, i.e. removed.
minSF_VS=smin(SF_VS)                 'Minimum safety factor against dilatant damage
'
' Compute Minimum Safety Factor for Dilatancy
' Based on dilatant damage criteria for Cayuta Salt
' [DeVries et al., 2005]
'
sig0_CA=-1*{MPa_Pa}           'Dimensional constant (Pa)
T0_CA=1.95*{MPa_Pa}           'Unconfined tensile strength (Pa)
n_CA=0.693                    'Salt material constant (-)
D1_CA=0.773*{MPa_Pa}          'Salt material constant (Pa)
D2_CA=0.524                          'Salt material constant (-)
F_CA=(D1_CA*(I1T/sig0_CA)^n_CA+T0_CA)/(sqrt(3)*cos(Lode)-D2_CA*sin(Lode)) 'RD Sqrt(J2) (Pa)
DPOT_CA=SJ2/F_CA                     'Dilatant damage potential
DIL_CA=IFLZ(DPOT_CA-CUT,CUT,DPOT_CA) 'If DPOT<CUT then DIL=CUT, if DPOT>CUT then DIL=DPOT
SF_CA=IFEZ(STATUS,1/DIL_CA,100) 'Safety factor against dilatancy (SF=1/DPOT)
minSF_CA=smin(SF_CA)                 'Minimum safety factor against dilatant damage
'
' Compute Minimum Safety Factor for Dilatancy
' Based on dilatant damage criteria for Big Hill Salt
' [Sobolik & Ehgartner, 2009]
'
sig0_BH=-1*{MPa_Pa}           'Dimensional constant (Pa)
T0_BH=83540*{psf_Pa}                 'Unconfined tensile strength (Pa)
n_BH=0.3668                   'Salt material constant (-)
D1_BH=45200*{psf_Pa}                 'Salt material constant (Pa)
D2_BH=0.5632                         'Salt material constant (-)
F_BH=(D1_BH*(I1T/sig0_BH)^n_BH+T0_BH)/(sqrt(3)*cos(Lode)-D2_BH*sin(Lode)) 'RD Sqrt(J2) (Pa)
DPOT_BH=SJ2/F_BH                'Dilatant damage potential
DIL_BH=IFLZ(DPOT_BH-CUT,CUT,DPOT_BH) 'If DPOT<CUT then DIL=CUT, if DPOT>CUT then DIL=DPOT
SF_BH=IFEZ(STATUS,1/DIL_BH,100) 'Safety factor against dilatancy (SF=1/DPOT)
minSF_BH=smin(SF_BH)                 'Minimum safety factor against dilatant damage
'
' Delete unnecessary variables
'
delete CUT sig0_CA T0_CA n_CA D1_CA D2_CA sig0_BH T0_BH n_BH D1_BH D2_BH
delete I1T I1C SJ2
delete sig3 sig2 Deno Denom Denomi Psi APsi Lode
delete F_VS DPOT_VS DIL_VS
delete F_CA DPOT_CA DIL_CA
delete F_BH DPOT_BH DIL_BH
'
End
```

III-C. An example for the zoomed volume of the web salt

```
'
' West Hackberry Salt Dome
' Dilation Criteria for the web between caverns 109 and 110
' Journalized by B.Y.Park on September 30, 2010
' Consider safety factor of 1.5 for Van Sambeek criterion
'
save displx disply displz     'To see deformed mesh
'
{include("units.txt")}
'
' Time selection
' Simulation starts at 1/1/1945(TIME=0).
' Workovers start at beginning in 1/1/1984.
t_bgn=14244*{d_s}      '(=1/1/1984)
```

```
'
' Define time in term of year since 1/1/1984
TIME=(TIME-t_bgn)/{d_s}
'
' Select Salt Dome
blocks delete 2 3 4           'exclude caprock overburden farfield
'
' zoom around the web (SAND2009-1986, Table 1)
'{hor=300}     'ft, horizontal margin from center of cavern
'{ver=200}     'ft, vertical margin from top and bottom of cavern
'{wes=8.878}   'ft, Cavern 109
'{eas=23.11}   'ft, Cavern 110
'{sou=750.074} 'ft, Cavern 109
'{nor=1499.328}       'ft, Cavern 110
'{bot=-4600}   'ft, Cavern 109
'{top=-2600}   'ft, Cavern 109
zoom {wes-hor} {eas+hor} {sou+1} {nor-1} {bot-ver} {top+ver}
'
' Compute I1 and SJ2
I1T=sigxx+sigyy+sigzz         'I1 (psf), Positive for tension
I1C=-I1T                             'I1 (psf), Positive for compression
SJ2=VONMISES/SQRT(3.0)               'Sqrt(J2) (psf)
'
' Compute Lode angle
'
sig1=pmax(sigxx,sigyy,sigzz,sigxy,sigyz,sigzx) 'Maximum principal stress (psf)
sig3=pmin(sigxx,sigyy,sigzz,sigxy,sigyz,sigzx) 'Minimum principal stress (psf)
sig2=I1T-sig1-sig3                   'Intermediate principal stress (psf)
                                     'because I1T=sig1+sig2+sig3=sigxx+sigyy+sigzz
Deno=sig1-sig3                       'Denominator
Denom=ABS(sig1-sig3)-1.E-6           'Screen out when -1.E-6<Deno<1.E-6
Denomi=IFLZ(Denom,1.E-6,Deno)        'If Denom<0, Denomi=1.E-6; Otherwise Denomi=Deno
Psi=atan((2*sig2-sig1-sig3)/Denomi/sqrt(3)) 'Lode angle (rad)
APsi=ABS(Psi)-1.E-6                  'Screen out when -1.E-6<Psi<1.E-6
Lode=IFLZ(APsi,1.E-6,Psi)            'If APsi<0, Lode=1.E-6; Otherwise Lode=Psi (rad)
'
' Compute Maximum sig1 (psf)
'
Maxsig1=smax(sig1)
'
' Compute Minimum Safety Factor for Dilatancy
' Based on dilatant damage criteria for WIPP
' Sqrt(J2)=0.27*I1
' [Van Sambeek et al., 1993]
'
F_VS=0.27*I1C/1.5              'Consider safety factor of 1.5 (App.II) (psf)
DPOT_VS=SJ2/F_VS                     'Dilatant damage potential
CUT=0.01                             'Screen out when DPOT<0.01 i.e. SF>100
DIL_VS=IFLZ(DPOT_VS-CUT,CUT,DPOT_VS) 'If DPOT<CUT then DIL=CUT, if DPOT>CUT then DIL=DPOT
SF_VS=IFEZ(STATUS,1/DIL_VS,100) 'Safety factor against dilatancy (SF=1/DPOT)
' If STATUS=0, elements are active. STATUS=1, elements are inactive, i.e. removed.
minSF_VS=smin(SF_VS)                 'Minimum safety factor against dilatant damage
'
' Compute Minimum Safety Factor for Dilatancy
' Based on dilatant damage criteria for Cayuta Salt
' [DeVries et al., 2005]
'
sig0_CA=-1*{MPa_psf}          'Dimensional constant (psf)
T0_CA=1.95*{MPa_psf}          'Unconfined tensile strength (psf)
n_CA=0.693                    'Salt material constant (-)
D1_CA=0.773*{MPa_psf}         'Salt material constant (psf)
D2_CA=0.524                          'Salt material constant (-)
F_CA=(D1_CA*(I1T/sig0_CA)^n_CA+T0_CA)/(sqrt(3)*cos(Lode)-D2_CA*sin(Lode)) 'RD Sqrt(J2) (psf)
DPOT_CA=SJ2/F_CA                     'Dilatant damage potential
DIL_CA=IFLZ(DPOT_CA-CUT,CUT,DPOT_CA) 'If DPOT<CUT then DIL=CUT, if DPOT>CUT then DIL=DPOT
SF_CA=IFEZ(STATUS,1/DIL_CA,100) 'Safety factor against dilatancy (SF=1/DPOT)
minSF_CA=smin(SF_CA)                 'Minimum safety factor against dilatant damage
'
' Compute Minimum Safety Factor for Dilatancy
' Based on dilatant damage criteria for Big Hill Salt
' [Sobolik & Ehgartner, 2009]
'
sig0_BH=-1*{MPa_psf}          'Dimensional constant (psf)
T0_BH=83540                   'Unconfined tensile strength (psf)
n_BH=0.3668                   'Salt material constant (-)
D1_BH=45200                   'Salt material constant (psf)
D2_BH=0.5632                         'Salt material constant (-)
F_BH=(D1_BH*(I1T/sig0_BH)^n_BH+T0_BH)/(sqrt(3)*cos(Lode)-D2_BH*sin(Lode)) 'RD Sqrt(J2) (psf)
DPOT_BH=SJ2/F_BH                'Dilatant damage potential
DIL_BH=IFLZ(DPOT_BH-CUT,CUT,DPOT_BH) 'If DPOT<CUT then DIL=CUT, if DPOT>CUT then DIL=DPOT
SF_BH=IFEZ(STATUS,1/DIL_BH,100) 'Safety factor against dilatancy (SF=1/DPOT)
```

```
minSF_BH=smin(SF_BH)                'Minimum safety factor against dilatant damage
'
' Delete unnecessary variables
'
delete CUT sig0_CA T0_CA n_CA D1_CA D2_CA sig0_BH T0_BH n_BH D1_BH D2_BH
delete I1T I1C SJ2 T_BGN
delete sig3 sig2 Deno Denom Denomi Psi APsi Lode
delete F_VS DPOT_VS DIL_VS
delete F_CA DPOT_CA DIL_CA
delete F_BH DPOT_BH DIL_BH
'
end
```

III-D. An example for the zoomed volume containing two caverns

```
'
' Bryan Mound Salt Dome
' Dilation Criteria for the web between caverns 112 and 114
' Journalized by B.Y.Park on August 12, 2010
' Consider safety factor of 1.5 for Van Sambeek criterion
'
save displx disply displz     'To see deformed mesh
'
{include("units.txt")}
'
' Time selection
' Simulation starts at 1/1/1945(TIME=0).
' Workovers start at beginning in 1/1/1984.
t_bgn={14244*d_s}      '(=1/1/1984)
'
' Define time in term of year since 1/1/1984
TIME=(TIME-t_bgn)/{d_s}
'
' Select Salt Dome
blocks delete 2 3 4           'exclude caprock overburden farfield
'
' zoom around the web
' Node 3916716    -8.564840E+02 -1.983660E+03 -2.280000E+03 (lower left)
' Node 3635512    -2.418810E+02 -1.370640E+03 -2.360000E+03 (upper right)
' Node 3803244     5.183780E+02 -3.923108E+02 -4.041000E+03 (bottom center)
' Node 3589036    -2.418810E+02 -1.570890E+03 -2.133600E+03 (top center)
' C:\Sandia.dat\SPR\P2D\Calculation\Radius of WH SPR with leach.xls
'
zoom -856 -242 -1983 -1371 -4171 -2002
'
' Compute I1 and SJ2
I1T=sigxx+sigyy+sigzz         'I1 (psf), Positive for tension
I1C=-I1T                              'I1 (psf), Positive for compression
SJ2=VONMISES/SQRT(3.0)                'Sqrt(J2) (psf)
'
' Compute Lode angle
'
sig1=pmax(sigxx,sigyy,sigzz,sigxy,sigyz,sigzx) 'Maximum principal stress (psf)
sig3=pmin(sigxx,sigyy,sigzz,sigxy,sigyz,sigzx) 'Minimum principal stress (psf)
sig2=I1T-sig1-sig3                    'Intermediate principal stress (psf)
                              'because I1T=sig1+sig2+sig3=sigxx+sigyy+sigzz
Deno=sig1-sig3                        'Denominator
Denom=ABS(sig1-sig3)-1.E-6            'Screen out when -1.E-6<Deno<1.E-6
Denomi=IFLZ(Denom,1.E-6,Deno)         'If Denom<0, Denomi=1.E-6; Otherwise Denomi=Deno
Psi=atan((2*sig2-sig1-sig3)/Denomi/sqrt(3)) 'Lode angle (rad)
APsi=ABS(Psi)-1.E-6                   'Screen out when -1.E-6<Psi<1.E-6
Lode=IFLZ(APsi,1.E-6,Psi)             'If APsi<0, Lode=1.E-6; Otherwise Lode=Psi (rad)
'
' Compute Maximum sig1 (psf)
'
Maxsig1=smax(sig1)
'
' Compute Minimum Safety Factor for Dilatancy
' Based on dilatant damage criteria for WIPP
' Sqrt(J2)=0.27*I1
' [Van Sambeek et al., 1993]
'
F_VS=0.27*I1C/1.5               'Consider safety factor of 1.5 (App.II) (psf)
DPOT_VS=SJ2/F_VS                      'Dilatant damage potential
CUT=0.01                              'Screen out when DPOT<0.01 i.e. SF>100
DIL_VS=IFLZ(DPOT_VS-CUT,CUT,DPOT_VS) 'If DPOT<CUT then DIL=CUT, if DPOT>CUT then DIL=DPOT
SF_VS=IFEZ(STATUS,1/DIL_VS,100) 'Safety factor against dilatancy (SF=1/DPOT)
' If STATUS=0, elements are active. STATUS=1, elements are inactive, i.e. removed.
minSF_VS=smin(SF_VS)                  'Minimum safety factor against dilatant damage
```

```
'
' Compute Minimum Safety Factor for Dilatancy
' Based on dilatant damage criteria for Cayuta Salt
' [DeVries et al., 2005]
'
sig0_CA=-1*{MPa_psf}          'Dimensional constant (psf)
T0_CA=1.95*{MPa_psf}          'Unconfined tensile strength (psf)
n_CA=0.693                    'Salt material constant (-)
D1_CA=0.773*{MPa_psf}         'Salt material constant (psf)
D2_CA=0.524                        'Salt material constant (-)
F_CA=(D1_CA*(I1T/sig0_CA)^n_CA+T0_CA)/(sqrt(3)*cos(Lode)-D2_CA*sin(Lode)) 'RD Sqrt(J2) (psf)
DPOT_CA=SJ2/F_CA                   'Dilatant damage potential
DIL_CA=IFLZ(DPOT_CA-CUT,CUT,DPOT_CA) 'If DPOT<CUT then DIL=CUT, if DPOT>CUT then DIL=DPOT
SF_CA=IFEZ(STATUS,1/DIL_CA,100) 'Safety factor against dilatancy (SF=1/DPOT)
minSF_CA=smin(SF_CA)               'Minimum safety factor against dilatant damage
'
' Compute Minimum Safety Factor for Dilatancy
' Based on dilatant damage criteria for Big Hill Salt
' [Sobolik & Ehgartner, 2009]
'
sig0_BH=-1*{MPa_psf}          'Dimensional constant (psf)
T0_BH=83540                   'Unconfined tensile strength (psf)
n_BH=0.3668                   'Salt material constant (-)
D1_BH=45200                   'Salt material constant (psf)
D2_BH=0.5632                       'Salt material constant (-)
F_BH=(D1_BH*(I1T/sig0_BH)^n_BH+T0_BH)/(sqrt(3)*cos(Lode)-D2_BH*sin(Lode)) 'RD Sqrt(J2) (psf)
DPOT_BH=SJ2/F_BH                'Dilatant damage potential
DIL_BH=IFLZ(DPOT_BH-CUT,CUT,DPOT_BH) 'If DPOT<CUT then DIL=CUT, if DPOT>CUT then DIL=DPOT
SF_BH=IFEZ(STATUS,1/DIL_BH,100) 'Safety factor against dilatancy (SF=1/DPOT)
minSF_BH=smin(SF_BH)               'Minimum safety factor against dilatant damage
'
' Delete unnecessary variables
'
delete CUT sig0_CA T0_CA n_CA D1_CA D2_CA sig0_BH T0_BH n_BH D1_BH D2_BH
delete I1T I1C SJ2
delete sig3 sig2 Deno Denom Denomi Psi APsi Lode
delete F_VS DPOT_VS DIL_VS
delete F_CA DPOT_CA DIL_CA
delete F_BH DPOT_BH DIL_BH
'
end
```

DISTRIBUTION

1 U.S. Department of Energy
Attn: D. Johnson, FE-40
Deputy Assistant Secretary for Petroleum Reserves
1000 Independence Avenue SW
Washington, D.C. 20585

1 US Department of Energy
Attn: Deputy Director, RW-2
Office of Civilian Radioactive Waste Mgmt.
Forrestal Building
Washington, DC 20585

Electronic copy only to Wayne Elias at Elias.Wayne@spr.doe.gov for distribution to DOE and DM

1	MS0372	J. G. Arguello Jr.	1525
1	MS0376	J. E. Bean	1525
1	MS0706	D. J. Borns	6912
5	MS0706	B. L. Ehgartner	6912
1	MS0706	D. L. Lord	6912
1	MS0706	C. A. Rautman	6912
1	MS0706	A. R. Sattler	6912
1	MS0706	Anna C.S. Lord	6912
1	MS0735	J. A. Merson	6910
1	MS0751	R. E. Finley	6210
1	MS0751	T. W. Pfeifle	6914
1	MS0751	S. R. Sobolik	6914
5	MS0751	B. Y. Park	6914
1	MS1395	M. Y. Lee	6211
1	MS1395	C. G. Herrick	6211
1	MS0899	Technical Library	9536 (electronic copy)
1	MS0731	823 Library	10662

Sandia National Laboratories